Interference Management in Wireless Networks: Physical Layer Communication Strategies, MAC Layer Interactions, and High Layer Messaging Structures

Leonard Henry Grokop

Electrical Engineering and Computer Sciences
University of California at Berkeley

Technical Report No. UCB/EECS-2008-118
http://www.eecs.berkeley.edu/Pubs/TechRpts/2008/EECS-2008-118.html

September 16, 2008

Acknowledgement

Foremost I would like to thank my advisor Professor David Tse for his tireless mentorship and support. Through the hundreds of one-on-one meetings we had during my graduate education, he taught me how to formulate and solve research problems by abstracting the key elements of a system into a mathematical model, and then examining simple cases in order to develop the intuition required to find a solution. I am indebted to my colleagues in Wireless Foundations for the time they dedicated to discussing various research problems with me, and for the spirit of camaraderie they helped foster in our laboratory. I am also indebted to Professors Venkat Anantharam, Michael Gastpar and Anant Sahai for their research collaboration and their excellent teaching.

Interference Management in Wireless Networks: Physical Layer Communication Strategies, MAC Layer Interactions, and High Layer Messaging Structures

by

Leonard H. Grokop

B.Sc. (University of Melbourne) 2001
B.E. (Hons.) (University of Melbourne) 2001
M.S. (University of California, Berkeley) 2005

A dissertation submitted in partial satisfaction
of the requirements for the degree of

Doctor of Philosophy

in

Electrical Engineering and Computer Sciences

in the

GRADUATE DIVISION

of the

UNIVERSITY OF CALIFORNIA, BERKELEY

Committee in charge:

Professor David Tse, Chair
Professor Kannan Ramchandran
Professor David Aldous

Fall 2008

The dissertation of Leonard H. Grokop is approved:

Professor David Tse, Chair	Date
Professor Kannan Ramchandran	Date
Professor David Aldous	Date

University of California, Berkeley

Fall 2008

Interference Management in Wireless Networks: Physical Layer Communication Strategies, MAC Layer Interactions, and High Layer Messaging Structures

by

Leonard H. Grokop

Abstract

Interference Management in Wireless Networks: Physical Layer Communication Strategies, MAC Layer Interactions, and High Layer Messaging Structures

by

Leonard H. Grokop

Doctor of Philosophy in Computer Science

University of California, Berkeley

Professor David Tse, Chair

Wireless communications research of previous decades has mostly focused on systems built from point to point channels. In such systems physical communication links are essentially interference free, and interference management is at most a peripheral issue. Whilst these approaches have obvious advantages in terms of simplicity of design and maintenance, they typically suffer from low spectral efficiencies. In this thesis we research a number of new approaches spanning a range of communication layers, aimed at improving spectrum management.

In the first chapter the fully connected K-user interference channel is studied in a multipath environment with bandwidth W. We show that when each link consists of D physical paths, the total spectral efficiency can grow *linearly* with K. This result holds not merely in the limit of large transmit power P, but for any fixed P, and is therefore a stronger characterization than degrees of freedom. It is achieved via a form of interference alignment in the time domain. A caveat of this result is that W must grow with K, a phenomenon we refer to as *bandwidth scaling*. Our insight comes from examining channels with single path links ($D = 1$), which we refer to as line-of-sight (LOS) links. For such channels we build a time-indexed interference

graph and associate the communication problem with finding its maximal independent set. This graph has a stationarity property that we exploit to solve the problem efficiently via dynamic programming. Additionally, the interference graph enables us to demonstrate the necessity of bandwidth scaling for any scheme operating over LOS interference channels. Bandwidth scaling is then shown to also be a necessary ingredient for interference alignment schemes used on general K-user interference channels.

In the second chapter we consider the problem of two wireless networks operating on the same (presumably unlicensed) frequency band. Pairs within a given network cooperate to schedule transmissions, but between networks there is competition for spectrum. To make the problem tractable, we assume transmissions are scheduled according to a random access protocol where each network chooses an access probability for its users. A game between the two networks is defined. We characterize the Nash Equilibrium behavior of the system. Three regimes are identified; one in which both networks simultaneously schedule all transmissions; one in which the denser network schedules all transmissions and the sparser only schedules a fraction; and one in which both networks schedule only a fraction of their transmissions. The regime of operation depends on the pathloss exponent α, the latter regime being desirable, but attainable only for $\alpha > 4$. This suggests that in certain environments, rival wireless networks may end up naturally cooperating. To substantiate our analytical results, we simulate a system where networks iteratively optimize their access probabilities in a greedy manner. We also discuss a distributed scheduling protocol that employs carrier sensing, and demonstrate via simulations, that again a near cooperative equilibrium exists for sufficiently large α.

In the third chapter we examine messaging structures. Much of the existing work on the broadcast channel focuses only on the sending of private messages. We examine the scenario where the sender also wishes to transmit common messages to subsets

of receivers. For an L-user broadcast channel there are $2^L - 1$ subsets of receivers and correspondingly $2^L - 1$ independent messages. The set of achievable rates for this channel is a $2^L - 1$-dimensional region. There are fundamental constraints on the geometry of this region. For example, observe that if the transmitter is able to simultaneously send L rate-one private messages, errorfree to all receivers, then by sending the same information in each message, it must be able to send a single rate-one common message, errorfree to all receivers. This swapping of private and common messages illustrates that for any broadcast channel, the inclusion of a point $\mathbf{R}^*$ in the achievable rate region implies the achievability of a set of other points that are not merely componentwise less than $\mathbf{R}^*$. We formerly define this set and characterize it for $L = 2$ and $L = 3$. Whereas for $L = 2$ all the points in the set arise only from operations relating to swapping private and common messages, for $L = 3$ a form of network coding is required.

Professor David Tse, Chair Date

This thesis is dedicated to the memory of my grandfather David Pearl, who came to Australia as a Holocaust survivor from Europe. His ethic of hard work and diligence provided me with opportunities I might not otherwise have had, and serves as a guiding example in my life.

Contents

Preface

The primary issue in the design of wireless adhoc networks is managing the interference that transmissions generate at nearby receivers. The simplest approach to this problem, and the one most commonly adopted in practice, is to assign users orthogonal subchannels of the available spectrum —each user gets a slice of the pie, so to speak. This is typically done in such a way as to ensure that neighboring communication links (we refer to a communication link as a *user*) are assigned different subchannels. The drawback to this approach is that when the density of users in the system increases, the spectral efficiency of each user diminishes —each user gets a smaller slice of pie. Is this an innate characteristic of the communication medium, or is it possible to design schemes that circumvent this deleterious effect? This question is the focus of the first chapter of this thesis, where we show that it is indeed possible to design physical layer communication strategies for which the spectral efficiency of each user diminishes arbitrarily slowly as the number of users increases. We develop a framework for efficiently designing optimal communication schemes for line-of-sight channels by way of a time-indexed interference graph. The ideas can then be extended to channels with both line-of-sight and non line-of-sight components.

In the second chapter we investigate the scenario where two co-located wireless adhoc networks share the same frequency spectrum. Within each network devices cooperate in scheduling transmissions at the MAC layer, but between networks their is no incentive to do so. Users would still hope to receive an equal slice of the pie, but due to the competitive nature of the situation, this desirable outcome seems unlikely. We formulate the problem as a game between two random-access networks and characterize the Nash equilibrium behavior of the system. The behavior turns out to depend crucially on the pathloss exponent (the rate at which the signal fades with

increasing distance). We identify three distinct regimes and show that surprisingly, when the path loss exponent is large enough, each network behaves as if it were operating in isolation.

The last problem we tackle concerns messaging structures. For broadcast and multiple access channels with three users we characterize the complete set of messaging structures that are achievable for any channel for which a given messaging structure is achievable.

Acknowledgements

Foremost I would like to thank my advisor Professor David Tse for his tireless mentorship and support. Through the hundreds of one-on-one meetings we had during my graduate education, he taught me how to formulate and solve research problems by abstracting the key elements of a system into a mathematical model, and then examining simple cases in order to develop the intuition required to find a solution. I am indebted to my colleagues Salman Avestimehr, Guy Bresler, Cheng Chang, Krish Eswaran, Raul Etkin, Paolo Minero, Bobak Nazer, Vinod Prabhakaran, Anand Sarwate, Rahul Tandra, and Aaron Wagner, for the time they dedicated to discussing various research problems with me, and for the spirit of camaraderie they helped foster in our laboratory. I am also indebted to Professors Venkat Anantharam, Michael Gastpar and Anant Sahai for their research collaboration and their excellent teaching. I would also like to thank Professor Roy Yates for his friendship and collaboration during his sabbatical year at Berkeley, Professor Raymond Herbert for his ever-present enthusiasm and inspiration at the piano, and Professor Lucien Polak for encouraging me to pursue graduate studies in electrical engineering in the United States.

Chapter 1

Interference Alignment for Line-of-Sight Channels

1.1 Introduction

The problem of communicating efficiently in wireless adhoc networks has received much attention of late, the focus being on how to deal with interference in a shared medium. Traditional approaches based on orthogonalizing users (eg. time-division multiple access (TDMA) or frequency-division multiple access (FDMA) schemes) or reusing the spectrum (eg. code-division multiple access (CDMA), certain modes of 802.11) suffer from poor spectral efficiency. In particular as the number of users in the system grows, the spectral efficiency of each link vanishes. More recent approaches include using multi-hop [12], distributed MIMO [24], [11], and interference alignment [20],[5],[14]. This work is belongs to the latter category. Interference alignment is a technique that uses appropriate precoding to compact interfering signals into small dimensional subspaces at each receiver. At the same time, the subspace occupied by the data remains linearly independent of the interference. It was first applied to a

multiple MIMO base station problem in [20] and shown to be capable of achieving multiplexing gains distinctly greater than those achievable using conventional signalling schemes. The technique was then extended in [14] to show that there were exactly $4M/3$ degrees of freedom (the asymptotic gradient of spectral efficiency with respect to $\log_2 \mathsf{SNR}$) in the MIMO X channel (two MIMO transmitters each desiring to send data to two MIMO receivers) with $M > 1$ antennas at each transceiver. Following this, a more sophisticated interference alignment technique was developed in [5] for the K-user interference channel with an infinite number of independently faded sub-channels, and used to demonstrate that contrary to conventional wisdom, the total degrees of freedom of the channel is $K/2$.

Whilst the last approach demonstrates the potential benefits that interference alignment techniques can provide, it suffers from a number of limitations. Perhaps the foremost is that whilst a degrees of freedom characterization is useful in the high SNR limit, it may not be meaningful at moderate SNR's. This stems from the fact that degrees of freedom characterizes the asymptotic slope of the spectral efficiency curve and not its actual value. In particular, it is unclear whether at any fixed SNR the total spectral efficiency of the system is increasing in proportion to K, or increasing at all. The point here is that [5] does not contain a scaling law result the likes of [12] and [24], that is, it does not tell us what happens to the system capacity as more users enter the fray. We address this question by constructing a communication scheme that achieves a scaling of system capacity arbitrarily close to linear.

There is another key limitation. It is natural to interpret the parallel channels used in the interference alignment scheme of [5] as corresponding to sub-channels in the frequency domain. This is due to various difficulties associated with realizing the scheme over independently faded parallel channels in time, most notably the very rapid and accurate channel measurement that must take place, and the substantial delay incurred. But in order for a large number of frequency channels to undergo

independent fading, significant scattering/multipath is required.

In this work we examine the K-user interference channel with *limited multipath*. We start by assuming each of the K^2 links consists only of a single physical path with complex gain h_{ij} and delay τ_{ij} seconds. This model is a good representation for a line-of-sight (LOS) channel. Following this we generalize to the case where each link consists of D physical paths. We illustrate a simple and elegant representation of interference alignment in the time domain, in terms of aligning symbols on a time-indexed interference graph. This interference graph proves to be an extremely useful tool for both conceptualizing and solving various problems relating to interference in LOS channels. We identify the problem of communicating on the LOS interference channel with the problem of finding a maximal independent set in the interference graph, and show how this problem can be solved efficiently using dynamic programming principles. The simplicity of this approach makes it quite versatile and potentially capable of being extended to tackle at a variety of related problems.

For the remainder of this work power spectral density (PSD) is used in place of signal-to-noise ratio, as we will later wish to compare schemes that use different bandwidths. Depending on the link delays, it may be possible to achieve a spectral efficiency as high as $\frac{1}{2}\log_2(1+|h_{ii}|^2\mathsf{PSD}/N_0)$ bps/Hz for each user i, regardless of the number of interferers. This is exactly half the spectral efficiency achievable in the absence of interference. We characterize the precise channel conditions for which this is possible and show that they occur in at least 1/16 of all scenarios for the 3-user interference channel.

This of course, says little about the typical gains one can expect by aligning interference in the time domain. To address this question, we treat the link delays as independent and uniformly distributed random variables in $[0, T_d)$, where T_d is the delay-spread of the channel. Previous work such as [20], [5], [14] has focused on degrees of freedom as a metric for performance, which is a measure of the scaling

of spectral efficiency with PSD when the power spectral density is large. We focus on the *scaling of spectral efficiency with* K when the number of users is large. The main result of this work is the construction of a communication scheme that achieves a spectral efficiency arbitrarily close to $O(1)\log_2(1 + |h_{ii}|^2\mathsf{PSD}/N_0)$ for each user i as $K \to \infty$. Thus our result characterizes the best possible scaling of spectral efficiency with K for any fixed PSD, as compared with [20], [5], [14], where the best possible scaling of spectral efficiency with PSD, for any fixed K, is characterized. In this sense, our characterization has a similar flavor to characterizations of scaling laws for wireless adhoc networks such as [12], [24]. However, our scheme requires no cooperation between users.

A caveat of our result is that the bandwidth must scale sufficiently with K. Interpreting the parallel channel model of [5] in the frequency domain, one sees that the bandwidth there must also scale with K. Interestingly enough, the bandwidth scaling required for our scheme is essentially the same as that required in [5], namely $O(K^{2K^2})$. However, whereas the scheme in [5] requires coding over blocks of length $O(K^{2K^2})$, which creates significant encoding and decoding complexity issues as well as substantial delay, our scheme requires no block coding, and consequently does not incur any delay or suffer from complexity issues.

Essentially, in order to align interference into a small dimensional subspace and keep it linearly independent of the data subspace, a high degree of resolvability of the received signals is required. We establish this concretely for the LOS channel in the context of the interference graph, showing that if the bandwidth scales sublinearly with K, then the total spectral efficiency of the system (the sum of all users spectral efficiencies) will scale sublinearly, and hence almost all of the users will witness vanishing spectral efficiencies as K increases.

This suggests that the greatest performance gains can be reaped in systems with

large delay spreads[1] Perhaps the best example of such a system is the backbone of a mesh network, used to wirelessly connect rural areas. Such systems are well approximated by a LOS model, have large delay spreads, and are relatively static, making channel measurement simpler and more accurate.

The structuring of the rest of the paper is as follows. In section 1.2 we describe the model of the K-user LOS interference channel. Section 1.3 provides a summary of the main result concerning the achievability of non-vanishing spectral efficiencies as the number of users grows. The time-indexed interference graph is introduced in section 1.4. In the same section we present an algorithm for optimizing the spectral efficiency efficiently via dynamic programming. We also address the questions of bandwidth scaling, and of characterizing the class of channels for which the spectral efficiency can reach its maximum value. In section 1.5 we present our construction that establishes the main result. Following this, in section 1.6, we establish the relationship between time and frequency domain interference alignment techniques. Section 1.7 contains further discussion, extensions and open problems.

1.2 Model

We consider the K-user interference channel in which there are K transmitters and K receivers. Transmitter i wishes to send data to receiver i but its transmission constitutes interference at all other receivers. We often refer to each tx-rx pair as a *user*. There are thus K^2 links in total, K direct links and $K(K-1)$ cross-links. Each link consists of a single physical path. Denote the gain and delay (in seconds) of the link between transmitter j and receiver i by $h_{ij} \in \mathbb{C}$ and $\tau_{ij} \in [0, \infty)$, respectively. We assume the h_{ij} and τ_{ij} are fixed for the duration of communication. Denote the

[1]Delay spread is the length of the impulse response of the channel

signal transmitter j sends by $x_j(t)$. Then the baseband signal at the ith receiver is

$$y_i(t) = \sum_{j=1}^{K} h_{ij} x_j(t - \tau_{ij}) + z_i(t)$$

where the $z_i(t)$ are i.i.d. white noise processes with power spectral density N_0 Watts/Hz. Denote the carrier frequency f_c and the bandwidth that the signals $x_j(t)$ are constrained to lie in by W Hz. Assuming the use of ideal sinc pulses, the passband signal after sampling is given by

$$y_i[m] = \sum_{j=1}^{K} h_{ij} e^{-2\pi f_c \tau_{ij}} \sum_{l=0}^{\infty} \mathrm{sinc}(l - \tau_{ij} W) x_j[m - l] + z_i[m]$$

where the $z_i[m]$ are i.i.d. $\mathcal{CN}(0, N_0 W)$. We use the following conventional approximation for the sinc pulse,

$$\mathrm{sinc}(t) \approx \begin{cases} 1, & \text{if } -1/2 < t < 1/2; \\ 0, & \text{otherwise,} \end{cases}$$

see page 27 of [28]. Let l_{ij} denote the integer round-off of the real number $\tau_{ij} W$. This leads to

$$y_i[m] = \sum_{j=1}^{K} h_{ij} e^{-2\pi f_c \tau_{ij}} x_j[m - l_{ij}] + z_i[m].$$

In a wireless model one typically makes an assumption about the statistics of the channel. For example, in a channel with ISI, the tap coefficients are often modeled as i.i.d. Rayleigh random variables. In models where there is a dominant path, Rician random variables are used instead. Likewise in this work we make a statistical assumption on the channel, but limit this statistical assumption only to the link delays, taking the τ_{ij} to be i.i.d. uniform in $[0, T_d)$, where T_d denotes the delay-spread of the channel in seconds. This means that if we define L to be one plus the integer

round off of T_dW, the l_{ij} are i.i.d. uniform in $\{0, \ldots, L-1\}$. No assumption is made on the link gains h_{ij}, other than they all being non-zero.

We refer to this as the K-user *line-of-sight (LOS)* interference channel, as this is the most common scenario giving rise to such a model.

There is a straightforward extension of this model to the case where each link consists of D physical paths, such that the ith received signal is

$$y_i(t) = \sum_{j=1}^{K} \sum_{d=1}^{D} h_{ij,d} x_j(t - \tau_{ij,d}) + z_i(t).$$

Here $h_{ij,d} \in \mathbb{C}$ and $\tau_{ij,d} \in [0, \infty)$ are the complex gain and delay of the dth physical path between transmitter j and receiver i. This leads to the following generalization of the passband model after sampling

$$y_i[m] = \sum_{j=1}^{K} \sum_{d=1}^{D} h_{ij,d} e^{-2\pi f_c \tau_{ij,d}} x_j[m - l_{ij,d}] + z_i[m].$$

The natural extension of our statistical assumption for the LOS channel is to treat the delays $l_{ij,d}$ as i.i.d. uniform in $\{0, \ldots, L-1\}$. In doing so we are assuming independent delays not just across physical paths of different links, but also across the physical paths corresponding to the same link.

We refer to this as the *K-user D-path interference channel*.

1.3 Preview of Main Result

Theorem 1.3.1. *For any $\epsilon > 0$, there exists a communication scheme on the K-user LOS interference channel such that if $W > (2K(K-1))^{K(K-1)+\epsilon}$, the expected spectral*

efficiency of user i tends to

$$\frac{1}{(K(K-1))^{\epsilon}} \log_2 \left(1 + |h_{ii}|^2 \frac{\mathsf{PSD}}{N_0}\right) \tag{1.1}$$

as $K \to \infty$.

Section 1.5 is devoted to proving this result. Here the expectation of spectral efficiency is taken over the random direct delays l_{ii}. Roughly speaking this result says that as K scales, it is possible for each user to communicate at a spectral efficiency arbitrarily close to $O(1)\log_2(1 + \frac{\mathsf{PSD}}{N_0})$, so long as the bandwidth scales as fast as $O((2K(K-1))^{K(K-1)})$. In other words, communication at spectral efficiencies that vanish arbitrarily slowly with K is possible if the bandwidth scales sufficiently. In this result, and throughout this work, we assume that all cross delays l_{ij} for $i \neq j$ are known at all transmitters and receivers. This result is of a similar nature to the scaling laws of [24], in that we show the growth of system capacity with the number of users is arbitrarily close to linear. Unfortunately, as is the case in [5], the required bandwidth scaling is great. A result presented later on (theorem 1.4.2) addresses the question of whether bandwidth scaling is necessary.

For the case where each link consists of D physical paths we have the following generalization.

Theorem 1.3.2. *For any $\epsilon > 0$, there exists a communication scheme on the K-user D-path interference channel such that if $W > (2DK(DK-1))^{DK(DK-1)+\epsilon}$, the expected spectral efficiency of user i tends to*

$$\frac{1}{(DK(DK-1))^{\epsilon}} \log_2 \left(1 + \max_{d \in \{1,\ldots,D\}} |h_{ii,d}|^2 \frac{\mathsf{PSD}}{N_0}\right) \tag{1.2}$$

as $K \to \infty$.

As is evident from the statement of the theorem, there is a tradeoff between

the number of physical paths per link and the bandwidth scaling required. Again, the question of whether this bandwidth scaling is necessary is addressed in a result presented later on.

1.4 The Interference Graph

The key insight leading to theorem 1.3.1 comes from formulating the communication problem in a graph theoretical setting. We start with an example. Consider a 3-user LOS interference channel where the direct links are all zero, i.e. $l_{11} = 0$, $l_{22} = 0$ and $l_{33} = 0$, and the cross-links are say, $l_{21} = 3$, $l_{31} = 1$, $l_{12} = 1$, $l_{32} = 4$, $l_{13} = 3$, $l_{23} = 0$. Choose a length T for the communication block. Create a directed graph $\mathcal{G}_{3,T}(l_{12}, l_{13}, l_{21}, l_{23}, l_{31}, l_{32}) = (\mathcal{V}, \mathcal{E})$ as follows. Let the vertex set be

$$\mathcal{V} = \{v_1(0), \ldots, v_1(T-1)\} \cup \{v_2(0), \ldots, v_2(T-1)\} \cup \{v_3(0), \ldots, v_3(T-1)\}.$$

The vertex $v_i(t)$ represents the tth time slot for the ith transmitter. Form the edge set $\mathcal{E}$ as follows. Add a directed edge $e_{21}(0)$ starting from vertex $v_1(0)$ and ending at vertex $v_2(l_{21}) = v_2(3)$. This represents the fact that, owing to a delay of 3 time slots, a transmission during time slot 0 by transmitter 1 arrives at receiver 2 during time slot 3. Also add a directed edge $e_{31}(0)$ starting from $v_1(0)$ and ending at $v_3(l_{31}) = v_3(1)$. This represents the fact that, owing to a delay of 1 time slot, a transmission during time slot 0 by transmitter 1 arrives at receiver 3 during time slot 1. Likewise add directed edges $e_{12}(0)$ and $e_{32}(0)$ from vertex $v_2(0)$ to $v_1(l_{12}) = v_1(1)$ and $v_3(l_{32}) = v_3(4)$, respectively, and directed edges e_{13} and e_{23} from vertex $v_3(0)$ to $v_1(l_{13}) = v_1(3)$ and $v_2(l_{23}) = v_2(0)$, respectively. This set of six edges encapsulates all of the interference generated by transmissions during time slot 0. As the channel is time-invariant the same interference structure applies for later time slots. Thus for each

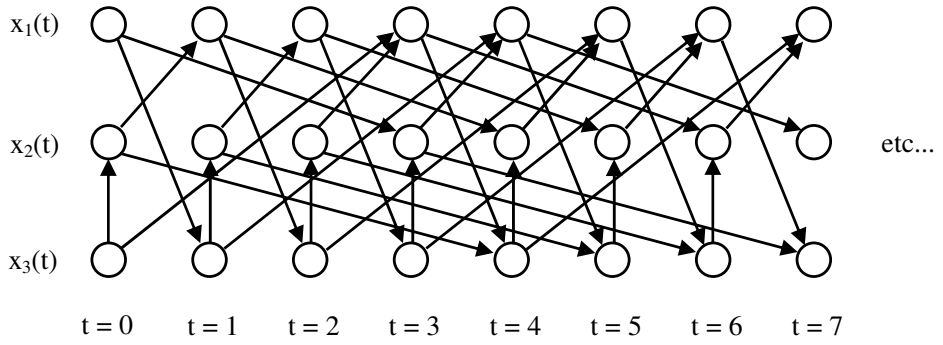

Figure 1.1: The interference graph associated with the LOS channel with direct-delays $l_{11} = 0, l_{22} = 0, l_{33} = 0$ and cross-delays $l_{21} = 3, l_{31} = 1, l_{12} = 1, l_{32} = 4, l_{13} = 3, l_{23} = 0$.

$t = 1, 2, \ldots, T-1$ add a directed edge from $v_1(t)$ to $v_2(t + l_{21})$, provided $t + l_{21} \leq T$, a directed edge from $v_1(t)$ to $v_3(t + l_{31})$, provided $t + l_{31} \leq T$, a directed edge from $v_2(t)$ to $v_1(t + l_{12})$, provided $t + l_{12} \leq T$, etc... See figure 1.1 for an illustration.

In this example all direct delays were zero, whereas in general this is not the case. However as each transmitter j can merely offset it's transmitted sequence $x_j[m]$ by $-l_{jj}$, we can effectively assume without loss of generality that $l_{jj} = 0$. More concretely we define the *normalized cross-delays*

$$l'_{ij} \triangleq l_{ij} - l_{jj}.$$

Note that $l'_{ij} \in \{-L + 1, \ldots, L - 1\}$, that is, it is possible for l'_{ij} to be negative. At this point one may wonder why the interference graph need be directed, since the feasibility of a given transmit pattern is independent of edge direction. The answer is it need not be, but we define it as such to aid in conceptualizing the problem.

In general we have

Definition 1.4.1. *The time-indexed interference graph (or simply interference graph for short) of length T associated with the K-user LOS interference channel with nor-*

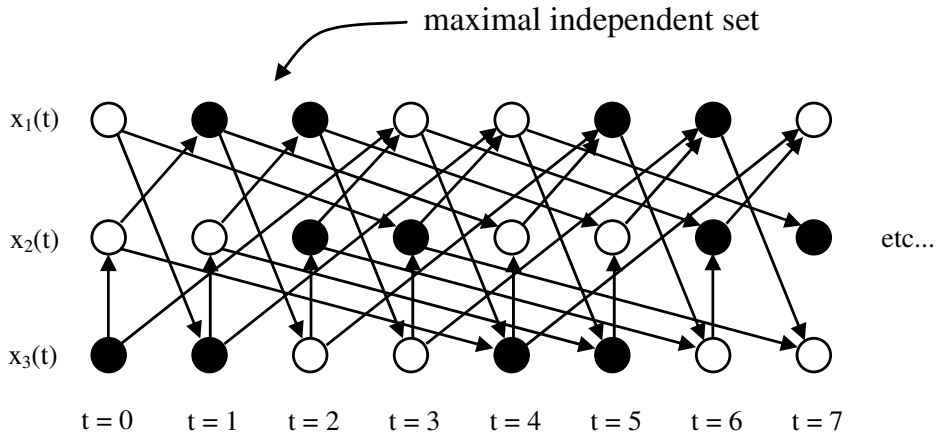

Figure 1.2: A feasible transmit pattern corresponds to an independent set. The vertices of a maximal independent set are shaded. For a symmetric channel, the maximal independent set maximizes total spectral efficiency.

malized cross-delays $\{l'_{ij}\}_{i\neq j}$*, is the directed graph* $\mathcal{G}_{K,T}(\{l'_{ij}\}_{i\neq j}) = (\mathcal{V}, \mathcal{E})$ *where*

$$\mathcal{V} = \bigcup_{j=1}^{K} \{v_j(1), \ldots, v_j(T)\}$$
$$\mathcal{E} = \bigcup_{i=1}^{K} \bigcup_{j=1, j\neq i}^{K} \{e_{ij}(1), \ldots, e_{ij}(T - l'_{ij})\},$$

with edge $e_{ij}(t)$ *stemming from vertex* $v_j(t)$ *and ending at vertex* $v_i(t + l'_{ij})$*.*

This graph has KT vertices and approximately $K(K-1)T$ edges. As a transmission during time slot t is interfered with by one time slot at each other user, and itself interferes with one time slot at each other user, each vertex has both in-degree $K-1$ and out-degree $K-1$. To reduce the notational burden, we often refer to the graph $\mathcal{G}_{K,T}(\{l'_{ij}\}_{i\neq j})$ simply as $\mathcal{G}$, where the parameters of the interference graph are implicit.

One can similarly define a time-indexed interference graph for the D-path interference channel, but in the interest of brevity and clarity we do not discuss it here.

A *transmit pattern* is a subset of time slots during which data symbols are sent,

one data symbol being sent per time slot. A transmit pattern is called *feasible* if each data symbol is received during a time slot that contains no interference from other transmissions. Thus a feasible transmit pattern corresponds to an *independent set* on the interference graph. Occasionally we will drop the adjective "feasible" when it is clear that the transmit pattern in question is such. As each data symbol arriving at receiver i during a time slot containing no interfering symbol, is capable of conveying $\log_2(1 + |h_{ii}|^2 \frac{\mathsf{PSD}}{N_0})$ bps/Hz, user i's spectral efficiency will be

$$R_i = N_i \log_2 \left(1 + |h_{ii}|^2 \frac{\mathsf{PSD}}{N_0}\right),$$

where N_i is the number of vertices in $\{v_i(1), \ldots, v_i(T)\}$ that are in the independent set. Let us assume for the meantime that $h_{ii} = 1$ for all i. Then the total spectral efficiency is directly proportional to the size of the independent set. Thus the problem of designing a communication scheme to maximize total spectral efficiency reduces to finding the *maximal independent set* of the interference graph. Denote the size of the maximal independent set of a graph $\mathcal{G}$ (called the *independence number*) by $\alpha(\mathcal{G})$. Then the maximum total spectral efficiency for a graph $\mathcal{G}$ is

$$\alpha(\mathcal{G}) \log_2 \left(1 + \frac{\mathsf{PSD}}{N_0}\right).$$

For the preceding example, the maximal independent set is illustrated in figure 1.2. Whenever an independent set contains two vertices that possess a mutual neighbor, the interference generated by these two transmissions aligns at the mutual neighboring vertex. This is *interference alignment in the time domain*. For the example in figure 1.2, the neighbors of each unshaded vertex are all shaded, that is, data transmissions occur at all neighbors of an unshaded vertex. This is not always the case. Suppose we use a TDMA based communication scheme where user 1 transmits on consecutive

time slots for a long period whilst users 2 and 3 remain silent. Then after a small guard interval user 2 transmits on consecutive time slots whilst users 1 and 3 remain silent. Finally user 3 transmits, and then back to user 1 and so on. In this round robin scheme, each unshaded vertex is connected to only a single shaded one and no interference alignment occurs.

The problem of finding the maximal independent set is a well-known NP-hard problem, meaning that for an arbitrary graph, there is no known algorithm capable of solving the problem in time sub-exponential in the number of vertices. Knowing this it may appear that finding an optimal transmit pattern requires a computation time that is exponential in the block length T, however the interference graph is not an arbitrary graph. In particular it is stationary in the sense that, ignoring boundary effects, the structure of the graph is invariant to time shifts. In the next section we present an algorithm that exploits this property to find the maximum independent set in linear time. More generally, when the link gains h_{ii} are arbitrary the algorithm solves the problem of finding an independent set that maximizes spectral efficiency. We refer to this set as the *optimal independent set*.

1.4.1 Finding the maximal independent set efficiently

In this section we concentrate on the LOS channel, but the ideas can be extended to the D-path channel. Given an interference graph $\mathcal{G}$ we now illustrate how dynamic programming principles can be employed to compute the maximal independent set efficiently. Let each vertex $v_j(t) \in \{0, 1\}$ with $v_j(t) = 1$ if $v_j(t)$ is included in the transmit pattern, that is, if a data symbol is transmitted by user j during time slot t, and $v_j(t) = 0$ otherwise. There is a slight abuse of notation here as we have used $v_j(t)$ to represent both an element of the vertex set $\mathcal{V}$ and an indicator function for whether or not a data symbol is transmitted by transmitter j during time slot t.

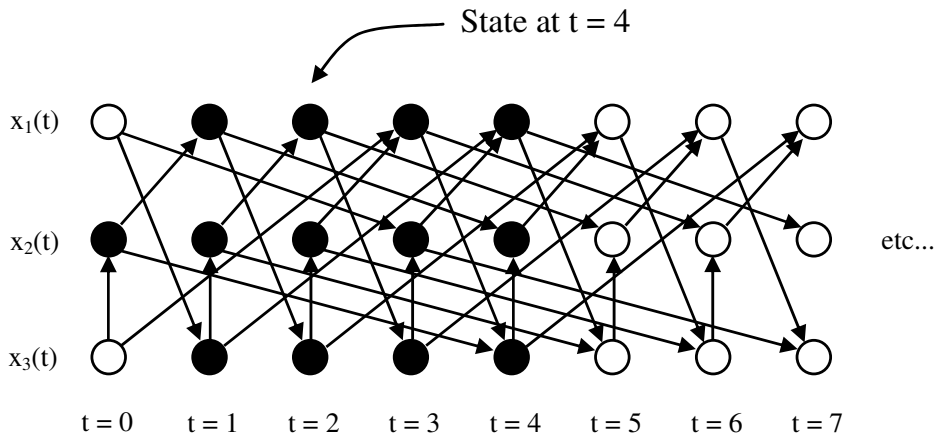

Figure 1.3: The LOS interference channel of figure 1.1. The state at time $t = 4$ is a function of the shaded vertices, each taking on one of two values.

Concretely stated, the optimization problem we will solve is

$$\min_{\substack{\{v_j(t)\} \in \{0,1\}^{KT} \\ \text{s.t. } v_i(s) + v_j(t) \leq 1, \forall (v_i(s), v_j(t)) \in \mathcal{E}}} -\sum_{j=1}^{K} r_j \left(\sum_{t=0}^{T-1} v_j(t), \right) \tag{1.3}$$

where $r_i = \log_2(1 + |h_{ii}|^2 \, \mathsf{PSD} \, / N_0)$. This is the problem of finding the optimal independent set. This cost is just the sum of the spectral efficiencies of the users weighted by the number of data symbols they send. We use a negative sign so as to justify the description of this metric as a *cost*, i.e. something we are trying to minimize. In the event that all direct gains are equal, r_j is independent of j and the problem reduces to finding the maximal independent set of $\mathcal{G}$.

To solve this problem efficiently, we start by defining

$$l_j^* \triangleq \max\{\max_i l'_{ij}, \max_i -l'_{ji}\}.$$

This is the length of the longest edge that connects a vertex at a time t, to a vertex belonging to user j for time $\leq t$. When all the l'_{ij} are positive, l_j^* simply represents the

longest edge stemming from user j. In the example of figure 1.1, $l_1^* = 3$, $l_2^* = 4$ and $l_3^* = 3$. When some of the l'_{ij} are negative, l_j^* represents the longest edge connecting user j to another user in the forward time direction. Thus the total amount of memory in the system is $\max_j l_j^*$. If this seems somewhat contrived, recall that although the interference graph is a directed graph, it need not be defined as such, as the effect of vertex $v_i(t)$ causing interference at vertex $v_j(t')$ is identical to the effect of vertex $v_j(t')$ causing interference at vertex $v_i(t)$. What matters for the dynamic programming formulation in this section, is not whether $v_i(t)$ is causing interference with $v_j(t')$ or vice versa, but whether $t > t'$, $t = t'$ or $t < t'$. In our algorithm we move through vertices in order of increasing time t. *The state of the system at time t is defined by those vertices at times $\leq t$ that are connected to vertices at times $\geq t$.*

More precisely, define the state vector at time t to be

$$\mathbf{s}(t) = \begin{pmatrix} v_1(t) \\ \vdots \\ v_1(t - l_1^*) \\ \vdots \\ \vdots \\ v_K(t) \\ \vdots \\ v_K(t - l_K^*) \end{pmatrix}. \tag{1.4}$$

This is the collection of all vertices at times $\leq t$, that interfere with, or are interfered with by vertices at times $\geq t$. Figure 1.3 illustrates which vertices are included in the state vector. As each $v_j(t)$ takes on one of two values, the state space consists of *at most* $2^{\sum_{j=1}^{K}(l_j^*+1)}$ possible states. Some states may be infeasible because two of their vertices are connected by an edge. Thus define the state space as the space of

all feasible states

$$\mathcal{S} = \left\{\mathbf{s}_1, \ldots, \mathbf{s}_{|\mathcal{S}|}\right\}$$

with each $\mathbf{s}_i \in \{0,1\}^{\sum_{j=1}^{K}(l_j^*+1)}$. Each state in $\mathcal{S}$ corresponds to an *independent set* in the subgraph made up of vertices in $\mathbf{s}(t)$. Thus there are typically far fewer than $2^{\sum_{j=1}^{K}(l_j^*+1)}$ states. A second example is given in figures 1.4 and 1.5. In this example there are a total of 28 states as shown in figure 1.5.

For notational convenience we label the elements of $\mathbf{s}_i$ as such

$$\mathbf{s}_i = \begin{pmatrix} s_i^{(1,0)} \\ \vdots \\ s_i^{(1,l_1^*)} \\ \vdots \\ \vdots \\ s_i^{(K,0)} \\ \vdots \\ s_i^{(K,t-l_K^*)} \end{pmatrix}.$$

Denote the set of feasible state transitions from $\mathbf{a} \in \mathcal{S}$ to $\mathbf{b} \in \mathcal{S}$ by

$$\mathcal{F} = \left\{(\mathbf{a}, \mathbf{b}) : b^{(j,k+1)} = a^{(j,k)}, \text{ for } j = 1, \ldots, K \text{ and } k = 0, \ldots, l_j^* - 1\right\}$$

For the example of figures 1.4 and 1.5 the set of feasible state transitions is

$$\mathcal{S} = \{(\mathbf{s}_1, \mathbf{s}_2), (\mathbf{s}_1, \mathbf{s}_8), (\mathbf{s}_1, \mathbf{s}_{11}), (\mathbf{s}_2, \mathbf{s}_3), \ldots\}$$

With the state space clearly defined, it is straightforward to derive the actual algorithm, which is akin to the Viterbi algorithm. It begins by initializing the costs

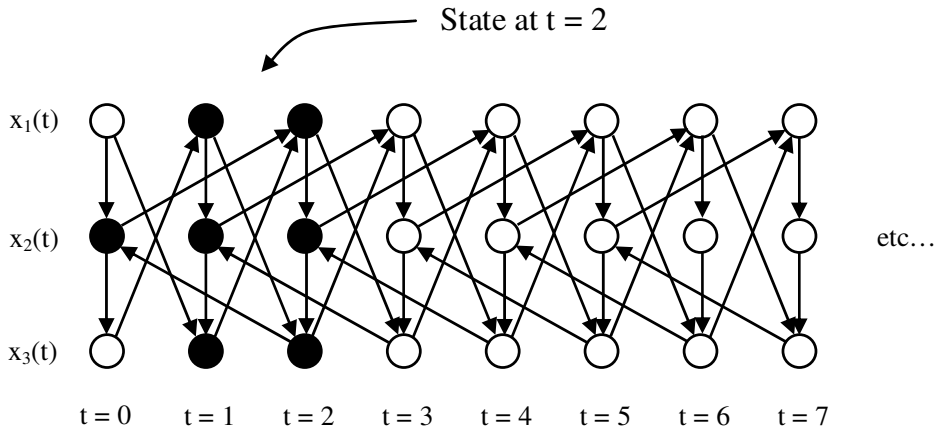

Figure 1.4: A LOS interference channel with normalized cross delays $l'_{21} = 0$, $l'_{31} = 1$, $l'_{12} = 2$, $l'_{32} = 0$, $l'_{13} = 1$ and $l'_{23} = -2$. The state at time $t = 2$ is a function of the shaded vertices.

to zero, that is

$$c_{\mathbf{s}_j}(0) = 0,$$

for all $\mathbf{s}_j \in \mathcal{S}$. Each iteration of the algorithm involves finding the minimum cost path entering each state. At times $t = 1, \ldots, T$ compute

$$\mathbf{s}_{i^*}(t, \mathbf{s}_j) = \arg \min_{\substack{\mathbf{s}_i \in \mathcal{S} \\ (\mathbf{s}_i, \mathbf{s}_j) \in \mathcal{F}}} c_{\mathbf{s}_i}(t-1),$$

for each $\mathbf{s}_j \in \mathcal{S}$, which is the minimum cost state at time $t-1$ from which we can transition into state $\mathbf{s}_j$ at time t. Then compute

$$c_{\mathbf{s}_j}(t) = c_{\mathbf{s}_{i^*}(t,\mathbf{s}_j)}(t-1) - \sum_{k=1}^{K} r_k s_j^{(k,0)},$$

for each $\mathbf{s}_j \in \mathcal{S}$, which is the minimum cost of a path that ends up at state $\mathbf{s}_j$ at time

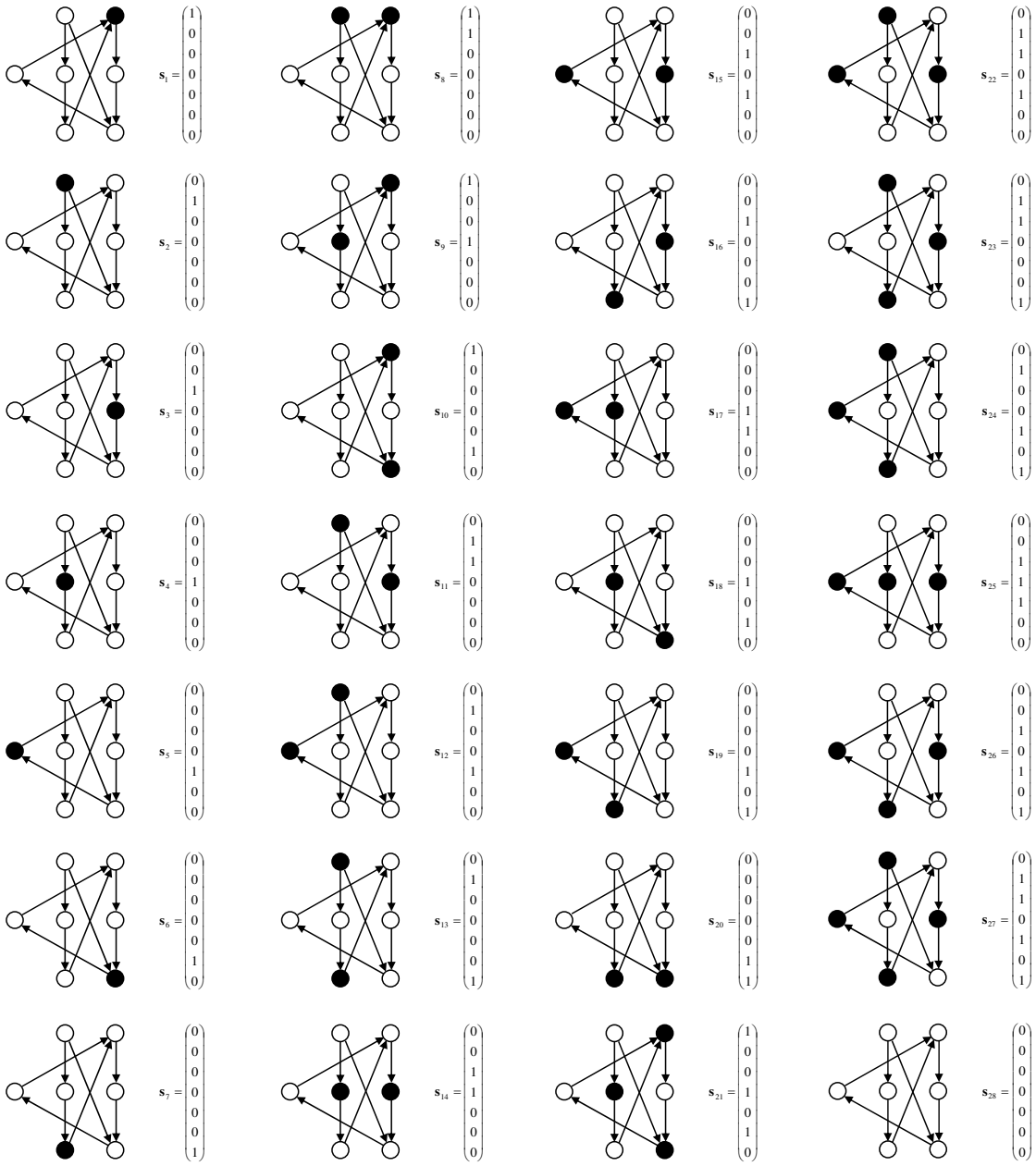

Figure 1.5: An illustration of the entire state space $\mathcal{S}$ for the example of figure 1.4. For each state, both the state vector is given and the corresponding independent set shaded.

t. When time $t = T$ is finally reached, compute

$$\mathbf{s}^*(T) = \arg\min_{\mathbf{s}_i \in \mathcal{S}} c_{\mathbf{s}_i}(T),$$

which is the optimal termination state. The optimal independent set is then found by working backwards. Start by setting the Tth column of vertices $v_1(T), \ldots, v_K(T)$ according to $\mathbf{s}^*(T)$. That is, set $v_j(T) = [s_i^*(T)]^{(j,0)}$ for $j = 1, \ldots, K$. Then set the $T-1$th column according to $\mathbf{s}_{i^*}(T, \mathbf{s}^*(T))$, that is, set $v_j(T-1) = [s_i^*(T, \mathbf{s}^*(T))]^{(j,0)}$ for $j = 1, \ldots, K$. Continue by setting $v_j(T-2) = [s_i^*(T-1, s_i^*(T, \mathbf{s}^*(T)))]^{(j,0)}$, etc...

We now briefly examine the complexity of this algorithm. As the state space consists of all independent sets of a subgraph defined by $2^{\sum_{j=1}^{K}(l_j^*+1)}$ vertices, given a set of delays l'_{ij}, it takes $O(2^{\sum_{j=1}^{K}(l_j^*+1)})$ time steps to enumerate. Once this is done, the algorithm takes $O(T|\mathcal{S}|)$ time steps to solve problem (1.3). Roughly speaking, $l'_{ij} = O(L)$, and $|\mathcal{S}| = O(LK \log LK)$. Thus the algorithm takes

$$O(TLK \log LK) + O(2^{LK})$$

time steps to compute the optimal independent set.

As the state space defined in equation 1.4 is finite, for large T the optimal independent set will have a periodic form with period less than or equal to the number of states $|\mathcal{S}|$. Thus, if there is no restriction on how large T can be, once the period of the maximal independent set is found, we can simply set T equal to it, without compromising optimality. In this case, the entire problem can be solved in

$$O(LK \log LK 2^{LK \log LK}) + O\left(2^{LK}\right) = O\left((LK)^{LK+1} \log LK\right)$$

time steps.

1.4.2 Bandwidth scaling

Theorem 1.3.1 shows that if the bandwidth scales sufficiently quickly with K, the spectral efficiency per user can be made to vanish arbitrarily slowly. A natural question to ask is whether it is *necessary* for the bandwidth to scale with K, in order for this desirable property to hold. The following converse result establishes that this is indeed the case.

Theorem 1.4.2. *If the bandwidth scales sufficiently slowly with K such that*

$$\lim_{K\to\infty} \frac{\log W}{\log \frac{K}{\log K}} = 0$$

then

$$\lim_{K\to\infty} \frac{\log \alpha(\mathcal{G})/T}{\log K} = 0 \tag{1.5}$$

with probability one.

As the total spectral efficiency

$$\sum_{i=1}^{K} R_i \leq \frac{\alpha(\mathcal{G})}{T} \log_2 \left(1 + \max_i |h_{ii}|^2 \frac{\mathsf{PSD}}{N_0}\right)$$

theorem 1.4.2 implies

$$\lim_{K\to\infty} \frac{\log \left(\sum_{i=1}^{K} R_i\right)}{\log K} = 0,$$

which is equivalent to $\lim_{K\to\infty} R_i = 0$ for almost all users $i \in \{1, \ldots, K\}$.

Roughly speaking the above result says that if the bandwidth scales slower than $O(K/\log K)$, then the spectral efficiency resulting from any feasible transmit pattern will vanish as $K \to \infty$. Note there is a gap between this converse result and the achievability result of theorem 1.3.1. Theorem 1.3.1 demonstrates that it is sufficient for the bandwidth to scale like $O((2K(K-1))^{K(K-1)})$, but theorem 1.4.2 shows that it

is necessary for the bandwidth to scale only as fast as $O(K/\log K)$. This establishes that the slowest possible bandwidth scaling lies somewhere between $O(K/\log K)$ and $O((2K(K-1))^{K(K-1)})$. It is unclear, which if any of these bounds is tight.

Proof. Remove those edges that connect vertices of different time slots in the interference graph, $(v_i(t), v_j(t'))$ for $t' \neq t$. This provides an upper bound on the independence number. Now consider a single column $\mathcal{V}(t) = \{v_1(t), \ldots, v_K(t)\}$ of this graph in isolation. For any pair of vertices in $\mathcal{V}(t)$, there exists an edge connecting them independently with probability $1-(1-1/L)^2$ (probability $1/L$ for each of the two possible directions). Thus the graph consisting of vertices $\mathcal{V}(t)$ and the random subset of edges connecting them, is precisely the Erdős-Rényi graph $\mathcal{G}_{K,1-(1-1/L)^2}$. A well known result (see for example [4]) is that

$$\lim_{n\to\infty} \frac{\alpha(\mathcal{G}_{n,p})}{\log n} = \frac{2}{\log(1/(1-p))}$$

with probability one. Hence the independence number of $\mathcal{G}_{K,2/L}$ satisfies

$$\begin{aligned}\lim_{n\to\infty} \frac{\alpha(\mathcal{G}_{K,2/L})}{\log K} &= \frac{2}{\log(1/(1-1/L)^2)} \\ &\leq L.\end{aligned}$$

As L is directly proportional to W, if $\lim_{K\to\infty} \log W/\log \frac{K}{\log K} = 0$ then the same limit applies for L and

$$\lim_{K\to\infty} \frac{\log \alpha(\mathcal{G}_{K,2/L})}{\log K} = 0.$$

Now as the independence number of the interference graph satisfies $\alpha(\mathcal{G}) \leq T\alpha(\mathcal{G}_{K,2/L})$, equation (1.5) follows. □

1.4.3 When is the maximal independent set maximal?

We now turn to the problem of analysis. Ideally we would like a simple characterization of the size of the maximal independent set in terms of the parameters of the system, K, T, and the normalized cross-delays l'_{ij}. It is unclear if such a characterization exists. Instead we present two results. The first characterizes when the independence number is equal to its maximum possible value, and shows how the maximal independent set can be found almost instantly in this event. The second, which is theorem 1.3.1, demonstrates that surprisingly large independent sets exist on average, when both the number of users and the bandwidth are sufficiently high. In this section we present the former result, in the next section we present the latter. What we will be revealed in this section is that the problem of determining whether or not the independence number is equal to its maximum possible value, is a group theoretic one.

We assume in this section that the direct gains are all equal so that the optimal independent set is equivalent to the maximal independent set. Owing to the absence of some edges, the boundary of the interference graph has a slightly different structure than it's interior. In order to circumvent this problem, we let $T \to \infty$ so that these boundary effects are negligible.

Definition 1.4.3. *The independence rate of sequence of interference graphs*

$$\mathcal{G}_{K,1}(\{l'_{ij}\}_{i\neq j}), \mathcal{G}_{K,2}(\{l'_{ij}\}_{i\neq j}), \ldots$$

is

$$\mathsf{IR}(\mathcal{G}_K(\{l'_{ij}\}_{i\neq j})) \triangleq \lim_{T\to\infty} \frac{\alpha(\mathcal{G}_{K,T}(\{l'_{ij}\}_{i\neq j}))}{T}.$$

We write $\mathsf{IR}(\mathcal{G}_K)$ for short. Start with the following observation.

Lemma 1.4.4. *For any number of users K and any channel $\{l'_{ij}\}_{i\neq j}$*

$$\mathsf{IR}(\mathcal{G}_K) \leq \frac{K}{2}.$$

This means that for large T we can only include at most half the vertices of the interference graph in any feasible transmit pattern. We now ask, when is the independence rate *exactly equal* to $K/2$? The following result succinctly answers this question for $K = 3$. Define

$$\begin{aligned} l &\triangleq l'_{31} + l'_{13} + l'_{32} + l'_{21} + l'_{12} + l'_{23} \\ l_1 &\triangleq l'_{13} + l'_{32} + l'_{21} \\ l_2 &\triangleq l'_{21} + l'_{12} \\ l_3 &\triangleq l'_{31} + l'_{13}. \end{aligned}$$

If $l_i \neq 0$, define γ_i to be the exponent of 2 in the prime factorization of l_i, that is $l_i = 2^{\gamma_i}\beta_i$ where β_i represents the rest of the prime factorization. If $l_i = 0$ then define $\gamma_i = \infty$. Similarly if $l \neq 0$, define γ to be the exponent of 2 in the prime factorization l, i.e. $l = 2^{\gamma}\beta$. If $l = 0$ then define $\gamma = \infty$.

Theorem 1.4.5. $\mathsf{IR}(\mathcal{G}_3) = 3/2$ *if and only if* $\gamma_1 < \gamma_2$, $\gamma_1 < \gamma_3$ *and* $\gamma_1 < \gamma$, *in which case there are exactly* $2^{\gcd(l_1, l_2/2, l_3/2, l/2)}$ *feasible transmit patterns achieving it.*

To clarify, if for example both $\gamma_1 = \infty$ and $\gamma_2 = \infty$, then the above conditions are not satisfied and $\mathsf{IR}(\mathcal{G}) < 3/2$. This theorem provides a necessary and sufficient condition such that all users can transmit half the time without interfering with one another. The most probable way this condition can be met is if l_1 is an odd number, and l, l_2 and l_3 are all even numbers. Each of these events roughly occurs independently with probability $1/2$, hence the probability all four occur simultaneously is

$1/16$. Thus with probability $\gtrsim 1/16$ there exists a feasible transmit pattern enabling all users to transmit half the time without interfering with one another. There are of course other ways in which our condition can be met, for example, if l_1 is even, but not a multiple of 4, and l, l_2 and l_3 are all multiples of 4, however this, and all other configurations satisfying the condition of theorem 1.4.5 likely occur with probability much less than $1/16$. The proof of theorem 1.4.5 is given in the appendix.

Example 1.4.6. *For the channel in figure 1.11, we have* $l = 2$ *and* $l_1 = 1, l_2 = 2, l_3 = 2$. *This means* $\gamma = 1, \gamma_1 = 0, \gamma_2 = 1, \gamma_3 = 1$, *so a feasible transmit pattern achieving independence number* $3/2$ *exists. As* $\gcd(l_1, l_2/2, l_3/2, l/2) = 1$ *there are only two feasible transmit patterns: the first is shown in the figure as a sequence of shaded vertices, the second is obtained by complementing the transmit pattern, i.e. unshading the shaded vertices, and shading the unshaded ones.*

How does theorem 1.4.5 generalize for an arbitrary number of users, K? Define a *cycle* on the interference graph to be the indices of a tuple of edges with connecting vertices, that start and end on the same row. For example $((1,2),(2,3),(3,1))$ and $((3,2),(2,3))$ are examples of cycles for $K = 3$. The *length* of a cycle is the sum of the normalized cross-delays associated with it. For example, the cycle $((1,2),(2,3),(3,1))$ has length $l'_{12} + l'_{23} + l'_{31}$.

Define the set of cycles containing an even number of terms as

$$\mathcal{Y}_e = \{((i_1,i_2),(i_2,i_3),\ldots,(i_{2n},i_1)) : i_1 \neq i_2 \neq \cdots \neq i_{2n} \text{ and } i_j \in \{1,\ldots,K\}\},$$

and the set of cycles containing an odd number of terms as

$$\mathcal{Y}_o = \{((i_1,i_2),(i_2,i_3),\ldots,(i_{2n+1},i_1)) : i_1 \neq i_2 \neq \cdots \neq i_{2n+1} \text{ and } i_j \in \{1,\ldots,K\}\}.$$

Then we claim it can be shown that

Claim 1.4.7. $\mathsf{IR}(\mathcal{G}_K) = K/2$ *if and only if the exponents of 2 in the prime factorizations of the lengths of all cycles containing an odd number of terms, are the same, and this exponent is strictly less than the exponent of 2 in the prime factorization of the length of every cycle containing an even number of terms. That is, the exponent of 2 in the prime factorization of*

$$\sum_{(i,j)\in Y_o} l'_{ij},$$

is the same for all $Y_o \in \mathcal{Y}_o$*, and this value is strictly less than the exponent of 2 in the prime factorization of*

$$\sum_{(i,j)\in Y_e} l'_{ij},$$

for any $Y_e \in \mathcal{Y}_e$*.*

1.5 Achieving Non-Vanishing Spectral Efficiency

We now prove theorem 1.3.1 by presenting a construction with expected spectral efficiency that can be made to vanish arbitrarily slowly as $K \to \infty$. First, a high-level overview of the proof. The idea is to construct a transmit pattern that has close to $O(1)$ independence rate as $K \to \infty$. At the heart of the transmit pattern is a *generalized arithmetic progression*. If the bandwidth scales appropriately with the number of users then this progression will have desirable interference alignment properties, but care has to be taken in constructing a transmit pattern out of it. In particular, the progression will be very sparse, meaning that many identical versions of this progression must be interleaved, each with a different timing offset. The trick to making the analysis work is to use a randomization argument to show that a good set of offsets exists.

Proof. (of Theorem 1.3.1) First some notation that will be used throughout the proof. Let

$$N \triangleq K(K-1)$$

and

$$A \triangleq \frac{L}{N^{N+\epsilon}}.$$

We use $\oplus$ to denote addition modulo L. Let

$$\mathcal{T} \triangleq \left\{ \bigoplus_{1 \le i \ne j \le K} \alpha_{ij} l_{ij} : \{\alpha_{ij}\}_{i \ne j} \in \{0, \ldots, N-1\}^N \right\}.$$

This is the set of all linear combinations of the cross-delays (not normalized) with integer coefficients ranging from 0 to N. Define

$$\mathcal{S} \triangleq \bigcup_{a=1}^{A} (m_a \oplus \mathcal{T})$$

See figure 1.6 for an illustration. Each user transmits one data symbol at each time slot in the set

$$\mathcal{X} \triangleq \bigcup_{k=0}^{\infty} (\mathcal{S} + kL).$$

The above construction corresponds to concatenating data blocks $\mathcal{S}$ of length L. The modulo L addition used in constructing $\mathcal{S}$ and $\mathcal{T}$, ensures a seamless transition at the block boundaries. This is illustrated in figure 1.7. The construction is defined in this seemingly convoluted way in order to make the analysis simple and elegant. However there is an easier way of conceptualizing this construction: take multiple copies of the generalized arithmetic progression $\left\{ \sum_{1 \le i \ne j \le K} \alpha_{ij} l_{ij} : \{\alpha_{ij}\}_{i \ne j} \in \{0, \ldots, N-1\}^N \right\}$, and throw them down on the infinite time axis with offsets $m_1, \ldots, m_A, L+m_1, \ldots, L+m_A, 2L+m_1, \ldots, 2L+m_A, \ldots$. Although this construction is periodic with period

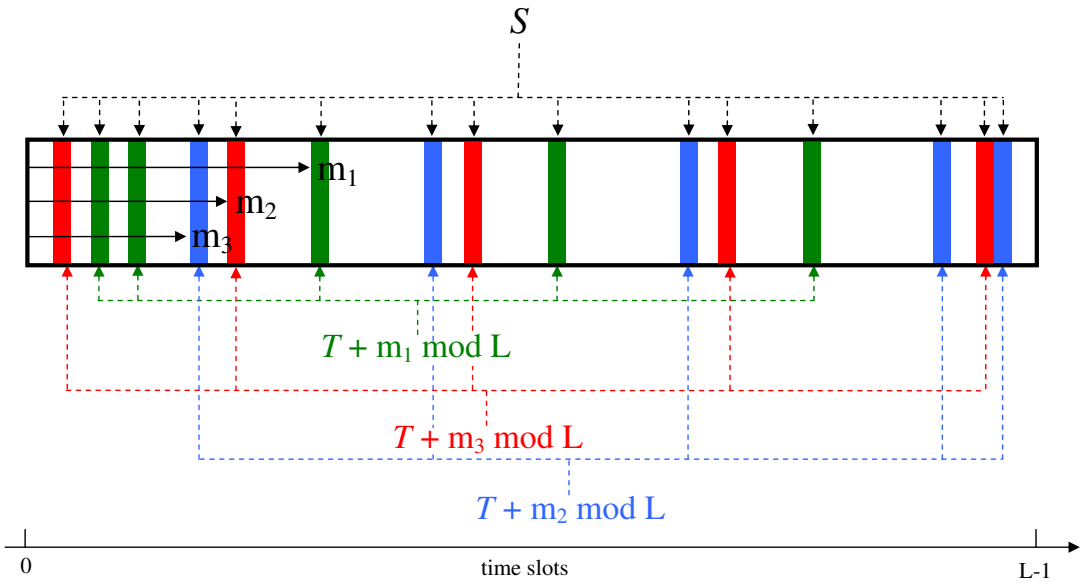

Figure 1.6: The construction $\mathcal{S}$ is formed by interleaving a sufficient number of generalized arithmetic progressions $\mathcal{T}$ with random offsets m_i. The colored bars indicate time slots during which data symbols are sent.

L, locally, the offsets of these progressions will appear as a Poisson process with intensity $A/L = 1/N^{N+\epsilon}$. As there are N^N points in each progression, the density of points in $\mathcal{X}$ will be $1/N^\epsilon$ and hence the spectral efficiency will go to zero with K like $1/(K(K-1))^\epsilon$.

We will show that there exists a choice of

$$(m_1, \ldots, m_A) \in \{0, \ldots, L-1\}^A$$

such that the expected spectral efficiency of this scheme approaches (1.2) as $K \to \infty$. More specifically, we show that for the above construction, at each receiver the expected fraction of time slots containing a data symbol but no interference is large. Each such data symbol is then able to convey $\log_2(1 + |h_{ii}|^2 \,\mathsf{PSD}\, / N_0)$ bps/Hz of information and the expected spectral efficiency achieved by the scheme for user i is the fraction of such time slots multiplied by $\log_2(1 + \mathsf{PSD}\, / N_0)$.

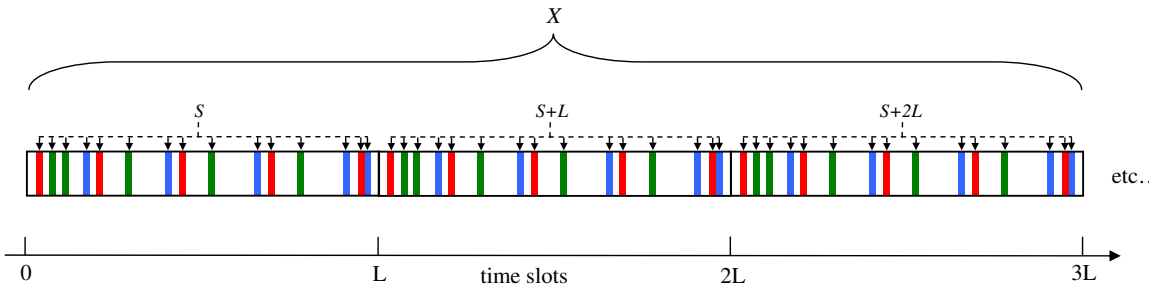

Figure 1.7: The construction $\mathcal{X}$ is formed by concatenating blocks of $\mathcal{S}$. The modulo L structure of $\mathcal{S}$ ensures a seamless transition from block to block.

Since our construction $\mathcal{X}$ consists of a concatenation of identical blocks of length L, we analyze its performance over a single block extending from time slot 0 to $L-1$. At receiver i the set of time slots containing interference is

$$\mathcal{F}_i \triangleq \bigcup_{j=1, j\neq i}^{K} (\mathcal{S} \oplus l_{ij}) \,. \tag{1.6}$$

Denote the number of time slots at receiver i, that contain a data symbol from transmitter i, but no interference by $S_i \triangleq |\{t \in (\mathcal{S} \oplus l_{ii}) \backslash \mathcal{F}_i\}|$. Then conditioning on the cross delays we have

$$\mathbb{E}S_i = \frac{1}{L^{K(K-1)}} \sum_{\{l_{ij}\}_{i\neq j}} \mathbb{E}_{\{l_{ii}\}_i}[S_i | \{l_{ij}\}_{i\neq j}]. \tag{1.7}$$

Define

$$s(k) \triangleq \begin{cases} 1, & \text{if } k \in \mathcal{S} \\ 0, & \text{otherwise.} \end{cases}$$

That is, $s(k) = 1$ if a transmission takes place at time slot k, and zero otherwise. Similarly define

$$f_i(k) \triangleq \begin{cases} 1, & \text{if } k \in \mathcal{F}_i \\ 0, & \text{otherwise.} \end{cases}$$

That is, $f_i(k) = 1$ if there is interference during time slot k at receiver i and zero otherwise. Conditioned on the cross delays, S_i is the correlation function between the set of transmit times $\mathcal{S}$ and the set of interference free times $\mathcal{F}_i^c$, evaluated at an offset of l_{ii}, specifically

$$S_i(l_{ii}) = \sum_{k=0}^{L-1} s(k \oplus l_{ii})(1 - f_i(k))$$

Thus

$$\begin{aligned}
E_{\{l_{ii}\}_i}[S_i|\{l_{ij}\}_{i\neq j}] &= \frac{1}{L}\sum_{l_{ii}=0}^{L-1} S_i(l_{ii}) \\
&= \frac{1}{L}\sum_{l_{ii}=0}^{L-1}\sum_{k=0}^{L-1} s(k \oplus l_{ii})(1 - f_i(k)) \\
&= \frac{1}{L}\sum_{k=0}^{L-1}(1 - f_i(k))\sum_{l_{ii}=0}^{L-1} s(k \oplus l_{ii}) \\
&= \frac{1}{L}\sum_{k=0}^{L-1}(1 - f_i(k))\sum_{l_{ii}=0}^{L-1} s(l_{ii}) \\
&= \frac{1}{L}\sum_{k=0}^{L-1}(1 - f_i(k))|\mathcal{S}| \\
&= |\mathcal{S}|\left(1 - \frac{|\mathcal{F}_i|}{L}\right)
\end{aligned}$$

where in the above sequence of equations we have used the identities $|\mathcal{S}| \equiv \sum_{k=0}^{L-1} s(k)$ and $|\mathcal{F}_i| \equiv \sum_{k=0}^{L-1} f_i(k)$. Substituting back into equation (1.7) we find the fraction of time slots at receiver i containing data but no interference is

$$\frac{\mathbb{E}S_i}{L} = \frac{1}{L^{K(K-1)}}\sum_{\{l_{ij}\}_{i\neq j}} \frac{|\mathcal{S}|}{L}\left(1 - \frac{|\mathcal{F}_i|}{L}\right). \tag{1.8}$$

The above expression makes intuitive sense as if we uniformly select a time slot at

random from $\{0, \ldots, L-1\}$, then conditioned on the $\{l_{ij}\}_{i \neq j}$, the quantity $|\mathcal{S}|/L$ is the probability this time slot contains a data symbol, and $1 - |\mathcal{F}_i|/L$ is the probability it does not contain an interference symbol. We now compute appropriate bounds on the terms $|\mathcal{S}|$ and $|\mathcal{F}_i|$. From equation (1.6) we have

$$\begin{aligned}
\mathcal{F}_i &= \bigcup_{j \neq i} (\mathcal{S} \oplus l_{ij}) \\
&= \bigcup_{j \neq i} \left(\left[\bigcup_{a=1}^{A} (m_a \oplus \mathcal{T}) \right] \oplus l_{ij} \right) \\
&= \bigcup_{a=1}^{A} \left[\bigcup_{j \neq i} (\mathcal{T} \oplus l_{ij}) \right] \oplus m_a
\end{aligned}$$

But

$$\bigcup_{j \neq i} (\mathcal{T} \oplus l_{ij}) \subset \left\{ \bigoplus_{1 \leq i \neq j \leq K} \alpha_{ij} l_{ij} : \{\alpha_{ij}\}_{i \neq j} \in \{0, \ldots, N\}^N \right\},$$

and this set has at most $(N+1)^N$ elements. This is the interference alignment property. Hence

$$\begin{aligned}
\frac{|\mathcal{F}_i|}{L} &\leq A \frac{1}{L} \left| \bigcup_{j \neq i} (\mathcal{T} \oplus l_{ij}) \right| \\
&\leq \frac{A(N+1)^N}{L} \\
&< \frac{(N+1)^N}{N^{N+\epsilon}} \\
&= N^{-\epsilon} \left(1 + \frac{1}{N} \right)^N \\
&< e N^{-\epsilon}.
\end{aligned}$$

We now bound $|\mathcal{S}|$. We first show that $|\mathcal{T}| = N^N$ almost surely as $N \to \infty$. In order to have $|\mathcal{T}| < N^N$, there must exist two sets of coefficients $\{\alpha_{ij}\}_{i \neq j} \neq \{\alpha_{ij}\}'_{i \neq j}$

both elements of $\{0, \ldots, N-1\}^N$, satisfying

$$\bigoplus_{i \neq j} \alpha_{ij} l_{ij} = \bigoplus_{i \neq j} \alpha'_{ij} l_{ij}.$$

This is equivalent to requiring there to exist some $\{\overline{\alpha}_{ij}\}_{i \neq j} \in \{-N+1, \ldots, N-1\}^N \backslash \mathbf{0}$ satisfying

$$\bigoplus_{i \neq j} \overline{\alpha}_{ij} l_{ij} = 0.$$

Using the union bound we have

$$\begin{aligned}
\Pr\left(|\mathcal{T}| < N^N\right) &= \Pr\left(\exists \{\overline{\alpha}_{ij}\}_{i \neq j} \in \{-N+1, \ldots, N-1\}^N \backslash \mathbf{0} \text{ s.t. } \bigoplus_{i \neq j} \overline{\alpha}_{ij} l_{ij} = 0\right) \\
&\leq \sum_{\{\overline{\alpha}_{ij}\}_{i \neq j} \in \{-N+1, \ldots, N-1\}^N} \Pr\left(\bigoplus_{i \neq j} \overline{\alpha}_{ij} l_{ij} = 0\right).
\end{aligned}$$

As conditioned on all cross delays other than l_{12}, there is at most one value of l_{12} that satisfies $\sum_{i \neq j} \overline{\alpha}_{ij} l_{ij} = 0$, and the cross delays are uniformly distributed over $\{0, \ldots, L-1\}$, we have

$$\begin{aligned}
\Pr\left(|\mathcal{T}| < N^N\right) &\leq \sum_{\{\overline{\alpha}_{ij}\}_{i \neq j} \in \{-N+1, \ldots, N-1\}^N} \frac{1}{L} \\
&= \frac{(2N)^N}{L} \\
&\leq \frac{(2N)^N}{(2N)^{N+\epsilon}} \\
&= (N)^{-\epsilon} \\
&\to 0
\end{aligned}$$

as $N \to \infty$ (or equivalently, as $K \to \infty$).

At this point it should start to become clear why it is that in this particular

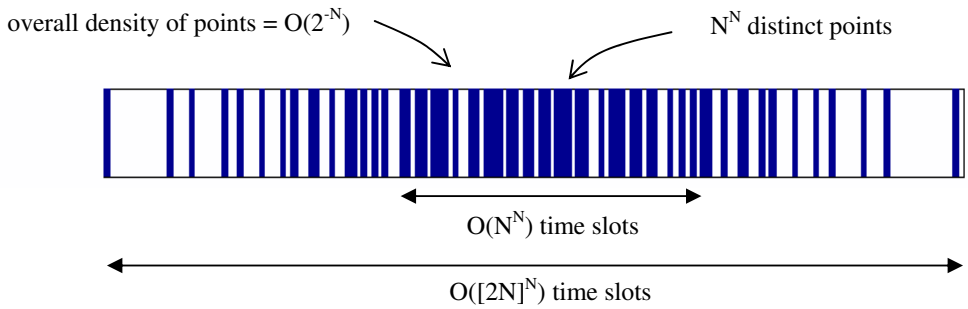

Figure 1.8: An illustration of the generalized arithmetic progression $\mathcal{T}$ without the modulo L wrap around. There are N^N points spread over $O((2N)^N)$ time slots, however almost all points are concentrated at the center in a width of $O(N^N)$. Hence the density of points is $O(2^{-N})$.

construction the bandwidth must scale like $(2N)^N$. From the above calculation we see that in order to make all the points in the generalized arithmetic progression $\mathcal{T}$ distinct, we require the l_{ij} to be large. How large? It may seem that as there are N^N integers in $\mathcal{T}$, the minimum being 0 and the maximum being roughly the same order as l_{ij}, we require $l_{ij} = O(N^N)$. However, the structure of the generalized arithmetic progression is such that the bulk of its points are concentrated around the center, such that we actually require at least $l_{ij} = O((2N)^N)$ to separate these center points out, as the above calculation shows. But such a large order of l_{ij} makes $\mathcal{T}$ very sparse, in fact if $l_{ij} = O((2N)^N)$ then $\mathcal{T}$'s density is a mere $O(2^{-N})$. So to fill in the gaps we interleave multiple sequences $\mathcal{T}$. How many? $O(2^N)$. In general if $l_{ij} = O(L)$ then we must interleave $O(L/N^N) = A$ sequences. This explanation is illustrated in figure 1.8

We now use a probabilistic argument to demonstrate the existence of a good choice of $(m_1, \ldots, m_A)$. Let $m_a \sim$ i.i.d. $U(\{0, \ldots, L-1\})$. Let

$$t(k) \triangleq \begin{cases} 1, & \text{if } k \in \mathcal{T} \\ 0, & \text{otherwise.} \end{cases}$$

and

$$t_a(k) \triangleq \begin{cases} 1, & \text{if } k \in m_a \oplus \mathcal{T} \\ 0, & \text{otherwise.} \end{cases}$$

Thus $t_a(k) = t(k \oplus m_a)$. Then we can write

$$s(k) = t_1(k) + t_2(k)(1 - t_1(k)) + t_3(k)(1 - t_2(k))(1 - t_1(k)) \\ + \cdots + t_A(k)(1 - t_{A-1}(k)) \times \cdots \times (1 - t_1(k)).$$

This expression says that $k \in \mathcal{S}$ if $k \in m_1 \oplus \mathcal{T}$, or if $k \notin m_1 \oplus \mathcal{T}$ but $k \in m_2 \oplus \mathcal{T}$, or if $k \notin m_1 \oplus \mathcal{T}$ and $k \notin m_2 \oplus \mathcal{T}$ but $k \in m_3 \oplus \mathcal{T}$, etc... We can write the above expression alternatively as

$$\begin{aligned} s(k) &= t_1(k) + (1 - t_1(k))(t_2(k) + (1 - t_2(k))(t_3(k) + \dots)) \\ &= t(k \oplus m_1) + (1 - t(k \oplus m_1))(t(k \oplus m_2) + (1 - t(k \oplus m_2))(t(k \oplus m_3) + \dots)) \end{aligned}$$

Then taking the expectation over the distribution of $m_1, \ldots, m_A$

$$
\begin{aligned}
\frac{\mathbb{E}|\mathcal{S}|}{L} &= \frac{1}{L}\mathbb{E}\sum_{k=0}^{L-1} s(n) \\
&= \frac{1}{L}\mathbb{E}\sum_{k=0}^{L-1} t(k\oplus m_1) + (1-t(k\oplus m_1))(t(k\oplus m_2) \\
&\qquad\qquad + (1-t(k\oplus m_2))(t(k\oplus m_3)+\ldots)) \\
&= \frac{1}{L^{A+1}}\sum_{m_A=0}^{L-1}\cdots\sum_{m_1=0}^{L-1}\sum_{k=0}^{L-1} t(k\oplus m_1) + (1-t(k\oplus m_1))(t(k\oplus m_2) \\
&\qquad\qquad + (1-t(k\oplus m_2))(t(k\oplus m_3)+\ldots)) \\
&= \frac{1}{L^{A+1}}\sum_{k=0}^{L-1}\sum_{m_A=0}^{L-1}\cdots\sum_{m_1=0}^{L-1} t(k\oplus m_1) + (1-t(k\oplus m_1))(t(k\oplus m_2) \\
&\qquad\qquad + (1-t(k\oplus m_2))(t(k\oplus m_3)+\ldots)) \\
&= \frac{1}{L^{A+1}}\sum_{k=0}^{L-1}\sum_{m_A=0}^{L-1}\cdots\sum_{m_2=0}^{L-1} |\mathcal{T}| + (L-|\mathcal{T}|)t(k\oplus m_2) \\
&\qquad\qquad + (L-|\mathcal{T}|)(1-t(k\oplus m_2))(t(k\oplus m_3)+\ldots)) \\
&= \frac{1}{L^{A+1}}\sum_{k=0}^{L-1}\sum_{m_A=0}^{L-1}\cdots\sum_{m_2=0}^{L-1} |\mathcal{T}| + |\mathcal{T}|(L-|\mathcal{T}|) \\
&\qquad\qquad + (L-|\mathcal{T}|)^2(t(k\oplus m_3)+\ldots)) \\
&\qquad\qquad \vdots \\
&= \frac{|\mathcal{T}|}{L}\sum_{a=0}^{A-1}\left(1-\frac{|\mathcal{T}|}{L}\right)^a \\
&= 1-\left(1-\frac{|\mathcal{T}|}{L}\right)^A \\
&\to 1-\left(1-\frac{N^N}{L}\right)^{\frac{L}{N^{N+\epsilon}}} \qquad \text{a.s.} \\
&\to 1-e^{-\frac{N^N}{L}\frac{L}{N^{N+\epsilon}}} \\
&\to N^{-\epsilon}.
\end{aligned}
$$

Substituting back into equation (1.8)

$$\begin{aligned}\frac{\mathbb{E}S_i}{L} &= \frac{1}{L^{K(K-1)}} \sum_{\{l_{ij}\}_{i\neq j}} N^{-\epsilon}\left(1 - eN^{-\epsilon}\right) \\ &= N^{-\epsilon}\left(1 - eN^{-\epsilon}\right) \\ &\to N^{-\epsilon}\end{aligned}$$

as $N \to \infty$ (or equivalently $K \to \infty$). As each data symbol that is received without interference is capable of reliably communicating $\log_2(1 + |h_{ii}|^2 \mathsf{PSD}/\mathsf{N_0})$ bps/Hz, the expected spectral efficiency of each user i goes to

$$\frac{1}{(K(K-1))^{\epsilon}} \log_2\left(1 + |h_{ii}|^2 \mathsf{PSD}/\mathsf{N_0}\right)$$

as $K \to \infty$.

□

The proof of theorem 1.3.2 is a straightforward extension of the previous.

Proof. (of Theorem 1.3.2) If each receiver i treats physical paths $2, 3, \ldots, D$ from transmitter i as interference, then the received signals in the K user D path interference channel are statistically identical to those of the DK-user LOS interference channel. Thus the achievability result of theorem 1.3.1 carries over to the D path channel with K replaced by DK, and $|h_{ii}|^2$ replaced by $\max_{d\in\{1,\ldots,D\}} |h_{ii,d}|^2$. □

1.6 Frequency Domain Interpretation

In this section we reconcile the time domain version of interference alignment presented in this paper, and the frequency domain results of [5]. Specifically we show

how the three-user construction of [5] has a simple time domain structure for the LOS interference channel.

To begin, we need to transform the LOS model into the frequency domain. For this we use an OFDM architecture summarized in figure 1.9. Transmitter j has a stream of complex data symbols to send $\{x_j[0], x_j[1], \dots\}$ to receiver i. These are broken up into blocks of length n. Consider a single block denoted $\mathbf{x} = [x_j[0], \dots, x_j[n-1]]^T$. To send this block the transmitter computes the M-length vector $\overline{\mathbf{x}}_j = \mathbf{V}_j \mathbf{x}_j$, where $\mathbf{V}_j \in \mathbb{C}^{M \times n}$ is an encoding matrix to be specified later. Let $l_{\max} \triangleq \max_{i,j} l_{ij}$. To send $\overline{\mathbf{x}}_j$, tx j computes its IDFT and appends a cyclic prefix of length $l_{\max}$. Each receiver removes the cyclic prefix and computes the DFT. Specifically

$$\tilde{\mathbf{x}}_j = \begin{pmatrix} \mathbf{0}_{l_{\max} \times (M - l_{\max})} & \mathbf{I}_{l_{\max} \times l_{\max}} \\ & \mathbf{I}_{M \times M} \end{pmatrix} \mathbf{F}^*_{M \times M} \overline{\mathbf{x}}_j$$

and

$$\mathbf{y}_j = \mathbf{F}_{M \times M} \begin{pmatrix} \mathbf{0}_{M \times l_{\max}} & \mathbf{I}_{M \times M} \end{pmatrix} \tilde{\mathbf{y}}_j$$

where $\mathbf{F}_{M \times M}$ is the $M \times M$ DFT matrix,

$$\mathbf{F}_{M \times M} = \frac{1}{\sqrt{M}} \begin{pmatrix} 1 & 1 & 1 & \cdots & 1 \\ 1 & e^{j2\pi/M} & e^{j2\pi \cdot 2/M} & \dots & e^{j2\pi \cdot (n-1)/M} \\ 1 & e^{j2\pi \cdot 2/M} & e^{j4\pi \cdot (n-1)\theta} & \dots & e^{j2\pi \cdot 2(n-1)/M} \\ \vdots & \vdots & \vdots & \ddots & \vdots \\ 1 & e^{j2\pi \cdot (M-1)/M} & e^{j2\pi \cdot 2(M-1)\theta} & \dots & e^{j2\pi \cdot (M-1)(n-1)/M} \end{pmatrix}.$$

The result is a length M sequence

$$y_i[k] = \sum_{j=1}^{K} h_{ij} e^{-j2\pi(f_c \tau_{ij} + k l_{ij}/M)} \overline{x}_j[k] + z_i[k]$$

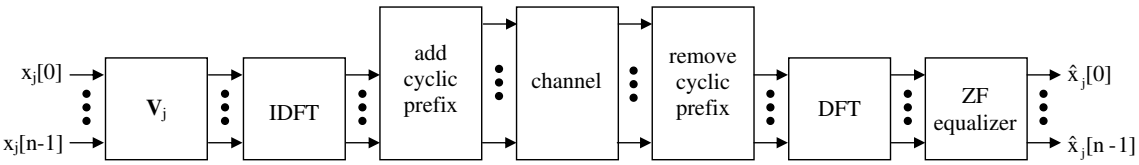

Figure 1.9: Illustration of the OFDM architecture used to reconcile the time and frequency domain versions of interference alignment.

for $k = 0, \ldots, M-1$. Let $\theta_{ij} \triangleq l_{ij}/M$. Then in matrix form

$$\mathbf{y}_i = \sum_{j=1}^{K} \mathbf{H}_{ij}\mathbf{V}_j\mathbf{x}_j + \mathbf{z}_i$$

where the link matrices are

$$\mathbf{H}_{ij} = h_{ij}e^{-j2\pi f_c \tau_{ij}} \begin{pmatrix} 1 & & & & \\ & e^{-j2\pi\cdot\theta_{ij}} & & & \\ & & e^{-j2\pi\cdot 2\theta_{ij}} & & \\ & & & \ddots & \\ & & & & e^{-j2\pi\cdot(M-1)\theta_{ij}} \end{pmatrix}. \qquad (1.9)$$

Choose W sufficiently large such that the l_{ij} are distinct. Note that M needs to be much larger than $l_{\max}$ in order for the overhead from the cyclic prefix to be small. Also, M must not have any of the l_{ij} as divisors, else the channel matrices will lose rank. Let $\overline{\mathbf{H}} \triangleq h_{ij}^{-1}e^{j2\pi f_c\tau_{ij}}\mathbf{H}$ and $\mathbf{T} \triangleq \overline{\mathbf{H}}_{12}\overline{\mathbf{H}}_{21}^{-1}\overline{\mathbf{H}}_{23}\overline{\mathbf{H}}_{32}^{-1}\overline{\mathbf{H}}_{31}\overline{\mathbf{H}}_{13}^{-1}$. Let $\mathbf{w} = [1 \ \cdots \ 1]^T$. Choose the encoding matrices as follows

$$\mathbf{V}_1 = \overline{\mathbf{H}}_{31}^{-1}\overline{\mathbf{H}}_{32}\mathbf{T}^2\mathbf{V}$$

$$\mathbf{V}_2 = \mathbf{T}\mathbf{V}$$

$$\mathbf{V}_3 = \overline{\mathbf{H}}_{13}^{-1}\overline{\mathbf{H}}_{12}\mathbf{V}$$

where

$$\mathbf{V} = [\mathbf{w}\ \mathbf{T}\mathbf{w}\ \mathbf{T}^2\mathbf{w}\ \cdots\ \mathbf{T}^{n-1}\mathbf{w}]$$

and let

$$n = (M-1)/2.$$

where M will be chosen to be an odd number. This is the three user construction of [**?**], but note the channel matrices $\mathbf{H}_{ij}$ do not consist of M independently faded tones. Rather, all tones are derived from a single parameter l_{ij}. Define

$$\theta = \theta_{12} - \theta_{21} + \theta_{23} - \theta_{32} + \theta_{31} - \theta_{13}$$
$$l = l_{12} - l_{21} + l_{23} - l_{32} + l_{31} - l_{13}$$

Then

$$\mathbf{V} = \frac{1}{\sqrt{M}} \begin{pmatrix} 1 & 1 & 1 & \cdots & 1 \\ 1 & e^{j2\pi\cdot\theta} & e^{j2\pi\cdot 2\theta} & \cdots & e^{j2\pi\cdot(n-1)\theta} \\ 1 & e^{j2\pi\cdot 2\theta} & e^{j2\pi\cdot 4\theta} & \cdots & e^{j2\pi\cdot 2(n-1)\theta} \\ \vdots & \vdots & \vdots & \ddots & \vdots \\ 1 & e^{j2\pi\cdot(M-1)\theta} & e^{j2\pi\cdot 2(M-1)\theta} & \cdots & e^{j2\pi\cdot(M-1)(n-1)\theta} \end{pmatrix}. \tag{1.10}$$

Lemma 1.6.1. *If M is prime the columns of $\mathbf{V}$ are a permuted subset of the columns of $\mathbf{F}_{M\times M}$, i.e.*

$$\mathbf{V} = \mathbf{F}_{M\times M}\pi_{l,M} \tag{1.11}$$

where $\pi_{l,M}$ is an $M \times n$ permutation matrix, i.e. each column of $\pi_{l,M}$ is a unique column of $\mathbf{I}_{M\times M}$.

Proof. Consider the matrix element $\mathbf{V}(2,k) = e^{j2\pi kl/M}/\sqrt{M} = e^{j2\pi\cdot(kl \mod M)/M}/\sqrt{M}$

for some $k \in \{0, \ldots, M-1\}$. Let M be prime. Then the set

$$\{1, e^{j2\pi/M}, e^{j2\pi\cdot 2/M}, \ldots, e^{j2\pi\cdot(M-1)/M}\}$$

together with the multiplication operation forms a group. Thus each $\mathbf{V}(2,k)$ corresponds to a unique $\mathbf{F}_{M\times M}(2,k')$ for some $k' \in \{0,\ldots,M-1\}$. Now observe that $\mathbf{V}(j,k) = \mathbf{V}(2,k)^{(j-1)}$ and $\mathbf{F}_{M\times M}(j,k') = \mathbf{F}_{M\times M}(2,k')^{(j-1)}$. Thus $\mathbf{F}_{M\times M}(j,k') = \mathbf{V}_{M\times M}(j,k)$. In other words each column of $\mathbf{V}$ corresponds to a unique column of $\mathbf{F}_{M\times M}$, which establishes the result. □

Lemma 1.6.1 enables us to write the encoding matrices $\mathbf{V}_j$ in a revealing form. Define

$$\mathbf{\Gamma}_1 \triangleq \overline{\mathbf{H}}_{31}^{-1}\overline{\mathbf{H}}_{32}\mathbf{T}^2 \tag{1.12}$$

$$\mathbf{\Gamma}_2 \triangleq \mathbf{T} \tag{1.13}$$

$$\mathbf{\Gamma}_3 \triangleq \overline{\mathbf{H}}_{13}^{-1}\overline{\mathbf{H}}_{12}. \tag{1.14}$$

Then

$$\tilde{\mathbf{x}}_j = \begin{pmatrix} \mathbf{0}_{l_{\max}\times(M-l_{\max})} & \mathbf{I}_{l_{\max}\times l_{\max}} \\ & \mathbf{I}_{M\times M} \end{pmatrix} \mathbf{F}^*_{M\times M}\mathbf{\Gamma}_j\mathbf{F}_{M\times M}\pi_{l,M}\mathbf{x}_j.$$

Examining the above expression reveals that the encoding operation for tx j corresponds to transmitting consecutive data symbols l time slots apart, but cyclicly wrapped around such that roughly half of all time slots contain data symbols and no two data symbols share the same time slot. As the operation $\mathbf{F}^*_{M\times M}\mathbf{\Gamma}_j\mathbf{F}_{M\times M}$ corresponds to delaying the input stream, the entire transmission sequence is just offset by this amount.

Based on equations (1.12)-(1.14) we can define the delay d_j for user j's transmis-

sion sequence as

$$\begin{aligned} d_1 &\triangleq 2l_{12} - 2l_{21} + 2l_{23} - l_{32} + l_{31} - 2l_{13} \\ d_2 &\triangleq l_{12} - l_{21} + l_{23} - l_{32} + l_{31} - l_{13} \\ d_3 &\triangleq l_{12} - l_{13}. \end{aligned}$$

Then we see that transmitter j will send its first symbol $x_j[1]$ in time slot $d_j \mod M$, its second symbol $x_j[2]$ in time slot $d_j + l \mod M$, its third in time slot $d_j + 2l \mod M$, etc... The last symbol will be sent at time $d_j + (n-1)l \mod M$. More precisely transmitter j sends

$$\tilde{x}_j[m] = \begin{cases} x_j[k], & \text{if } m = kl + d_j \mod M \text{ for some } k \\ 0, & \text{otherwise} \end{cases}$$

at times $m = 0, 1, \ldots, M-1$.

The manner by which this transmission scheme achieves interference alignment is now simple to understand. Tx 1, transmits it's first data symbol $x_1[1]$, such that it arrives at rx 3 at the same time as tx 2's first data symbol $x_2[1]$. Tx 2 transmits $x_2[1]$ such that it arrives at the same time as $x_3[1]$ at rx 1. Tx 3 transmits $x_3[1]$ such that it arrives at rx 2 at the same time as $x_1[2]$, etc... See example 1.6.3 and figure 1.10.

From figure 1.10 it is clear how decoding should be performed —receivers merely decode each data symbol by looking at the time slot in which it was received. But let us reconcile this with the decoding methodology of [**?**], where the received sequence is passed through a ZF equalizer. This corresponds to projecting the vector $\mathbf{y}_j$ onto the subspace orthogonal to the interference. At the first receiver

$$\mathbf{y}_1 = \begin{pmatrix} \mathbf{H}_{11}\mathbf{V}_1 & \mathbf{H}_{12}\mathbf{U} \end{pmatrix} \begin{pmatrix} \mathbf{x}_1 \\ \mathbf{x}_g \end{pmatrix} + \mathbf{z}_1$$

where

$$\mathbf{U} = [\mathbf{w}\ \mathbf{T}\mathbf{w}\ \mathbf{T}^2\mathbf{w}\ \cdots\ \mathbf{T}^n\mathbf{w}].$$

and $\mathbf{x}_g$ represents a combination of interfering symbols from the 2nd and 3rd users. It is straightforward to see that we can write the space orthogonal to $\mathbf{U}$ as

$$\mathbf{U}^c = \mathbf{F}_{M\times M}\pi_{l,M}^c$$

where $\pi_{l,M}^c$ is a permutation matrix orthogonal to $\pi_{l,M}$ in the sense that ${\pi_{l,M}^c}^*\pi_{l,M} = \mathbf{0}$. Simply put, $\mathbf{U}^c$ is a matrix whose columns are those columns of $\mathbf{F}_{M\times M}$ that are not present in $\mathbf{V}$. Thus the first receiver computes $\hat{\mathbf{x}}_1 = \mathbf{G}_1^*\mathbf{y}_1$ where

$$\mathbf{G}_1^* = (\mathbf{U}^{c*}\mathbf{H}_{12}^{-1}\mathbf{H}_{11}\mathbf{V}_1)^{-1}\mathbf{U}^{c*}\mathbf{H}_{12}^{-1}.$$

If we write out the decoder in detail

$$\mathbf{G}_1^*\mathbf{y}_1 =$$
$$({\pi_{l,M}^c}^*\mathbf{F}_{M\times M}^*\mathbf{H}_{12}^{-1}\mathbf{H}_{11}\mathbf{\Gamma}_1\mathbf{F}_{M\times M}\pi_{l,M})^{-1}{\pi_{l,M}^c}^*\mathbf{F}_{M\times M}^*\mathbf{H}_{12}^{-1}\mathbf{F}_{M\times M}\begin{pmatrix}\mathbf{0}_{M\times l_{\max}} & \mathbf{I}_{M\times M}\end{pmatrix}\tilde{\mathbf{y}}_j$$

we see that the first few operations correspond to removing the cyclic prefix, delaying the resulting stream by l_{12} and then selecting the interference free subset of this. The last operation is in general undefined, as the matrix we invert may not be full rank. However in certain scenarios the matrix equals identity and is then invertible.

The reason for this phenomenon is that the last operation corresponds to recovering the data from the interference free subspace, which may contain fewer than n dimensions of $\mathbf{x}_j$. In the case of many independently faded OFDM sub-channels such as is assumed in [**?**], one could always project the subspace spanned by the data onto the interference free subspace without losing information, however for single path

channels each data dimension is either orthogonal or overlapping with an interference dimension.

The scenario in which the above decoder is well defined (i.e. data and interference subspaces are orthogonal) is given by the following condition.

Lemma 1.6.2. *If*

$$\begin{aligned} l_{11} &= d_1 + nl \mod M \\ l_{22} &= d_2 + nl \mod M \\ l_{33} &= d_3 + nl \mod M \end{aligned}$$

then the interference subspace is orthogonal to the data subspace.

Thus if each of the direct delays takes on a single, specific value, the signal space will be orthogonal to the interference space at each of the receivers and we will be able to decode all data symbols.

Example 1.6.3. *Suppose the link delays are* $l_{11} = 0$, $l_{22} = 5$, $l_{33} = 9$, $l_{12} = 5$, $l_{13} = 4$, $l_{21} = 4$, $l_{23} = 6$, $l_{31} = 5$, $l_{32} = 4$. *Then* $d_1 = 7$, $d_2 = 4$ *and* $d_3 = 1$. *Also* $l = 5-4+6-4+5-4 = 4$. *Note that for illustrative purposes the direct delays have been precisely chosen such that the data and interference subspaces are orthogonal. Choose the data block length* M *to be the prime 13, and use a cyclic prefix of length* 9. *The total length of cyclic prefix plus data block is 21. Then tx 1 will transmit its 0th data symbol, namely* $x_1[0]$, *in time slot* $d_1 \mod M = 7 \mod 13 = 7$. *It's second data symbol* $x_1[1]$ *will be transmitted in time slot* $l + d_1 \mod M = 4 + 7 \mod 13 = 11$. *It's third data symbol* $x_1[2]$ *will be transmitted in time slot* $2l + d_1 \mod M = 15 \mod 13 = 2$, *etc.. These data symbols will arrive at rx 2 delayed by* $l_{21} = 4$ *time slots. Thus* $x_1[0]$ *will appear as interference at rx 2 during time slot* $7 + 4 = 11$, $x_1[1]$ *will appear as interference during time slot* $11 + 4 = 15$, *etc... Similarly tx 1's data*

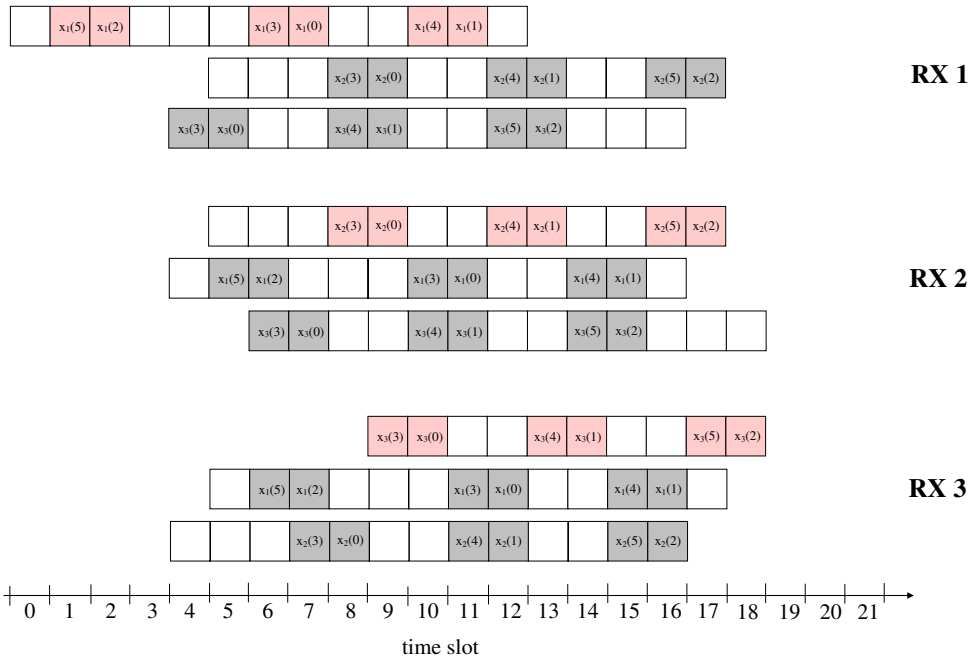

(a)

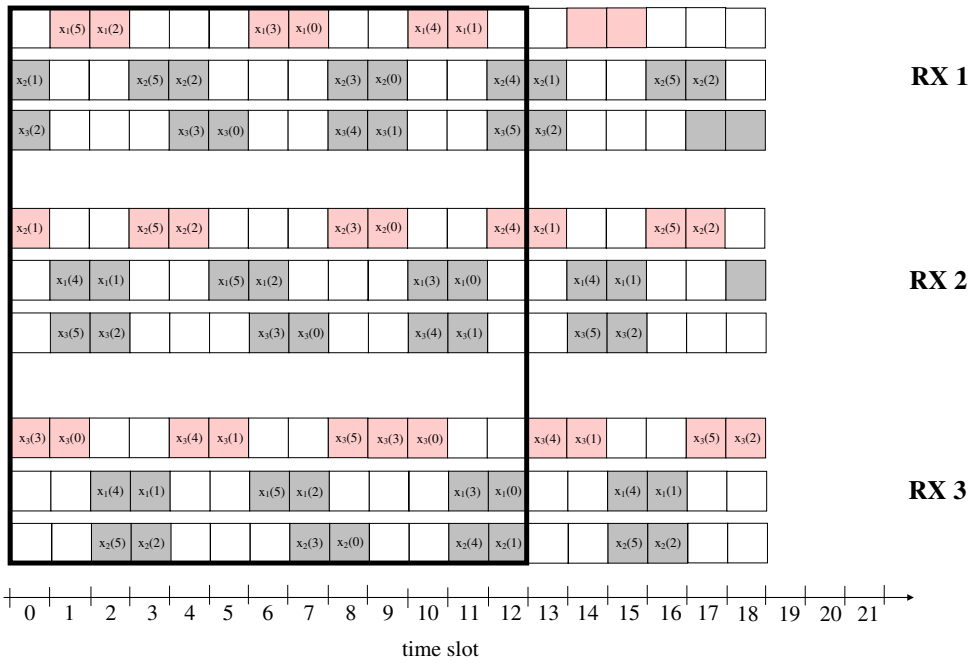

(b)

Figure 1.10: Illustration of 3 user interference alignment scheme of [5] in the time domain. See example 1.6.3 for a description. (a) Received sequences with the cyclic prefix omitted. (b) Received sequences incorporating the cyclic prefix.

symbols will arrive at rx 3 delayed by $l_{31} = 5$ time slots. Similarly one can do the same computation for tx 2's and tx 3's data symbols.

The details are given in figure 1.10. In part (a) of the figure the cyclic prefix has been omitted for illustrative purposes. It is incorporated into the picture in part (b). The red shaded boxes contain data symbols, the grey shaded boxes contain interference symbols. Notice the interference alignment property manifests itself as an overlapping of interfering data symbols. The shaded, but unlabeled boxes represent symbols belonging to the next OFDM block. The black box outlines those time slots that are used for decoding. The 9 time slots prior to these are discarded when the cyclic prefix is removed. The 9 unboxed time slots to the right of the black outline will also be discarded, but during the next OFDM block.

1.6.1 K-user channels

In the previous section we demonstrated that for three-user LOS channels, the frequency domain scheme of [5] has a simple analog in the time domain that works well when the block length is chosen to be a prime number, and the direct delays take on particular values. One would imagine that an analogous scheme for $K > 3$ users would therefore also exist and work well. This is not the case. In fact for the LOS interference channel with more than three users, the alignment scheme of [5] has various shortcomings which result in it achieving zero degrees of freedom in total. Our construction (in section 1.5) is inspired by the use of a generalized arithmetic progression in [5], but circumvents the schemes shortcomings by:

1. Truncating the generalized arithmetic progression appropriately.
2. Interleaving many replicas of the progression, with random offsets.
3. Scaling the bandwidth with K.

For example, to understand why truncation is necessary, recall the precoding matrices used in for the K-user channel in [5] are of the form

$$\mathbf{V}_j = \mathbf{S}_j \mathbf{B}$$

for $j = 2, \ldots, K$, where the matrix $\mathbf{B}$ is composed of the column vectors in the set

$$\mathcal{B} = \left\{ \left(\prod_{i,j \in \{2,3,\ldots,K\}, i \neq j, (i,j) \neq (2,3)} (\overline{\mathbf{H}}_{i1}^{-1} \overline{\mathbf{H}}_{ij} \mathbf{S}_j)^{\alpha_{ij}} \right) \mathbf{w} : \alpha_{ij} \in \{0, 1, \ldots, n-1\} \right\},$$

and $\mathbf{S}_j = \overline{\mathbf{H}}_{1j}^{-1} \overline{\mathbf{H}}_{13} \overline{\mathbf{H}}_{23}^{-1} \overline{\mathbf{H}}_{21}$. Observing equation (1.9), write the link matrices in the form

$$\overline{\mathbf{H}}_{ij} = \mathbf{Z}^{l_{ij}},$$

where

$$\mathbf{Z} \triangleq \begin{pmatrix} 1 & & & & \\ & e^{-j2\pi \cdot / M} & & & \\ & & e^{-j2\pi \cdot 2/M} & & \\ & & & \ddots & \\ & & & & e^{-j2\pi \cdot (M-1)/M} \end{pmatrix}.$$

Then we have

$$\mathcal{B} = \left\{ \mathbf{Z}^{\sum_{i,j \in \{2,3,\ldots,K\}, i \neq j, (i,j) \neq (2,3)} \alpha_{ij} \tilde{l}_{ij}} \mathbf{w} : \forall \alpha_{ij} \in \{0, 1, \ldots, n-1\} \right\}.$$

where $l_{ij} = -l_{ij} + l_{ij} - l_{1j} + l_{13} - l_{23} + l_{21}$. For sufficiently large n we will be able to find many pairs $(\{\alpha_{ij}\}, \{\alpha'_{ij}\})$ such that

$$\sum_{i,j \in \{2,3,\ldots,K\}, i \neq j, (i,j) \neq (2,3)} \alpha_{ij} \tilde{l}_{ij} = \sum_{i,j \in \{2,3,\ldots,K\}, i \neq j, (i,j) \neq (2,3)} \alpha'_{ij} \tilde{l}_{ij}.$$

Thus the precoding matrices *will loose rank* as many of their columns will be repeats of previous ones. This phenomenon of repeated elements is common in generalized arithmetic progressions over integer fields. See for example [27]. How much rank will be lost? Observe that the largest exponent of $\mathbf{Z}$ in $\mathcal{B}$ will be no greater than $(n-1)((K-1)(K-2)-1)\max l_{ij}$. But there are $n^{(K-1)(K-2)-1}$ columns in $\mathbf{B}$. Thus as $n \to \infty$ the rank of $\mathbf{B}$ will scale only like $O(n)$ due to repeated columns, whilst the dimension of the space scales like roughly $O(n^{(K-1)(K-2)-1})$. Hence the total degrees of freedom goes to zero unless the progression is truncated.

1.6.2 Bandwidth Scaling Revisited

The final issue we address in terms of reconciling time and frequency domain interpretations, is that of bandwidth scaling. We now demonstrate that bandwidth scaling is required in the scheme of [5] when the physical channel model is brought into the picture.

Theorem 1.6.4. *In a multipath fading channel with L taps, if the bandwidth satisfies*

$$\lim_{K\to\infty} \frac{\log W}{\log((K-1)(K-2)-1)^{(K-1)(K-2)-3}} = 0,$$

then the total degrees of freedom achieved by the K-user interference alignment scheme of [5] goes to zero as $K \to \infty$.

This means that the bandwidth must scale at least as fast as $O(((K-1)(K-2)-1)^{(K-1)(K-2)-3})$ which is roughly the same scaling that is required in theorem 1.3.1, namely $O(K^{2K^2})$.

Proof. For a general multipath channel with L taps, the link matrices are of the form

$$\mathbf{H}_{ij} = \sum_{l=0}^{L-1} a_{ij,l}\mathbf{Z}^l.$$

Using the commutativity of the diagonal $\mathbf{H}_{ij}$ matrices we can write

$$\mathbf{V}_j = \mathbf{S}_j \left(\prod_{i,j \in \{2,3,\ldots,K\}, i \neq j, (i,j) \neq (2,3)} \mathbf{H}_{i1}\mathbf{H}_{1j}\mathbf{H}_{23} \right)^{-n} \mathbf{C},$$

where the matrix $\mathbf{C}$ is composed of the column vectors in the set

$$\mathcal{C} = \left\{ \left(\prod_{i,j \in \{2,3,\ldots,K\}, i \neq j, (i,j) \neq (2,3)} (\mathbf{H}_{i1}\mathbf{H}_{1j}\mathbf{H}_{23})^{n-\alpha_{ij}} (\mathbf{H}_{ij}\mathbf{H}_{13}\mathbf{H}_{21})^{\alpha_{ij}} \right) \mathbf{w} : \alpha_{ij} \in \{0, 1, \ldots, n-1\} \right\}.$$

In [5] the minimum scaling of n with K required is

$$\lim_{K \to \infty} \frac{\log n}{\log (K-1)(K-2) - 1} > 0.$$

Each of the $\mathbf{H}_{ij}$ matrices is a polynomial of degree at most $L-1$ in the matrix $\mathbf{Z}$. Thus each column of $\mathbf{C}$ is a polynomial of degree at most $6n(L-1)((K-1)(K-2)-1)$ in the matrix $\mathbf{Z}$. This means the maximum rank of $\mathbf{C}$ is $6n(L-1)((K-1)(K-2)-1)+1$, as any c polynomials of degree $\leq d$ that are in general position, are linearly dependent for $c > d+1$. The total number of rows in $\mathbf{C}$ however, is at least $n^{(K-1)(K-2)-1}$. Thus the total degrees of freedom is no more than

$$\frac{6n(L-1)((K-1)(K-2)-1)}{n^{(K-1)(K-2)-1}}.$$

which goes to zero as $K \to \infty$, unless L (and hence W) scales like

$$\lim_{K \to \infty} \frac{\log L}{\log ((K-1)(K-2)-1)^{(K-1)(K-2)-3}} > 0.$$

□

1.7 Discussion and Conclusion

Although this work concentrated on the line-of-sight channel, where each link consists of only a single physical path, it is possible to generalize the concepts and constructions presented herein to the case where each link consists of D physical paths. This is done by modifying the interference graph such that each vertex interferes with D other vertices at each user. Intuitively this would cause the independence rate of the interference graph to decrease, but it can be shown by a simple modification of the proof of theorem 1.3.1, that when the D delays are i.i.d. for each link, the independence rate scales arbitrarily close to $O(K)$ as $K \to \infty$, so long as the bandwidth scales sufficiently with K. Put another way the spectral efficiency can again be made to vanish arbitrarily slowly as $K \to \infty$. The trick is to treat the additional paths as fictitious interferers who have no data of their own to send. The catch is that the scheme requires the bandwidth to scale much more quickly, like $O((2DK(DK-1))^{DK(DK-1)})$. Thus for all practical purposes, increasing the number of physical paths would likely lead to a decrease in the performance of time-domain based interference alignment schemes.

We demonstrated in section 1.4.2 that if the bandwidth scales sub-linearly in K, then the independence rate of the interference graph goes to zero as $K \to \infty$, and in section 1.5, that if the bandwidth scales like $O((2K(K-1))^{K(K-1)})$, then the independence rate scales arbitrarily close to $O(K)$. This brings us to an interesting open question. How does the independence rate scale in the intermediate regime where $O(K) \geq W < O((2K(K-1))^{K(K-1)})$? What if there are D physical paths?

There are several variations of the LOS interference channel for which the interference graph techniques discussed in this work are applicable, and for which fur-

ther study is warranted. These were alluded to earlier. For instance, the partial connected interference channel may be a more accurate model of a wireless adhoc network. It is possible that for such channels, a bandwidth scaling much less than $O((2K(K-1))^{K(K-1)})$ is sufficient in order for the independence rate to scale arbitrarily close $O(K)$. It is not clear how one would approach the problem of showing this if it were true, or disproving it otherwise. An interference channel with one dominant path per link and several sub-dominant ones, is also an interesting candidate for investigation. This channel is more commonly encountered in practice than the line-of-sight channel. It is likely that an optimization problem similar to 1.3 can be formulated for this scenario. It would be interesting to study whether time-domain based interference alignment can provide gains here. Presumably as the dominance of one physical path over the others diminishes, so too will the performance improvement.

Lastly we discuss some interesting fringe benefits associated with the communication schemes presented in this work. Whereas interference alignment in the frequency domain requires coding over very long blocks, which results in substantial delay due to the necessity of buffering data symbols at the encoder and received symbols at the decoder, no such delay is required for the time-indexed interference graph techniques detailed above. Data symbols are transmitted as soon as an appropriate time slot is reached, and detected when received. The only delay incurred is that stemming from the use of an error correction code. In the same respect, the encoding and decoding complexity are greatly reduced. Thus delay and complexity issues are non-existent.

Conditioning issues are also non-existent. Interference alignment in the frequency domain, although performing well at very high-PSD, suffers at moderate PSD if the data and interference subspaces are close to one another. Time domain interference alignment techniques are free from this problem as the data and interferences subspaces are orthogonal by design.

1.8 Appendix

1.8.1 Proof of Theorem 1.4.5

First suppose $l \neq 0$. From the interference graph form l infinite *chain graphs* $\mathcal{G}'_0, \ldots, \mathcal{G}'_{l-1}$. These graphs will be functions of K and $\{l_{ij}\}_{i \neq j}$ but for notational brevity we omit this notation. The ith chain graph $\mathcal{G}'_i$ has vertex and edges sets

$$\mathcal{V}'_i = \{v'_i(0), v'_i(1), \ldots\}$$
$$\mathcal{E}'_i = \{e'_i(0), e'_i(1), \ldots\}.$$

This is an undirected graph with edge $e'_i(j)$ joining vertices $v'_i(j)$ and $v'_i(j+1)$. We now associate the chain graphs with the interference graph. Let

$$\begin{aligned}
v'_i(6k) &= v_3(kl + i) \\
v'_i(6k+1) &= v_1(kl + i + l'_{31}) \\
v'_i(6k+2) &= v_3(kl + i + l'_{31} + l'_{13}) \\
v'_i(6k+3) &= v_2(kl + i + l'_{31} + l'_{13} + l'_{32}) \\
v'_i(6k+4) &= v_1(kl + i + l'_{31} + l'_{13} + l'_{32} + l'_{21}) \\
v'_i(6k+5) &= v_2(kl + i + l'_{31} + l'_{13} + l'_{32} + l'_{21} + l'_{12})
\end{aligned}$$

where the $v_k(t)$ are the vertices in the original interference graph. See figure 1.11 for an illustration. Note that the mapping from the interference graph to the l chain graphs is not one-one. In particular, each vertex in the interference graph is associated with a *pair* of vertices in the set of chain graphs. Paired vertices are called *twins* as they correspond to the same vertex from the original interference graph. We now think of a feasible transmit pattern as a collection of vertices from the set of chain graphs.

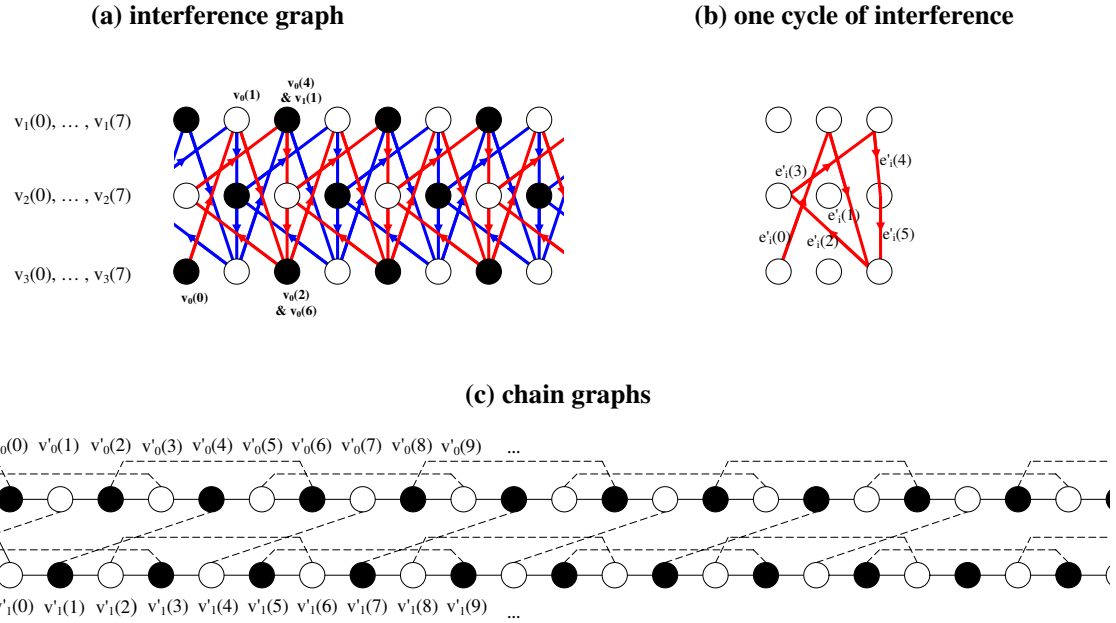

Figure 1.11: (a) A segment of the interference graph. Each row of vertices corresponds to the transmission opportunities for each of the users. The shaded vertices correspond to a feasible transmit pattern achieving an independence rate of $3/2$. A few of the vertices are labeled with their equivalent vertices in the chain graphs. In this example the normalized cross delays are $l'_{21} = 0$, $l'_{31} = 1$, $l'_{12} = 2$, $l'_{32} = 0$, $l'_{13} = 1$ and $l'_{23} = -2$. Thus $l = 0+1+2+0+1-2 = 2$ meaning that each cycle of interference moves two time slots to the right as illustrated in (b), which shows a single cycle from the interference graph, containing all six directed edges. (c) The corresponding chain graphs. As $l = 2$, there are two chains. A pair of twin vertices connected by a dashed line in the chain graphs, correspond to the same vertex in the original interference graph.

However, note that if a feasible transmit pattern results in a particular vertex (from the set of chain graphs) being included in the independent set, its twin will also be included. Likewise if a feasible transmit pattern results in a particular vertex being excluded, its twin will also be excluded. The key to characterizing the set of channels for which an interference rate of 3/2 is achievable lies in understanding which pairings are favorable, and which are not.

The pairings can be succinctly described by the following three equations

$$v_i'(6k) = v'_{i-l_3 \bmod l}(6(k + \lfloor l_3/l \rfloor) + 2) \tag{1.15}$$

$$v_i'(6k+1) = v'_{i-l_1 \bmod l}(6(k + \lfloor l_1/l \rfloor) + 4) \tag{1.16}$$

$$v_i'(6k+3) = v'_{i-l_2 \bmod l}(6(k + \lfloor l_2/l \rfloor) + 5) \tag{1.17}$$

for $i = 0, \ldots, l-1$ and $k = 0, 1, \ldots$.

In order to achieve an independence rate of 3/2, half of all vertices must be included in the transmit pattern. Denote the transmit pattern by $\mathcal{T}$. Because in each chain, all neighboring vertices are connected by an edge, this is only possible if in each chain, every second node is included in the transmit pattern. For each chain there are two ways of doing this, either $v_i'(2k) \in \mathcal{T}$ for all k, or $v_i'(2k+1) \in \mathcal{T}$ for all k. Let c_i denote the phase of the ith chain. If the former condition holds, we say the chain is *in phase* and write $c_i = I$. If the latter holds we say the chain is *out of phase* and write $c_i = O$. In the entire graph there are only 2^l combinations we need to examine, corresponding to all possible inphase/out of phase assignments for the l chains. A feasible transmit pattern achieving independence rate 3/2 exists if and only if each chain admits an I or O assignment and the assignment of I's and O's to the l chains does not violate conditions (1.15)-(1.17). Thus we wish to characterize those channels for which such an I/O assignment can be found.

At this point we consider an example. Suppose l divides l_1. We claim an indepen-

dence rate of 3/2 is not achievable. To see this argue by contradiction. Assume that $c_0 = I$. As l divides l_1, we have $l_1 \bmod l = 0$ and condition (1.16) pairs vertex $v_0(1)$ with vertex $v_0(6k' + 4)$ for some integer k'. But these vertices lie an odd distance apart on the same chain, so working backwards we see that we must have $c_0 = O$, a contraction. So suppose instead that $c_0 = 0$. Using the same logic as before we arrive at $c_0 = I$, again a contradiction. Thus the independence rate is less than 3/2.

From this example we see that condition (1.15) tells us if $c_0 = I$ then we must also have $c_{-l_3 \bmod l} = I$, as vertices $v'_0(0)$ and $v'_{-l_3 \bmod l}(6\lfloor l_3/l \rfloor + 2)$ are an even distance apart. Continuing this logic we see that we must also have $c_{-l_1 \bmod l} = O$, and $c_{-l_2 \bmod l} = I$. We can also conclude something else, as $c_{-l_1 \bmod l} = O$, we must have $c_{-2l_1 \bmod l} = I$ by condition (1.16). Continuing further, we must have $c_{-2l_1 - l_2 \bmod l} = I$ by condition (1.17) and so on.

By this point it should be clear that conditions (1.15)-(1.17) are satisfied if and only if for all integers k_1, k_2, k_3,

$$c_{2k_1 l_1 + k_2 l_2 + k_3 l_3 \bmod l} \neq c_{(2k_1+1) l_1 + k_2 l_2 + k_3 l_3 \bmod l} \tag{1.18}$$

Let $\mathcal{P}(l)$ denote the group consisting of integers $\{0, \ldots, l-1\}$ together with the addition modulo l operation. Consider the set of chains $c_{2k_1 l_1 + k_2 l_2 + k_3 l_3 \bmod l}$ for all integers k_1, k_2, k_3. This set forms a subgroup of $\mathcal{P}(l)$ with generator $\gcd(2l_1, l_2, l_3)$. We denote this subgroup by $\mathcal{P}_{\gcd(2l_1, l_2, l_3)}(l)$. It has $\gcd(2l_1, l_2, l_3, l) - 1$ cosets other than itself. The set of chains $c_{(2k_1+1) l_1 + k_2 l_2 + k_3 l_3 \bmod l}$ for all integers k_1, k_2, k_3, forms coset number $l_1 \bmod \gcd(2l_1, l_2, l_3, l)$. But as

$$2l_1 \bmod \gcd(2l_1, l_2, l_3, l) = 0,$$

either $l_1 \bmod \gcd(2l_1, l_2, l_3, l)$ equals $\gcd(l_1, l_2/2, l_3/2, l/2)$, or 0. If it is zero, condition

(1.18) above is violated. This occurs if and only if l_1 is a multiple of $\gcd(2l_1, l_2, l_3, l)$. Alternatively if it equals $\gcd(l_1, l_2/2, l_3/2, l/2)$ then we can choose the phases of half the cosets, namely cosets

$$0, 1, ..., \gcd(l_1, l_2/2, l_3/2, l/2) - 1$$

arbitrarily, and still satisfy (1.18). For this reason we refer to the chains

$$c_0, c_1, ..., c_{\gcd(l_1, l_2/2, l_3/2, l/2)-1}$$

as seed chains. This means that there are $2^{\gcd(l_1, l_2/2, l_3/2, l/2)}$ possible solutions that achieve independence rate 3/2. So what does it mean for l_1 to not be a multiple of $\gcd(2l_1, l_2, l_3, l)$? It means that

$$\gcd(l_1, 2l_1, l_2, l_3, l) \neq \gcd(2l_1, l_2, l_3, l).$$

In other words

$$\gcd(l_1, l_2, l_3, l) \neq \gcd(2l_1, l_2, l_3, l).$$

It is shown in lemma 1.8.1 that the above inequality is equivalent to having $\gamma_1 < \gamma_2$, $\gamma_1 < \gamma_3$ and $\gamma_1 < \gamma$. This establishes theorem 1.4.5 for $l \neq 0$.

Now suppose $l = 0$. This proof is a slight modification of the previous. From the interference graph from an infinite number of *cycle graphs* $\mathcal{G}'_0, \mathcal{G}'_1, \ldots$. The ith cycle graph $\mathcal{G}'_i$ has vertex and edge sets

$$\mathcal{V}'_i = \{v'_i(0), v'_i(1), v'_i(2), v'_i(3), v'_i(4), v'_i(5)\}$$
$$\mathcal{E}'_i = \{e'_i(0), e'_i(1), e'_i(2), e'_i(3), e'_i(4), e'_i(5)\},$$

where edge $e'_i(j \mod 6)$ joins vertices $v_i(j \mod 6)$ and $v_i(j+1 \mod 6)$, for $j = 0, 1, 2, 3, 4, 5$. Notice that for $l \neq 0$ we created a finite number of chain graphs, each with an infinite number of vertices, whereas for $l = 0$ we create an infinite number of cycle graphs, each with a finite number of vertices. We now associate the cycle graphs with the interference graph. Let

$$\begin{aligned}
v'_i(0) &= v_3(i) \\
v'_i(1) &= v_1(i + l'_{31}) \\
v'_i(2) &= v_3(i + l'_{31} + l'_{13}) \\
v'_i(3) &= v_2(i + l'_{31} + l'_{13} + l'_{32}) \\
v'_i(4) &= v_1(i + l'_{31} + l'_{13} + l'_{32} + l'_{21}) \\
v'_i(5) &= v_2(i + l'_{31} + l'_{13} + l'_{32} + l'_{21} + l'_{12})
\end{aligned}$$

where $v_k(t)$ are the vertices in the original interference graph. As before, the mapping from interference graph to the indefinite number of cycle graphs is not one-one. Each vertex in the interference graph is associated with a pair of vertices in the set of cycle graphs. The pairings are described by the following three equations

$$\begin{aligned}
v'_i(0) &= v'_{i-l_3}(2) \\
v'_i(1) &= v'_{i-l_1}(4) \\
v'_i(3) &= v'_{i-l_2}(5)
\end{aligned}$$

We want to assign each cycle graph i a phase, either $c_i = I$ or $c_i = O$ and we need to find necessary and sufficient conditions for a feasible assignment. Similarly to equation 1.18, the condition we are after is

$$c_{2k_1l_1+k_2l_2+k_3l_3} \neq c_{(2k_1+1)l_1+k_2l_2+k_3l_3}$$

for all integers k_1, k_2, k_3. By this point it should be clear, based on the proof for the $l \neq 0$ case, that the above condition is equivalent to

$$\gcd(l_1, l_2, l_3) \neq \gcd(2l_1, l_2, l_3).$$

This inequality is equivalent to having $\gamma_1 < \gamma_2$ and $\gamma_1 < \gamma_3$. Thus we see that the conditions for $l = 0$ case are the same as the $l \neq 0$ case if we set $\gamma = \infty$. This establishes the result in general.

Lemma 1.8.1. $\gcd(l_1, l_2, l_3, l) \neq \gcd(2l_1, l_2, l_3, l)$ *if and only if* $\gamma_1 < \gamma_2$, $\gamma_1 < \gamma_3$ *and* $\gamma_1 < \gamma$.

Proof. Suppose

$$\begin{aligned}
&\gcd(l_1, l_2, l_3, l) \neq \gcd(2l_1, l_2, l_3, l) \\
\Rightarrow &\gcd(2^{\gamma_1}\beta_1, 2^{\gamma_2}\beta_2, 2^{\gamma_3}\beta_3, 2^{\gamma}\beta) \neq \gcd(2^{\gamma_1+1}\beta_1, 2^{\gamma_2}\beta_2, 2^{\gamma_3}\beta_3, 2^{\gamma}\beta) \\
\Rightarrow &\gcd(2^{\gamma_1}, 2^{\gamma_2}, 2^{\gamma_3}, 2^{\gamma}) \gcd(\beta_1, \beta_2, \beta_3, \beta) \neq \gcd(2^{\gamma_1+1}, 2^{\gamma_2}, 2^{\gamma_3}, 2^{\gamma}) \gcd(\beta_1, \beta_2, \beta_3, \beta) \\
&\Rightarrow \min(\gamma_1, \gamma_2, \gamma_3, \gamma) \neq \min(\gamma_1 + 1, \gamma_2, \gamma_3, \gamma).
\end{aligned}$$

This can only hold if $\gamma_1 < \gamma_2$, $\gamma_1 < \gamma_3$ and $\gamma_1 < \gamma$. The proof in the opposite direction is identical. □

Chapter 2

Spectrum Sharing between Wireless Networks

2.1 Introduction

The recent proliferation of networks operating on unlicensed bands, most notably 802.11 and Bluetooth, has stimulated research into the study of how different systems competing for the same spectrum interact. Communication on unlicensed spectrum is desirable essentially because it is free, but users are subject to random interference generated by the transmissions of other users. Most research to date has assumed devices have no natural incentive to cooperate with one another. For instance, a wireless router in one apartment is not concerned about the interference it generates in a neighboring apartment. Following from this assumption, various game-theoretic formulations have been used to model the interplay between neighboring systems [31], [10], [3], [13], [21]. An important conclusion stemming from this body of work is that for single-stage games the Nash Equilibria (N.E.) are typically unfavorable, resulting in inefficient allocations of resources to users. A quintessential example is

the following. Consider a system where a pair of competing links is subjected to white-noise and all cross-gains are frequency-flat. Suppose the transmitters wish to select a one-time power allocation across frequency subject to a constraint on the total power expended (this problem is studied in [30], [6], [9] where it is referred to as the *Gaussian Interference Game*). It is straightforward to reason (via a waterfilling argument) that the selection by both users of frequency-flat power allocations, each occupying the entire band, constitutes a N.E.. This *full spread* power allocation can be extremely inefficient. Consider a symmetric system where the cross-gains and direct-gains are equal. At high SNR each link achieves a throughput of only 1 b/s/Hz, instead of $\frac{1}{2}\log_2(1+\mathsf{SNR})$ b/s/Hz, which would be obtained if the links cooperated by occupying orthogonal halves of the spectrum. At an SNR of 30 dB, the throughput ratio between cooperative behavior and this full spread N.E. behavior, referred to as the *price of anarchy*, is about 5. This example highlights an important point in relation to single-stage games between competing wireless links: users typically have an incentive to occupy all of the available resources.

In this work a different approach is taken. Rather than assuming total anarchy, that is, competition between *all* wireless links, we instead assume competition only between wireless links belonging to *different networks*. Wireless links belonging to the same network are assumed to *cooperate*. In short, we assume competition on the network level, not on the link level. In a practical setting this may represent the fact that neighboring wireless systems are produced by the same manufacturer, or are administered by the same network operator. Alternatively one may view the competition as being between coalitions of users [22].

To make the problem analytically tractable but still retain its underlying mechanics, we assume each network operates under a random-access protocol, where users from a given network access the channel independently but with the same probability. Analysis of random access protocols provides intuition for the behavior of sys-

tems operating under more complex protocols, as the access probability can broadly be interpreted as the average degrees of freedom each user occupies. For the case of competition on the link level, game-theoretic research of random-access protocols such as ALOHA have been conducted in [25] and [19]. In our model each network has a different density of nodes and chooses its access probability to maximize average throughput per user. Note this access protocol is essentially identical to one in which users select a random fraction of the spectrum on which to communicate. Thus an access probability of one corresponds to a full spread power allocation.

We first assume all links in the system have the same transmission range and afterwards show that the results are only trivially modified if each link is assumed to have an i.i.d. random transmission range. We characterize the N.E. of this system for a fixed-rate model, where all users transmit at the same data rate. We show that unlike the case of competing links, a N.E. always exists and is *unique*. Furthermore for a large range of typical parameter values, the N.E. is not full spread —nodes in at least one network occupy only a fraction of the bandwidth. We also identify two modes, delineated by the pathloss exponent α. For $\alpha > 4$, the N.E. behavior is distinctly different than for $\alpha < 4$ and possesses pseudo-cooperative properties. Following this we show that the picture for the variable-rate model, in which users individually tailor their transmission rates to match the instantaneous channel capacity, remains unchanged. Before concluding we present simulation results for the behavior of the system when the networks employ a greedy algorithm to optimize their throughput, operating under both a random access protocol, and a carrier sensing protocol.

In section II we formulate the system model explicitly. In section III.A we introduce the random access protocol and analyze its N.E. behavior in the fixed-rate model. In section III.B we analyze the variable-rate model. In section IV we extend our results to cover the case of variable transmission ranges. Section V presents simulation results and the carrier sensing protocol. Section VI summarizes and suggests

extensions. Section VII contains proofs of the main theorems presented.

2.2 Problem Setup

Consider two wireless networks consisting of $n\lambda_1$ and $n\lambda_2$ tx-rx pairs, respectively. Without loss of generality we will assume $\lambda_1 \leq \lambda_2$. The transmitting nodes are uniformly distributed at random in an area of size n. To avoid boundary effects suppose this area is the surface of a sphere. Thus λ_i is the density of transmitters (or receivers) in network i. For each transmitter, the corresponding receiver is initially assumed to be located at a fixed range of d meters with uniform random bearing. Time is slotted and all users are assumed to be time synchronized.

Both networks operate on the same band of (presumably unlicensed) spectrum and at each time slot a subset of tx-rx pairs are simultaneously scheduled in each network. When scheduled a tx-rx pair uses all of the spectrum. It is generally desirable to schedule neighboring tx-rx pairs in different time slots. This scheduling model is a form of TDM, but is more or less analogous to an FDM model where each tx-rx pair is allocated a subset of the spectrum (typically overlapping in some way with other tx-rx pairs in the network).

Transmitting nodes are full buffer in that they always have data to send. Transmissions are assumed to use Gaussian codebooks and interference from other nodes is treated as noise. Initially we analyse the model where all transmissions in network i occur at a common rate of $\log(1+\beta_i)$. We refer to β as the *target* SINR. Thus a transmission in network i is successful iff SINR $> \beta_i$. Later we explore the model where transmission rates are individually tailored to match the instantaneous capacities of the channels. The signal power attenuates according to a power law with *pathloss exponent* $\alpha > 2$. We assume a high-SNR or *interference limited* scenario where the thermal noise is insignificant relative to the received power of interfering nodes and

thus refer to the SIR as the SIR. For a given realization of the node locations the time-averaged throughput achieved by the jth tx-rx pair in network i is then

$$\overline{R}_j = f_j \mathbb{P}(\mathsf{SIR_j(t)} > \beta_i) \log(1 + \beta_i)$$

per complex d.o.f., where f_j is the fraction of time the jth tx-rx pair is scheduled. The average (represented by the bar above the R) is essentially taken over the distribution of the interference as at different times different subsets of transmitters are scheduled.

As for $\alpha > 2$ the bulk of the interference is generated by the strongest interferer, to make the problem tractable, we compute the SIR as the receive power of the desired signal divided by the receive power of the *nearest* interferers signal. We refer to this as the *Dominant Interferer* assumption. Denote the range of the nearest interferer to the jth receiver at time t by $r_j(t)$. Then

$$\mathsf{SIR}_j(t) = \frac{d^{-\alpha}}{r_j^{-\alpha}(t)}$$

The metric of interest to each network is its expected time-averaged rate per user,

$$\mathbb{E}\overline{R} = \mathbb{E}_g \left[f_j \mathbb{P}(\mathsf{SIR_j(t)} > \beta_i) \log(1 + \beta_i) \right]$$

The subscript g indicates this expectation is taken over the geographic distribution of the nodes. As the setup is statistically symmetric, this metric is equivalent to the expected *sum rate* of the system, divided by $n\lambda_i$, in the limit $n \to \infty$.

2.3 Random Access protocol

2.3.1 Fixed-Rate model

Suppose each network uses the following random access protocol. At each time slot each link is scheduled i.i.d. with probability p_i. The packet size is $\log(1+\beta_i)$ for all communications in network i. The variables β_i are optimized over.

Let us first compute the optimal access probability for the case of a single network operating in isolation on a licensed band, as a function of the node density and the transmission range. This problem has recently been studied independently in [15]-[17] with equivalent results derived. In [2] similar results are derived for the case where the SIR is computed based on all interferers, not just the nearest.

Let the r.v. $N_j(x)$ denote the number of interfering transmitters within range x of the jth receiver.

$$\begin{aligned}
\mathbb{E}\overline{R} &= \mathbb{E}_g\left[f_j\mathbb{P}(r_j(t) > \beta_i^{1/\alpha}d)\log(1+\beta_I)\right] \\
&= p_i\sum_{k=1}^{n\lambda_i-1}\mathbb{P}(N_j(\beta^{1/\alpha}d)=k)(1-p_i)^k\log(1+\beta_i) \\
&= p_i\sum_{k=1}^{n\lambda_i-1}\left(\frac{\pi\beta_i^{2/\alpha}d^2}{n}\right)^k\left(1-\frac{\pi\beta_i^{2/\alpha}d^2}{n}\right)^{n\lambda_i-k-1} \\
&\qquad\qquad \times\binom{n\lambda_i-1}{k}(1-p_i)^k\log(1+\beta_i) \\
&= p_i\left(1-p_i\frac{\pi\beta_i^{2/\alpha}d^2}{n}\right)^{n\lambda_i-1}\log(1+\beta_i) \\
&\to p_i\log(1+\beta_i)e^{-\pi\lambda_i d^2 p_i\beta_i^{2/\alpha}}
\end{aligned}$$

in the limit $n\to\infty$.

In order to obtain better insight into the problem at hand, a change of variables

is required. We refer to the set of all points within the transmission range as the *transmission disc*. The quantity $\pi\lambda_i d^2$ is the *average number of nodes (tx or rx) per transmission disc*. We often refer to it simply as the *number of nodes per disc* and represent it by the symbol

$$N_i \triangleq \pi\lambda_i d^2.$$

Assume N_i is larger than a certain threshold (we make this precise later). Maximizing over the access probability yields

$$\mathbb{E}\overline{R} \to \frac{\log(1+\beta_i)}{N_i \beta_i^{2/\alpha}} e^{-1} \tag{2.1}$$

with the optimal access probability being

$$p_i^* = \frac{1}{N_i \beta_i^{2/\alpha}}. \tag{2.2}$$

One can further optimize over the target SIR so that β_i is replaced by β_i^* in the above two equations. Inspection of equation (2.1) reveals that the optimal target SIR is a function of α alone. So if we define the quantity

$$\Lambda_i \triangleq N_i p_i,$$

Λ_i^* will be a constant, independent of N_i. The quantity Λ_i represents the *average number of (simultaneous) transmissions per transmission disc*. We sometimes refer to it simply as the *transmit density*. Whereas the domain of p_i is $[0, 1]$, the domain of Λ_i is $[0, N_i]$. Thus we see that for N_i sufficiently large, the access probability should be set such that an optimal number of transmissions per disc is achieved. What is this optimal number? What is the optimal target SIR?

For the purposes of optimizing equation (2.1), define the function $\Lambda^*(\alpha)$ as the

unique solution of the following equation

$$\frac{\alpha}{2} = \left(1 + \Lambda^{*\alpha/2}\right) \log\left(1 + \frac{1}{\Lambda^{*\alpha/2}}\right). \tag{2.3}$$

A plot of $\Lambda^*(\alpha)$ is given in figure 2.1. So as to avoid confusion, note that the symbol Λ^* represents a pre-defined function, not necessarily the same as the symbol Λ_i^*, which is a variable. As equation (2.1) is smooth and continuous with a unique maxima, by setting it's derivative to zero we find that the optimal target SIR is $\beta^* = \Lambda^{*-\alpha/2}$ and the optimal number of transmissions per disc is $\Lambda_i^* = \Lambda^*$, when N_i is larger than a certain threshold.

When N_i is smaller than this threshold, there aren't enough tx-rx pairs to reach the optimal number of transmissions per disc, even when all of them are simultaneously scheduled. In this case the solution lies on the boundary with $p_i^* = 1$. This corresponds to the scenario where the transmission range is short relative to the node density such that tx-rx pairs function as if in isolation. It is intuitive that in this case all transmissions in the network will be simultaneously scheduled. Our discussion is summarized in the following theorem.

Theorem 2.3.1. *(Optimal Access Probability) For a single network operating in isolation under the random access protocol, when $N_i > \Lambda^*$ the optimal access probability is $p_i^* = \frac{\Lambda^*}{N_i}$, where Λ^* is given by the unique solution of equation (2.3). The optimal target* SIR *is $\beta_i^* = \Lambda^{*-\alpha/2}$.*

When $N_i \leq \Lambda^*$, $p_i^* = 1$ and β_i^* is given by the unique solution to

$$\frac{\alpha}{2N_i\beta_i^{*2/\alpha}} = \left(1 + \frac{1}{\beta_i^*}\right) \log(1 + \beta_i^*).$$

The region satisfying $N_i > \Lambda^*$ is referred to as the *partial* reuse regime. The complement region is referred to as the *full reuse* regime. Note the optimal access probability

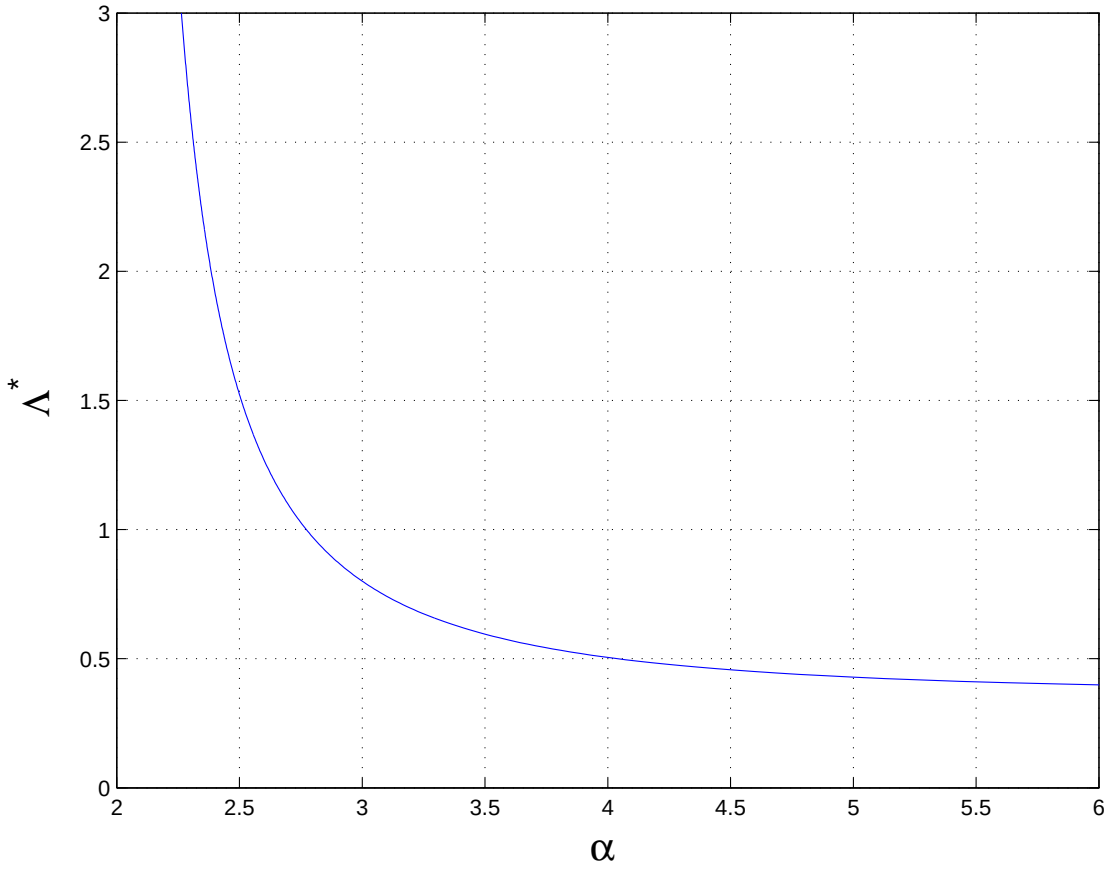

Figure 2.1: Optimal average number of transmissions per transmission disc as a function of the pathloss exponent.

of the above theorem is equivalent to the results of section IV.B in [15], and those discussed under the title *"Maximum Achievable Spatial Throughput and TC"* on page 4137 of [29].

Now we perform the same computation for the case where both networks operate on the same unlicensed band. In this case there is both *intra-network* and *inter-network* interference. It is straightforward to extend the above analysis to show that for network i

$$\mathbb{E}\overline{R}_i \to \frac{\Lambda_i}{N_i} \log(1+\beta_i) e^{-(\Lambda_1+\Lambda_2)\beta_i^{2/\alpha}}$$

in the limit $n \to \infty$. For a given Λ_2 the first network can optimize Λ_1 and β_1, and vice-versa. That is each network can iteratively adjust its access probability and target SIR in response to the other networks. In this sense a game can be defined between the two networks. A strategy for network i is a choice of $\Lambda_i \in [0, N_i]$ and $\beta_i > 0$. Its payoff function (also referred to as *utility function*) is the limiting form of $\mathbb{E}\overline{R}_i$ times N_i,

$$U_1\left((\Lambda_1,\beta_1),(\Lambda_2,\beta_2)\right) = \Lambda_1 \log(1+\beta_1) e^{-(\Lambda_1+\Lambda_2)\beta_1^{2/\alpha}} \tag{2.4}$$

$$U_2\left((\Lambda_1,\beta_1),(\Lambda_2,\beta_2)\right) = \Lambda_2 \log(1+\beta_2) e^{-(\Lambda_1+\Lambda_2)\beta_2^{2/\alpha}}. \tag{2.5}$$

Here we have scaled the throughput by N_i to emphasize the simple form of the payoff functions. At first glance this setup seems desirable but there is a redundancy in the way the strategy space has been defined. The problem is that the variable β_i only appears in U_i and thus should be optimized over separately rather than being included as part of the strategy. This leads to the following game setup.

Definition 2.3.2. *(Random Access Game) A strategy for network i in the Random*

Access Game is a choice of $\Lambda_i \in [0, N_i]$. *The payoff functions are*

$$U_1(\Lambda_1, \Lambda_2) = \max_{\beta_1 > 0} \Lambda_1 \log(1 + \beta_1) e^{-(\Lambda_1 + \Lambda_2)\beta_1^{2/\alpha}}$$
$$U_2(\Lambda_1, \Lambda_2) = \max_{\beta_2 > 0} \Lambda_2 \log(1 + \beta_2) e^{-(\Lambda_1 + \Lambda_2)\beta_2^{2/\alpha}}.$$

The above formulation is intuitively appealing as a networks choice of access probability constitutes its entire strategy. If we could explicitly solve the maximization problems, the variables β_i would be removed altogether. When Λ_1 and Λ_2 are large this can be done and

$$U_1(\Lambda_1, \Lambda_2) \approx \frac{\Lambda_1}{(\Lambda_1 + \Lambda_2)^{\alpha/2}} \cdot (\alpha/2)^{\alpha/2} e^{-\alpha/2} \tag{2.6}$$
$$U_2(\Lambda_1, \Lambda_2) \approx \frac{\Lambda_2}{(\Lambda_1 + \Lambda_2)^{\alpha/2}} \cdot (\alpha/2)^{\alpha/2} e^{-\alpha/2}, \tag{2.7}$$

but in general it is not possible. Instead, since we are only interested in analyzing the Nash equilibrium (N.E.) or equilibria of this game, we do the following.

Observe that the objective function within the maximization is smooth and continuous. This enables the order of maximization to be swapped. That is, for a given Λ_2, we first maximize over Λ_1 in equation (2.4) and then over the β_1. Likewise for equation (2.5). The benefit of this approach is that the maximizing Λ_i can be explicitly expressed as a function of β_i. This was demonstrated earlier for the single

network scenario. The resulting expressions are

$$U_1(\Lambda_1, \Lambda_2)$$
$$= \begin{cases} \Lambda_1 \log\left(1 + \Lambda_1^{-\alpha/2}\right) e^{-\Lambda_2/\Lambda_1 - 1}, & \Lambda_1 < N_1; \\ \max_{\beta_1 > 0} \log(1+\beta_1) e^{-(N_1+\Lambda_2)\beta_1^{2/\alpha}}, & \Lambda_1 = N_1. \end{cases}$$

$$U_2(\Lambda_1, \Lambda_2)$$
$$= \begin{cases} \Lambda_2 \log\left(1 + \Lambda_2^{-\alpha/2}\right) e^{-\Lambda_1/\Lambda_2 - 1}, & \Lambda_2 < N_2; \\ \max_{\beta_2 > 0} \log(1+\beta_2) e^{-(N_2+\Lambda_1)\beta_2^{2/\alpha}}, & \Lambda_2 = N_2. \end{cases}$$

The set of N.E. of the above game and their corresponding values of U_1 and U_2 are identical to those of the Random Access Game. Inspection of the above equations reveals a further simplification of the problem is at hand —the set of N.E. of the above game are identical to the set of N.E. of the following game (though the values of U_1 and U_2 at the equilibria may be different).

Definition 2.3.3. *(Transformed Random Access Game) A strategy for network i in the Transformed Random Access Game is a choice of $\Lambda_i \in [0, N_i]$. The payoff functions are*

$$U_1(\Lambda_1, \Lambda_2) = \Lambda_1 \log\left(1 + \Lambda_1^{-\alpha/2}\right) e^{-\frac{\Lambda_2}{\Lambda_1} - 1}$$
$$U_2(\Lambda_1, \Lambda_2) = \Lambda_2 \log\left(1 + \Lambda_2^{-\alpha/2}\right) e^{-\frac{\Lambda_1}{\Lambda_2} - 1},$$

We now analyze the N.E. of the Random Access Game by analyzing the N.E. of the Transformed Random Access Game. The first question of interest is whether or not there exists a N.E.? It turns out a unique N.E. always exists but its nature depends crucially on the pathloss exponent. There are two *modes*, $2 < \alpha < 4$ and

$\alpha > 4$. We start with the first.

Theorem 2.3.4. *(Random Access N.E. for $2 < \alpha < 4$) For $2 < \alpha < 4$ the unique N.E. occurs at $\Lambda_1^* = N_1$, and Λ_2^* defined by either the solution of*

$$N_1 = \Lambda_2 \left(\frac{\alpha}{2\left(1 + {\Lambda_2}^{\alpha/2}\right) \log\left(1 + {\Lambda_2}^{-\alpha/2}\right)} - 1 \right) \tag{2.8}$$

or N_1, whichever is smaller.

The N.E. described in theorem 2.3.4 occurs on the boundary of the strategy space. This is because for $2 < \alpha < 4$ each network tries to set its number of transmissions per disc higher than the other (see the proof of the theorem). The equilibrium is then only attained when at least one network has maxed out and scheduled all of its transmissions simultaneously.

The N.E. can be better understood when $N_1 \gg 1$ corresponding to the case in which transmissions span several intermediate nodes.

Theorem 2.3.5. *(Random Access N.E. for $2 < \alpha < 4$ and $N_1 \gg 1$) In the limit $N_1 \to \infty$ the N.E. occurs at*

$$(\Lambda_1^*, \Lambda_2^*) = \begin{cases} (N_1, N_2), & N_1 \leq N_2 \leq \dfrac{2}{\alpha - 2} N_1 \\ \left(N_1, \dfrac{2}{\alpha - 2} N_1\right), & \dfrac{2}{\alpha - 2} N_1 \leq N_2. \end{cases}$$

This result stems from using the limiting form $\log(1 + x) \to x$ as $x \to 0$ in the utility functions U_1 and U_2, as was done in equations (2.6) and (2.7). From it we see that if the denser network has more than $\approx 2/(\alpha - 2)$ times as many nodes as its rival, the N.E. will correspond to partial reuse, i.e. the denser network will only

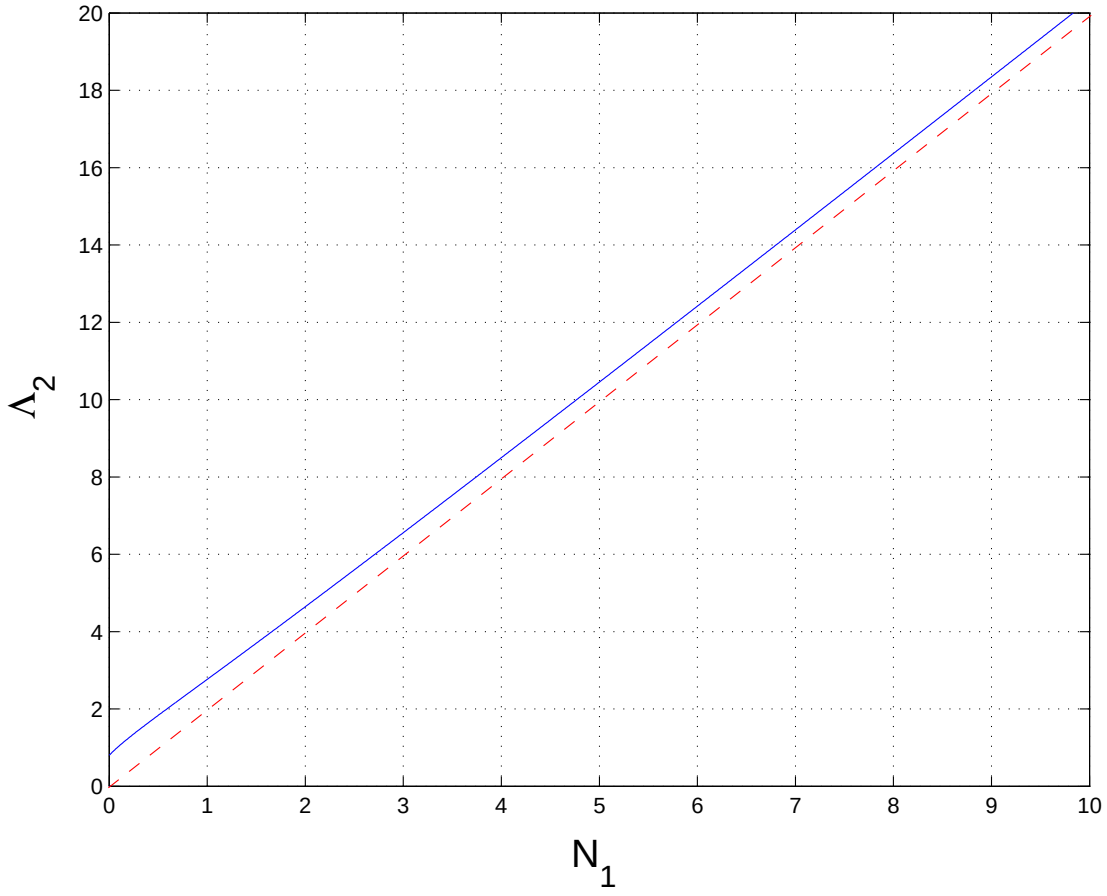

Figure 2.2: The solid line represents the solution to equation (2.8) for $\alpha = 3$. The N.E. value Λ_2^* is equal to the minimum of this line and N_2. The limiting solution used in theorem **??** is plotted as a dashed line.

occupy a fraction of the total available bandwidth. This is in stark contrast to the case of competing *individual transmissions* where the N.E. typically corresponds to a full spread, i.e. both competing links spread their power evenly across the entire bandwidth. The limit result of theorem **??** is plotted in figure 2.2 as a dashed line.

We now investigate the average throughput at equilibrium for the mode $2 < \alpha < 4$. We define the metric

$$U_e = U_1(\Lambda_1^*, \Lambda_2^*) + U_2(\Lambda_1^*, \Lambda_2^*)$$

This quantity has a natural interpretation. Recall $\mathbb{E}\overline{R}_i$ is the average throughput per tx-rx pair and N_i is the average number of tx-rx pairs per transmission disc in network i. Thus $U_i = N_i\mathbb{E}\overline{R}_i$ is the *average throughput per transmission disc* in network i. This is the average number of bits successfully received in network i within an area of size πd^2 per time slot, per d.o.f.. The quantity U_e is then the average throughput per transmission disc in the system, that is, the average number of bits successfully received *in both networks* within an area of size πd^2 per time slot, per d.o.f..

Theorem 2.3.6. *In the limit* $N_1 \to \infty$

$$U_e \to \begin{cases} \dfrac{c_1(\alpha)}{N_1^{\alpha/2-1}} & N_1 \le N_2 \le \frac{2}{\alpha-2}N_1 \\ \dfrac{c_2(\alpha)}{(N_1+N_2)^{\alpha/2-1}}, & \frac{2}{\alpha-2}N_1 \le N_2. \end{cases}$$

where $c_1(\alpha) = (\alpha/2-1)^{\alpha/2-1}\,(\alpha/2)e^{-\alpha/2}$ *and* $c_2(\alpha) = (\alpha/2)^{\alpha/2}e^{-\alpha/2}$.

The important property of this result is that as the number of nodes per transmission disc increases, U_e decreases roughly like $1/(N_1+N_2)^{\alpha/2-1}$. Let us compare this to the average throughput per transmission disc in the cooperative case, that is when the two networks behave as if they were a single network with $N_1 + N_2$ nodes per disc. From equation (2.1) this average throughput per disc is

$$U_c = \Lambda^* \log(1 + \Lambda^{*-\alpha/2})$$

which is independent of the number of nodes per disc. Thus as the number of nodes per disc grows, so does the price of anarchy

$$\frac{U_c}{U_e} = O\left(N_1^{\alpha/2-1}\right).$$

For $\alpha > 4$ the N.E. behavior is different. Whereas for $2 < \alpha < 4$ the solution always

lies on the boundary, for $\alpha > 4$ it typically does not.

Theorem 2.3.7. *(Random Access N.E. for $\alpha > 4$) For $\alpha > 4$ the unique N.E. occurs at*

$$(\Lambda_1^*, \Lambda_2^*) = (\sqrt{\Lambda^*(\alpha/2)}, \sqrt{\Lambda^*(\alpha/2)})$$

if $\sqrt{\Lambda^*(\alpha/2)} < N_1$, otherwise $\Lambda_1^* = N_1$ and Λ_2^* is defined by either the solution of equation (2.8) or N_2, whichever is smaller.

A plot of $\sqrt{\Lambda^*(\alpha/2)}$ versus α is given in figure 2.8. The condition $\sqrt{\Lambda^*(\alpha/2)} < N_1$ corresponds to network 1 having more than $\sqrt{\Lambda^*(\alpha/2)}$ nodes per transmission disc. We refer to this as the *partial/partial reuse* regime.

The interpretation of theorem 2.3.7 is that for $\alpha > 4$ in the partial/partial reuse regime, the solution lies in the strict interior of the strategy space. This is because on the boundary of the space network i can improve its throughput by undercutting the transmit density of network j, i.e. setting $\Lambda_i < \Lambda_j$. The symmetry of the N.E. ($\Lambda_1^* = \Lambda_2^*$) then follows by observing the utility functions are symmetric and the solution is unique.

There is a cooperative flavor to this equilibrium in that both networks set their transmission densities to the same level, and this level is comparable to the optimal single network density $\Lambda^*(\alpha)$. Moreover the equilibrium level does not grow with the number of nodes per transmission disc, as it does for $2 < \alpha < 4$. Actual cooperation between networks corresponds to setting the access probability based on equation (2.2), taking into account that the effective node density is $\lambda_1 + \lambda_2$. Thus the cooperative solution is

$$(\Lambda_1^*, \Lambda_2^*) = \left(\frac{\lambda_1}{\lambda_1 + \lambda_2} \Lambda^*, \frac{\lambda_2}{\lambda_1 + \lambda_2} \Lambda^* \right).$$

Under cooperation the average throughput per transmission disc is (from equation

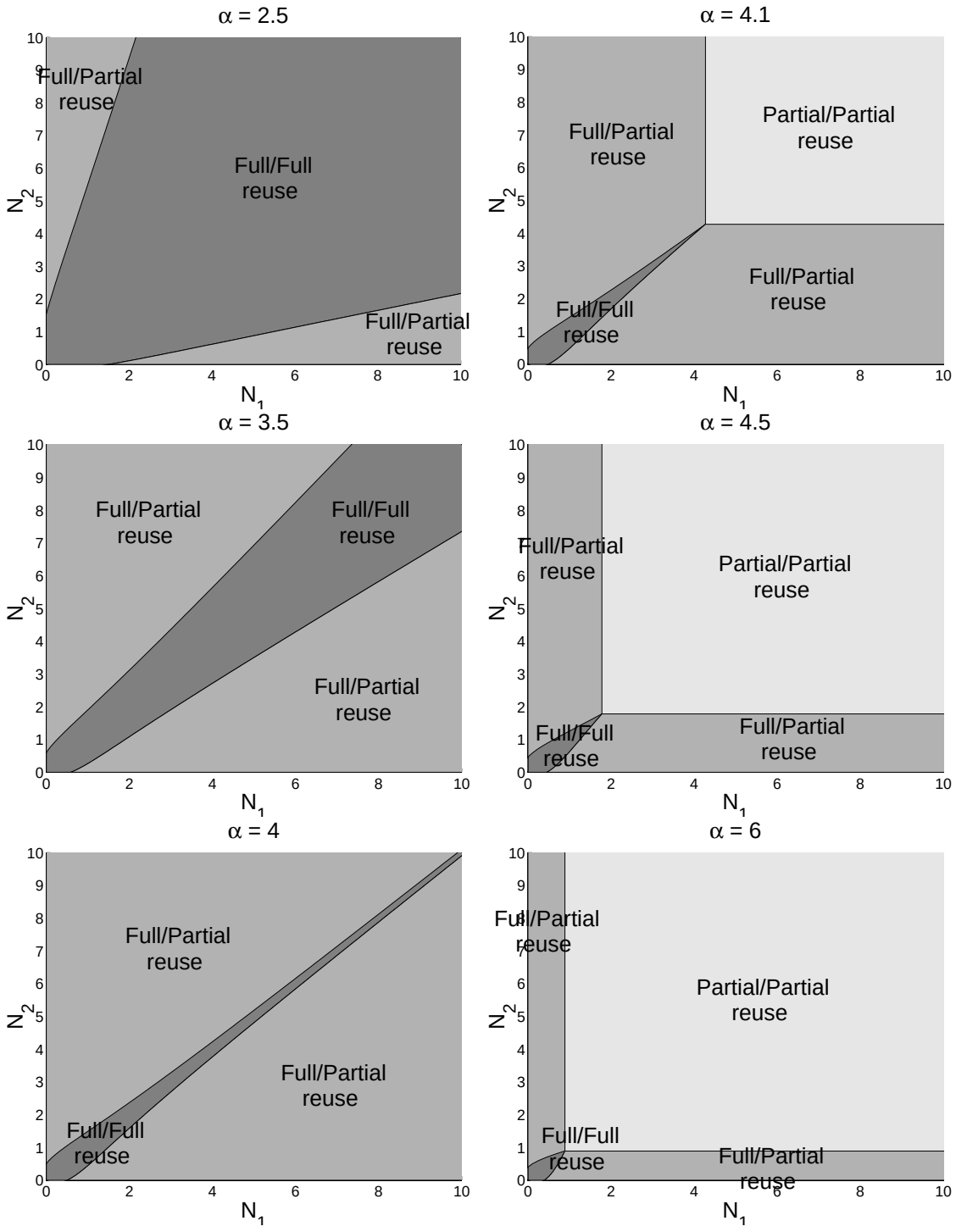

Figure 2.3: These plots can be used to determine which regime the N.E. is in. The x-axis and y-axis corresponds to the average number of nodes per transmission disc in network 1 and 2, respectively. Note the lower left vertex of the partial/partial reuse regime always occurs at $(\sqrt{\Lambda^*(\alpha)}, \sqrt{\Lambda^*(\alpha)})$ and the intersection of the full/full reuse regime with the axes always occurs at $(\Lambda^*(\alpha), 0)$ and $(0, \Lambda^*(\alpha))$.

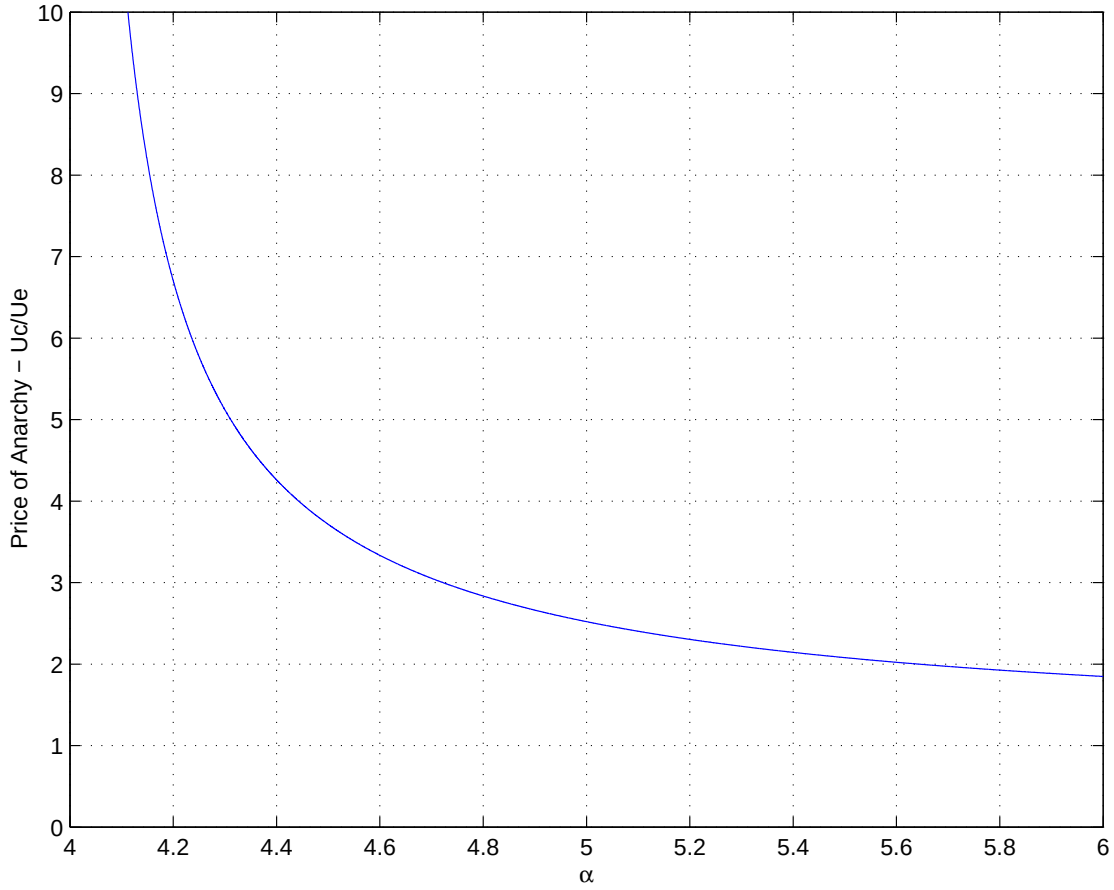

Figure 2.4: For $\alpha > 4$, the price of anarchy depends only on the pathloss exponent in the partial/partial reuse regime.

(2.1))

$$U_c = \frac{1}{e}\Lambda^*(\alpha)\log\left(1+\frac{1}{\Lambda^*(\alpha)^{\alpha/2}}\right).$$

Under cooperation in the partial/partial reuse regime it is

$$U_e = \frac{2}{e^2}\sqrt{\Lambda^*(\alpha/2)}\log\left(1+\frac{1}{\Lambda^*(\alpha/2)^{\alpha/4}}\right)$$

The price of anarchy is the ratio of these two quantities (U_e/U_c) and is plotted in figure 2.4. Comparing the two modes we see that whereas for $2 < \alpha < 4$ the price of

anarchy grows in an unbounded fashion with the number of nodes per transmission disc, for $\alpha > 4$ the price of anarchy in the partial/partial reuse regime is a constant depending only on α.

We now summarize the equilibria results. There are three regimes.

1. *Full/Full reuse*
   - $N_1 \leq \sqrt{\Lambda^*(\alpha/2)}$ and $N_1 \leq N_2 \left(\alpha/2(1+{N_2}^{\alpha/2})\log(1+{N_2}^{-\alpha/2}) - 1\right)$
   - both networks schedule all transmissions

2. *Full/Partial reuse*
   - $N_1 \leq \sqrt{\Lambda^*(\alpha/2)}$ and $N_1 > N_2 \left(\alpha/2(1+{N_2}^{\alpha/2})\log(1+{N_2}^{-\alpha/2}) - 1\right)$
   - denser network schedules all transmissions, sparser schedules only a fraction

3. *Partial/Partial reuse*
   - $N_1 > \sqrt{\Lambda^*(\alpha/2)}$
   - both networks schedule only a fraction of their transmissions

In the full/full reuse regime $(\Lambda_1^*, \Lambda_2^*) = (N_1, N_2)$. In the full/partial reuse regime the sparser network sets $\Lambda_1^* = N_1$ and the denser network sets Λ_2^* as the solution to equation (2.8). In the partial/partial reuse regime $(\Lambda_1^*, \Lambda_2^*) = (\sqrt{\Lambda^*(\alpha/2)}, \sqrt{\Lambda^*(\alpha/2)})$.

The regimes are essentially distinguished by which boundary constraints are active. For $2 < \alpha < 4$ the partial/partial reuse regime is not accessible. Figure 2.3 provides an illustrated means for determining which regime the system is in, for a range of values of the pathloss exponent. In these plots we consider all values of N_1 and N_2, not just those satisfying $N_1 \geq N_2$. Notice that as $\alpha \to 2$ the entire region corresponds to the full/full reuse regime, for $\alpha = 4$ almost the entire region corresponds to the full/partial reuse regime and for $\alpha \to \infty$ the entire region corresponds to the partial/partial reuse regime.

2.3.2 Variable-Rate model

In this section we examine the case where tx-rx pairs tailor their communication rates to suit instantaneous channel conditions, sending at rate $\log(1 + \mathsf{SIR}(\mathsf{t}))$ during the tth time slot. Various protocols can be used to enable tx-rx pairs to estimate their $\mathsf{SIR}(t)$.

Consider first the single, isolated network scenario. The expected time-averaged rate per user is now

$$\mathbb{E}\overline{R}_i = p_i \mathbb{E} \log(1 + \mathsf{SIR}).$$

As before, the rate is both time-averaged over the interference and averaged over the geographic distribution of the nodes. The SIR is the instantaneous value observed by a given rx node and is distributed according to

$$\begin{aligned} \mathbb{P}(\mathsf{SIR} > x) &= \mathbb{P}(r > x^{1/\alpha} d) \\ &= \left(1 - \frac{\pi x^{2/\alpha} d^2 p_i}{n}\right)^{n\lambda_i} \end{aligned}$$

where the variable r denotes the distance to the nearest interferer. Thus

$$\begin{aligned} \mathbb{E}\overline{R}_i &= p_i \int \mathbb{P}\left(\log(1 + \mathsf{SINR}) > s\right) ds \\ &= p_i \int \mathbb{P}\left(\mathsf{SINR} > x\right) \frac{dx}{1+x} \\ &= p_i \int_0^{\left(\frac{n}{p_i \pi d^2}\right)^{\alpha/2}} \left(1 - \frac{\pi x^{2/\alpha} d^2 p_i}{n}\right)^{n\lambda_i} \frac{dx}{1+x} \\ &\to p_i \int_0^{\infty} e^{-\pi p_i \lambda_i d^2 x^{2/\alpha}} \frac{dx}{1+x} \end{aligned}$$

in the limit $n \to \infty$. Changing variables and optimizing we have

$$\mathbb{E}\overline{R}_i \to \frac{1}{N_i} \max_{0 \le \Lambda_i \le 1} \Lambda_i \int_0^\infty e^{-\Lambda_i x^{2/\alpha}} \frac{dx}{1+x}. \tag{2.9}$$

Define $\Lambda'(\alpha)$ as the maximizing argument of the unconstrained version of the above optimization problem, or more specifically as the unique solution to

$$\int_0^\infty \frac{1 - \Lambda' x^{2/\alpha}}{1+x} e^{-\Lambda x^{2/\alpha}} dx = 0.$$

The function $\Lambda'(\alpha)$ is plotted in figure 2.8. Then

$$p_i^* = \min(\Lambda'(\alpha)/N_i, 1)$$

From this we see that the solution for the variable-rate case is the same as the fixed-rate solution, differing only by substitution of the function $\Lambda'(\alpha)$ for $\Lambda^*(\alpha)$.

Now we turn to the case of two competing wireless networks. Using an approach similar to the one above it can be shown that

$$\mathbb{E}\overline{R}_i \to \frac{1}{N_i} \Lambda_i \int_0^\infty e^{-(\Lambda_1+\Lambda_2)x^{2/\alpha}} \frac{dx}{1+x}.$$

In this way we can define the game between the two networks like so.

Definition 2.3.8. *(Variable Rate Random Access Game) A strategy for network i in the Variable Rate Random Access Game is a choice of* $\Lambda_i \in [0, \pi\lambda_i d^2]$. *The payoff functions are*

$$U_1(\Lambda_1, \Lambda_2) = \Lambda_1 \int_0^\infty e^{-(\Lambda_1+\Lambda_2)x^{2/\alpha}} \frac{dx}{1+x}$$
$$U_2(\Lambda_1, \Lambda_2) = \Lambda_2 \int_0^\infty e^{-(\Lambda_1+\Lambda_2)x^{2/\alpha}} \frac{dx}{1+x}.$$

From the above definition we see that the Fixed-Rate game is derived from the Variable-Rate game by merely applying a step-function lower bound to the players utility functions, with the width of the step-function optimized, i.e.

$$\begin{aligned}\int_0^\infty e^{-(\Lambda_1+\Lambda_2)x^{2/\alpha}} \frac{dx}{1+x} \\ &\geq \max_{\beta_i>0} e^{-(\Lambda_1+\Lambda_2)\beta_i^{2/\alpha}} \int_0^{\beta_i} \frac{dx}{1+x} \\ &= \max_{\beta_i>0} \log(1+\beta_i) e^{-(\Lambda_1+\Lambda_2)\beta_i^{2/\alpha}}.\end{aligned}$$

A plot comparing the expression on the left as a function of $\Lambda_1+\Lambda_2$, to the expression on the right as a function of $\Lambda_1+\Lambda_2$, for $\alpha=4$, is presented in figure 2.5. The figure suggests that both expressions share a similar functional dependency on $\Lambda_1+\Lambda_2$. It is therefore natural to wonder whether, as a consequence of this close relationship, the N.E. of the Variable-Rate game bears any relationship to the N.E. of the Fixed-Rate game?

As in the Fixed-Rate game, the utility functions of the Variable-Rate game can be explicitly evaluated when Λ_1 and Λ_2 are large yielding

$$\begin{aligned}U_1(\Lambda_1,\Lambda_2) &\approx \frac{\Lambda_1}{(\Lambda_1+\Lambda_2)^{\alpha/2}} \cdot \Gamma(\alpha/2+1) \\ U_2(\Lambda_1,\Lambda_2) &\approx \frac{\Lambda_2}{(\Lambda_1+\Lambda_2)^{\alpha/2}} \cdot \Gamma(\alpha/2+1).\end{aligned}$$

Comparing with equations (2.4) and (2.5) we see that for large Λ_1, Λ_2, the utility functions of the Variable-Rate game have exactly the same functional dependency on Λ_1, Λ_2 as the utility functions of the Fixed-Rate game, differing only in an α-dependent constant. These constants are plotted in figure 2.6. The plots illustrate the benefit in total system throughput that stems from playing the Variable-rate game in place of the Fixed-Rate game.

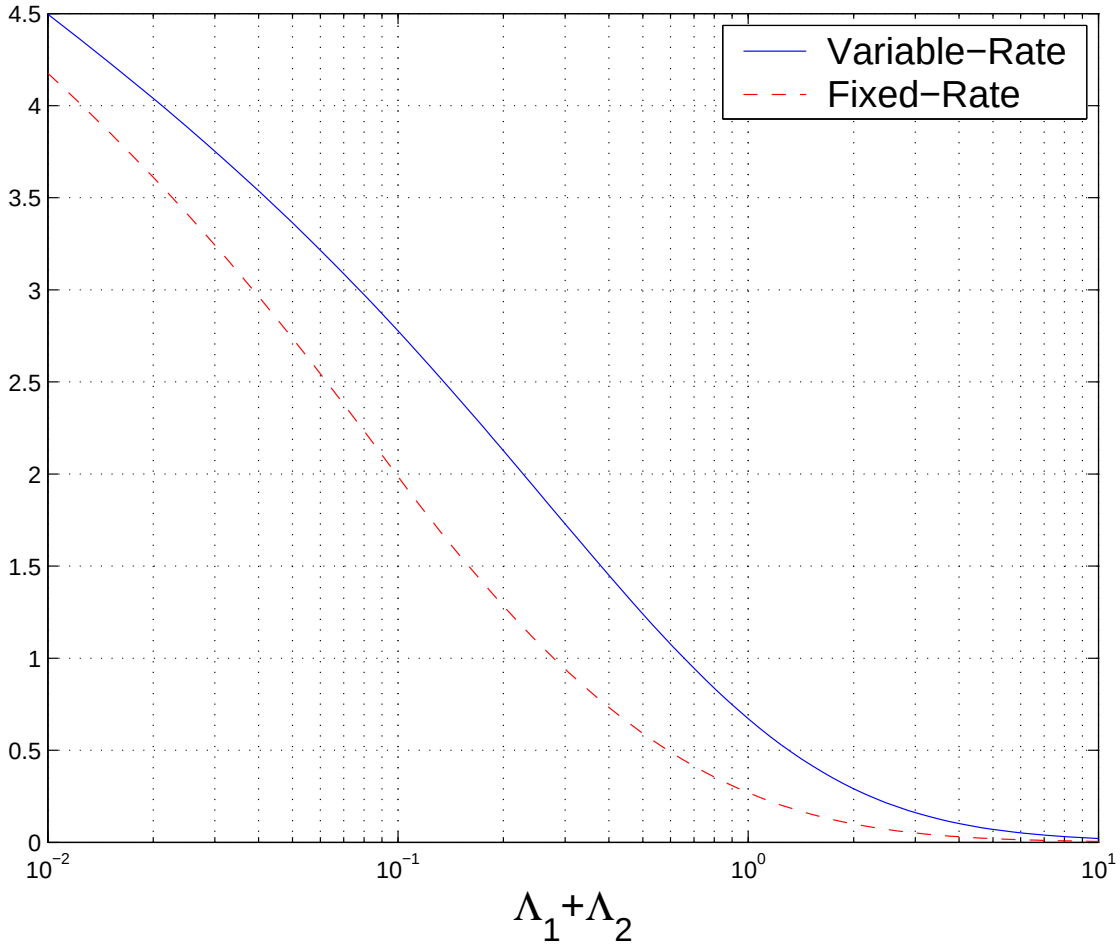

Figure 2.5: The utility functions used in the Fixed-Rate model are lower bounds of those used in the Variable-Rate model. In this sample plot $\alpha = 4$. The y-axis represents U_i/Λ_i.

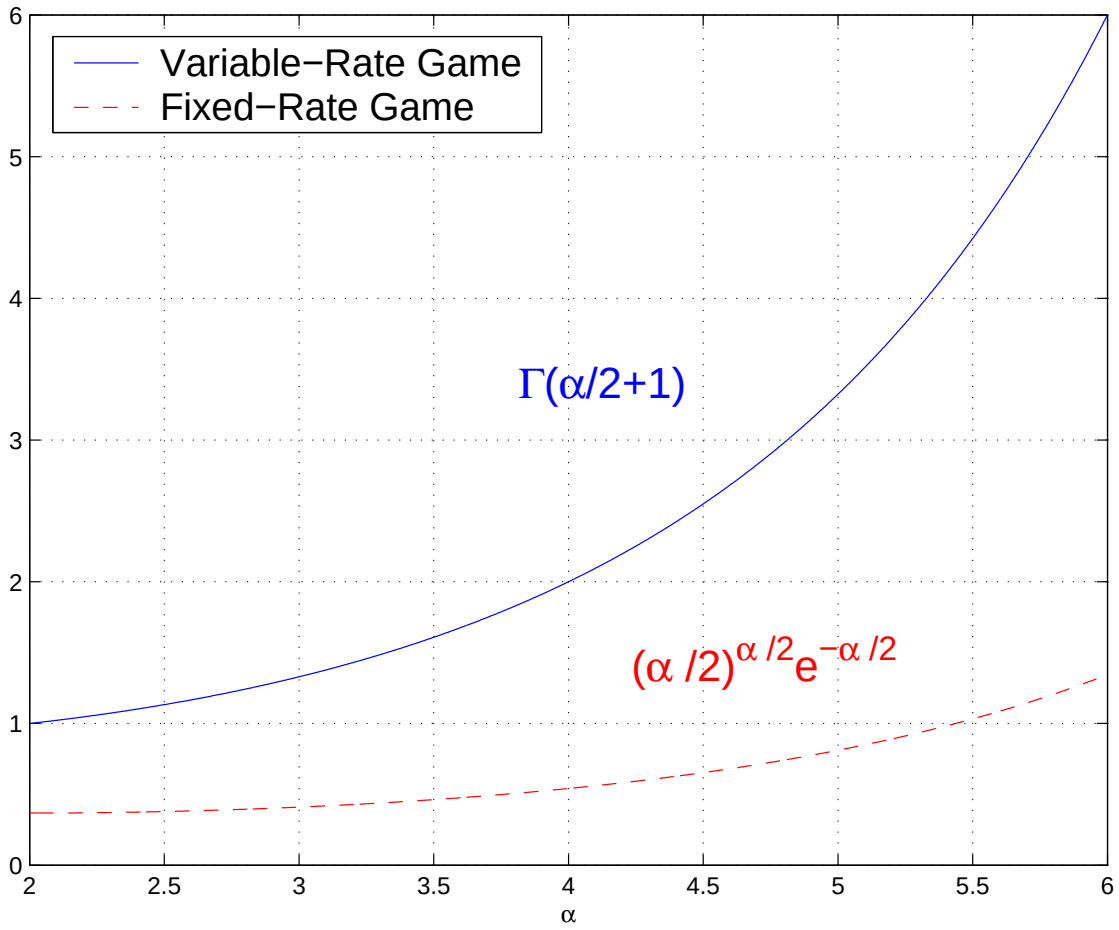

Figure 2.6: The total system throughputs at equilibrium for the Variable-Rate and Fixed-Rate games differ only by α-dependent constants. These constants are plotted above. For the Variable-Rate game the constant is $\Gamma(\alpha/2+1)$ versus $(\alpha/2)^{\alpha/2}e^{-\alpha/2}$ for the Fixed-Rate game.

As anticipated by the above discussion, the N.E. behavior of the Variable-Rate game parallels that of the Fixed-Rate game. The same two modes are present, $2 < \alpha < 4$ and $\alpha > 4$. These give rise to the same three spreading regimes, the only difference being that the boundaries delineating them are shifted slightly. The N.E. values $(\Lambda_1^*, \Lambda_2^*)$ in each regime take on a similar form.

Theorem 2.3.9. *The Variable-Rate Random Access Game has a unique N.E.* $(\Lambda_1^*, \Lambda_2^*)$ *which lies in one of three regions. Let* $\Lambda''(\alpha)$ *be the unique solution of*

$$\int_0^\infty \frac{1 - \Lambda'' x^{2/\alpha}}{1+x} e^{-2\Lambda'' x^{2/\alpha}} dx = 0. \tag{2.10}$$

for $\alpha > 4$*, and equal to positive infinity for* $\alpha \leq 4$*.*

- *(Full/Full reuse) If* $N_1 \leq \Lambda''(\alpha)$ *and* $N_2 \leq$ *the unique solution over* Λ *of*

$$\int_0^\infty \frac{1 - \Lambda x^{2/\alpha}}{1+x} e^{-(N_1+\Lambda)x^{2/\alpha}} dx = 0, \tag{2.11}$$

  then $(\Lambda_1^*, \Lambda_2^*) = (N_1, N_2)$*.*

- *(Full/Partial reuse) If* $N_1 \leq \Lambda''(\alpha)$ *and* $N_2 >$ *the unique solution of equation (2.11) then* $\Lambda_1^* = 1$ *and* Λ_2^* *is equal to this unique solution.*

- *(Partial/Partial reuse) If* $N_1 > \Lambda''(\alpha)$ *then* $(\Lambda_1^*, \Lambda_2^*) = (\Lambda''(\alpha), \Lambda''(\alpha))$*.*

A regime map is provided in figure 2.7. As is evident from the above theorem, it is not possible to characterize the behavior of the N.E. for the Variable-Rate game as explicitly as for the Fixed-Rate game. This is in part due to the more complex representation of the utility functions in terms of integrals, and in part due to the fact that the the function $\Lambda''(\alpha)$ cannot be represented in terms of the function $\Lambda'(\alpha)$, as in the case of the Fixed-Rate game, where one function equals the square-root of the other evaluated at $\alpha/2$.

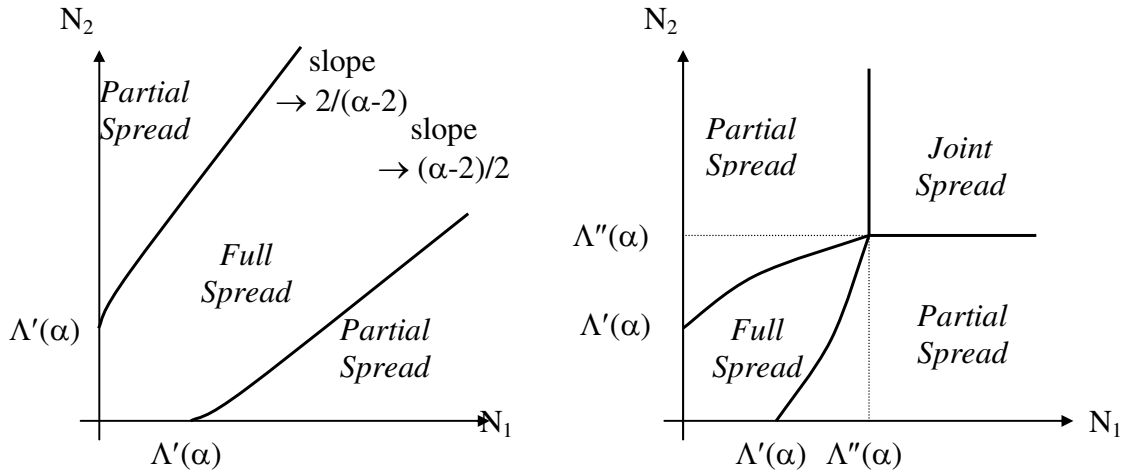

Figure 2.7: The three regimes for the N.E. of the Variable-Rate Game.

For large N_1 however, we can use the approximation adopted in theorem **??** to explicitly characterize the behavior of the N.E. in the full/partial reuse regime.

Theorem 2.3.10. *(Variable-Rate Random Access N.E. for $2 < \alpha < 4$ and $N_1 \gg 1$) In the limit $N_1 \to \infty$ the N.E. occurs at*

$$(\Lambda_1^*, \Lambda_2^*) = \begin{cases} (N_1, N_2), & N_1 \le N_2 \le \dfrac{2}{\alpha-2} N_1 \\ \left(N_1, \dfrac{2}{\alpha-2} N_1\right), & \dfrac{2}{\alpha-2} N_1 \le N_2. \end{cases}$$

Thus for $2 < \alpha < 4$ and large N_1, the behavior of the N.E. in the Variable-Rate game is identical to that of the Fixed-Rate game. As discussed earlier, the values of U_1 and U_2 at equilibrium are equal to those of the Fixed-Rate game times a constant $(\alpha/2)^{\alpha/2} e^{-\alpha/2} / \Gamma(\alpha/2+1)$.

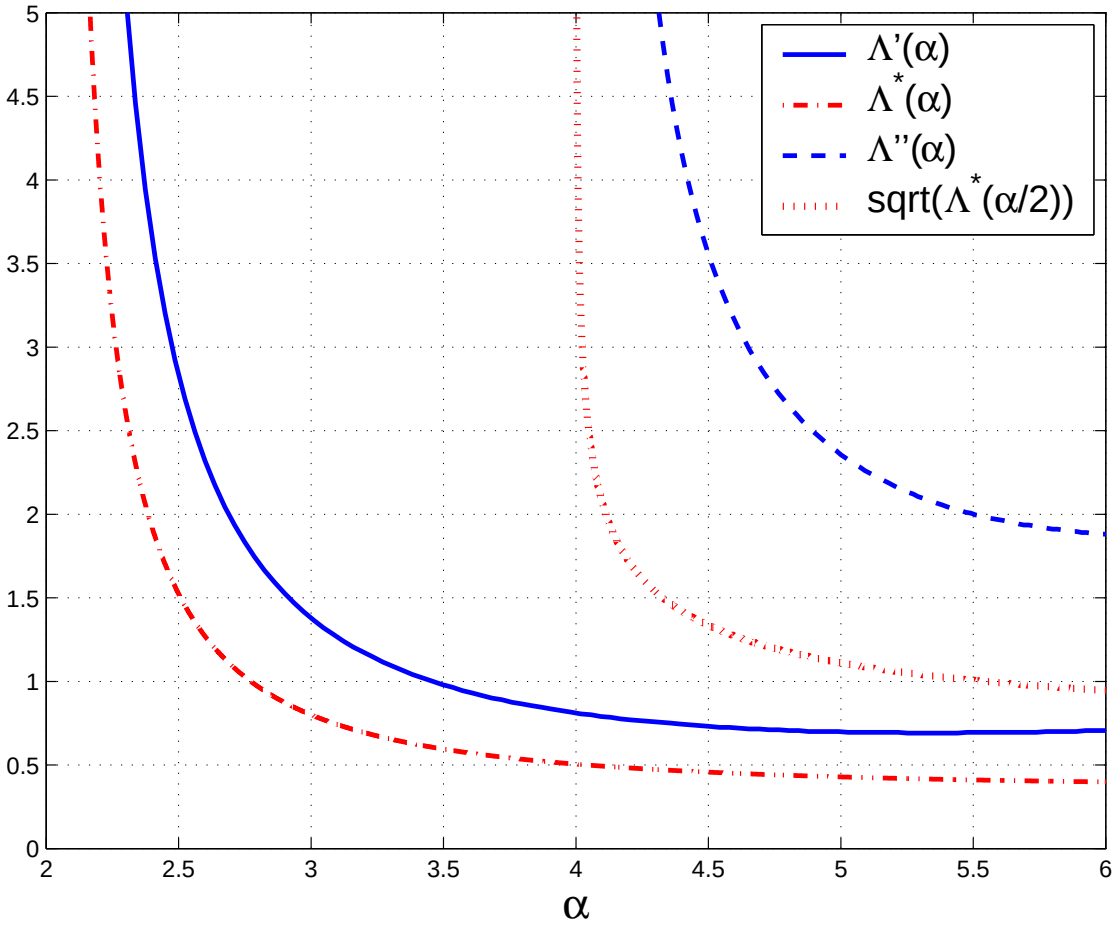

Figure 2.8: The functions $\Lambda''(\alpha)$ and $\Lambda'(\alpha)$ for the Variable-Rate model versus the equivalent functions $\Lambda^*(\alpha)$ and $\sqrt{(}\Lambda^*(\alpha/2))$ for the Fixed-Rate model.

2.3.3 Explanation of Behavior

The intuition behind our result is the following. The average throughput per link is essentially equal to the product of the fraction of time transmissions are scheduled, and the average number of bits successfully communicated per transmission. Adjusting the transmit density has a linear effect on the former term, but a non-linear effect on the latter. The latter depends on the SIR and the SIR essentially depends on the pathloss exponent via

$$\mathsf{SIR} \approx \left(\frac{\text{distance to transmitter}}{\text{distance to interferer}} \right)^{\alpha}$$

When the nearest interferer is closer than the transmitter, the ratio inside the parentheses is less than one, and a large value of α substantially hurts the SIR, dragging it to near zero and causing the link capacity to drop to near zero. However, when the nearest interferer is further away than the transmitter, the ratio is greater than one and a large value of α substantially improves the SIR, resulting in a large link capacity. Thus for large α the average number of bits successfully communicated per transmission is very sensitive to whether or not the transmission disc is empty.

This insensitivity for sufficiently small α means that increasing the transmit density in network i causes a linear increase in the fraction of time transmissions are scheduled, but has little effect on the number of bits successfully communicated per transmission, up until the point where the transmit density of network i starts to dwarf the transmit density of network j. Thus network i will wish to increase its transmit density until it is sufficiently larger than network j's. Likewise network j will wish to increase its transmit density until it is sufficiently larger than network i's. Ultimately this results in either

1. a full/full reuse solution, which occurs when the sparser network max's out

and winds up simultaneously scheduling all of its transmissions, and the denser network is insufficiently dense such that its optimal transmit density based on the sparser networks choice, results in it simultaneously scheduling all of its transmissions, or

2. a full/partial reuse solution, which occurs when the sparser network max's out and winds up simultaneously scheduling all of its transmissions but the denser network is sufficiently dense such that its optimal transmit density based on the sparser networks choice, results in it simultaneously scheduling only a fraction of its transmissions.

The opposite effect occurs for sufficiently large α, where the average number of bits successfully communicated per transmission depends critically on whether or not there is an interferer inside the transmission disc. In this scenario network i will set its active density to a level lower than network j's, in order to capitalize on those instances in which network j happens to not schedule any transmissions nearby to one of network i's receivers, resulting in the successful communication of a large number of bits. Likewise network j will set its active density to a level lower than network i's, and the system converges to the partial/partial reuse regime.

2.4 Variable Transmission Range

One of our initial assumptions was that all tx-rx pairs have the same transmission range d. In this section we consider the scenario where the transmission ranges of all tx-rx pairs in the system are i.i.d. random variables D_j. When the variance of D_j is large, some form of power control may be required to ensure long range transmissions are not unfairly penalized. A natural form of power control involves tx nodes setting their transmit powers such that all transmissions are received at the same SNR. This

means transmit power scales proportional to D_j^α. Denote the distance from the kth tx node to the jth rx node D_{ij}. Then the interference power from the kth tx node impinging on the jth rx node is proportional to $D_{kk}^\alpha / D_{kj}^\alpha$. In the fixed transmission range scenario this quantity was proportional to $1/D_{kj}^\alpha$. There we assumed the bulk of the interference was generated by the dominant interferer. Denote the scheduled set of tx nodes at time t by $\mathcal{A}(t)$. This assumption essentially evoked the following approximation

$$\sum_{k \in \mathcal{A}(\sqcup)} 1/D_{kj}(t)^\alpha \approx \max_{k \in \mathcal{A}(\sqcup)} 1/D_{kj}(t)^\alpha.$$

The equivalent approximation for the variable transmission range problem is

$$\sum_{k \in \mathcal{A}(\sqcup)} D_{kk}^\alpha / D_{kj}(t)^\alpha \approx \max_{k \in \mathcal{A}(\sqcup)} D_{kk}^\alpha / D_{kj}(t)^\alpha.$$

Thus for variable range transmission the dominant interferer is not necessarily the nearest to the receiver. Under this assumption the SIR at the jth rx node at time t is then

$$\mathsf{SIR}_j(t) = \frac{D_{k^*k^*}^{-\alpha}}{D_{k^*j^*}^{-\alpha}}$$

where k^* is the index of the tx node that is closest to the jth receiver relative to its transmission range.

Let us compute the throughput for the variable transmission range model under the Fixed-Rate Random Access protocol.

$$\mathbb{E}\overline{R} = p_i \mathbb{P}\left(\mathsf{SIR}_j(t) > \beta_i\right) \log(1 + \beta_i).$$

The probability the SIR is greater than the threshold

$$\begin{aligned}
\mathbb{P}(\mathsf{SINR_j(t)} > \beta_\mathsf{i}) &= \mathbb{P}\left(D_{kj} > \beta_i^{1/\alpha} D_{kk}, \forall k\right) \\
&= \left(\int_0^{\sqrt{n/\pi}/\beta_i^{1/\alpha}} \mathbb{P}\left(D_{kj} > \beta_i^{1/\alpha} x\right) \mathbb{P}_{D_{kk}}(x) dx\right)^{n\lambda} \\
&= \left(\int_0^{\sqrt{n/\pi}/\beta_i^{1/\alpha}} \left(1 - \frac{p_i \pi \beta_i^{2/\alpha} x^2}{n}\right) \mathbb{P}_{D_{kk}}(x) dx\right)^{n\lambda} \\
&= \left(1 - \frac{p_i \pi \beta_i^{2/\alpha}}{n} \int_0^{\sqrt{n/\pi}/\beta_i^{1/\alpha}} x^2 \mathbb{P}_{D_{kk}}(x) dx\right)^{n\lambda} \\
&= \left(1 - \frac{p_i \pi \beta_i^{2/\alpha} \mathbb{E} D_{kk}^2}{n}\right)^{n\lambda} \\
&\to e^{-p_i \pi \beta_i^{2/\alpha} \mathbb{E} D_{kk}^2}
\end{aligned}$$

as $n \to \infty$. For notational simplicity let $d \equiv D_{kk}$. If we define N_i as the average number of nodes per transmission disc, where the average is taken over both the geographical distribution of the nodes *and the distribution of the size of the transmission disc*, i.e.

$$N_i = \pi \lambda_i \mathbb{E}_d^2$$

we wind up with $\mathbb{E}\overline{R} \to p_i \log(1+\beta_i) e^{-N_i p_i \beta_i^{2/\alpha}}$, which is the same result as the fixed-transmission range model. It is straightforward to extend the analysis to the case of two competing networks. The throughput per user in network 1 is then

$$\mathbb{E}\overline{R} \to p_1 \log(1+\beta_1) e^{-(N_1 p_1 + N_2 p_2)\beta_1^{2/\alpha}}.$$

Likewise for network 2. From this we see that all results for the fixed-transmission range model extend to the variable-transmission range model by simply replacing d^2 by $\mathbb{E}d^2$.

2.5 Simulations

2.5.1 Random Access Protocol

In order to get a sense of the typical behavior of the players in the (Variable-Rate) Random Access game, and to justify the validity of the Dominant Interferer assumption, we simulate the behavior of the following greedy algorithm with the interference computed based on all transmissions in the network, not just the strongest.

Inputs: $p_1(0), p_2(0), \Delta$

Outputs: $\mathbf{p}_i = [p_i(1), \ldots, p_i(500)]$, for $i = 1, 2$.

For $t = 1$ to 500

Form estimate $\overline{R}_1(p_1(t-1) + \Delta, p_2(t-1))$

Form estimate $\overline{R}_1(p_1(t-1) - \Delta, p_2(t-1))$

If $\overline{R}_1(p_1(t-1) + \Delta, p_2(t-1)) > \overline{R}_1(p_1(t-1) - \Delta, p_2(t-1))$

$p_1(t) = \min(p_1(t-1) + \Delta, 1)$

Else

$p_1(t) = \max(p_1(t-1) - \Delta, 0)$

End

Form estimate $\overline{R}_2(p_1(t), p_2(t-1) + \Delta)$

Form estimate $\overline{R}_2(p_1(t), p_2(t-1) - \Delta)$

If $\overline{R}_2(p_1(t), p_2(t-1) + \Delta) > \overline{R}_2(p_1(t), p_2(t-1) - \Delta)$

$p_2(t) = \min(p_2(t-1) + \Delta, 1)$

Else

$p_2(t) = \max(p_2(t-1) - \Delta, 0)$

End

End

Each update time t, network 1 temporarily sets its access probability to $p_1(t-1)+\Delta$ and measures the resulting throughput, averaged over 200 transmission times. This is denoted $\overline{R}_1(p_1(t-1)+\Delta, p_2(t-1))$. It then repeats this measurement for an access probability of $p_1(t-1)-\Delta$. This is denoted $\overline{R}_1(p_1(t-1)-\Delta, p_2(t-1))$. It then either permanently increases its access probability to $p_1(t) = p_1(t-1) + \Delta$ or permanently decreases it to $p_1(t) = p_1(t-1) - \Delta$ depending on which option it estimates will lead to a higher throughput. Now network 2 performs the same operation. It uses a total of 400 time slots to measure the effect of increasing versus decresing its access probability and then either sets $p_2(t) = p_2(t-1)+\Delta$ or $p_2(t) = p_2(t-1)-\Delta$. If Δ is small, then both networks can perform these measurement operations simultaneously without significantly affecting the outcome.

The topology used in the simulations consisted of 400 tx nodes from network 1 and 200 tx nodes from network 2, all i.i.d. uniformly distributed in a square of unit area. For each tx node, its corresponding rx node was located at a point randomly chosen at uniform from a disc of radius 0.15. This corresponds to $N_1 = 400/\sqrt{(}800) \approx 14.14$ and $N_2 = 200/\sqrt{(}800) \approx 7.28$. A step-size of $\Delta = 0.02$ was used. When computing the throughputs, in order to avoid boundary effects, only transmissions emanating from those tx nodes in the interior of the network were counted. The results for $\alpha = 2.5, 3.5$ and 4.5 are displayed in figure 2.9. The observed behavior corresponds to the analytical results. For the values of N_1 and N_2 used, the N.E. lies in the Full/Full

regime for $\alpha = 2.5$, the Full/Partial regime for $\alpha = 3.5$, and the Partial/Partial regime for $\alpha = 4.5$, as can be seen from figure 2.3.

2.5.2 Carrier Sensing Multiple Access based protocol

The high level conclusion from our analysis of the Random Access protocol, is that the Nash Equilibrium is cooperative in nature for a sufficiently high pathloss exponent. Ideally we would like to be able to draw this conclusion for a more sophisticated class of scheduling protocols employing carrier sensing. Due to the analytical intractability of the problem, we present simulation results to illustrate this effect. We assume both networks operate under the following protocol. We present a centralized version of it due to space constraints, but claim there exists a distributed version that performs identically in most cases. During the scheduling phase, each tx-rx pair is assigned a unique token at random from $\{1, \ldots, n\}$. Tx nodes proceed with their transmission so long as they will not cause excessive interference to any rx node with a higher priority token. More precisely, a transmission is scheduled so long as for each rx node with higher priority, the difference between its received signal power in dB and the interference power from the lower priority tx node in dB, exceeds a silencing threshold γ_i ($i = 1$ for network 1 and $i = 2$ for network 2). Thus a game between the two networks can be defined where the strategies are the choices of silencing thresholds γ_1 and γ_2. We refer to this as the *CSMA game*. The silencing threshold for the CSMA game essentially plays the same role as the access probability in the Random Access game -it determines the degree of spatial reuse. A high value of γ leads to a low density of transmissions, a low value of γ leads to a high density.

We simulate the behavior that arises when both networks optimize their silencing thresholds in a greedy manner. Analogously to before, we have the following algorithm.

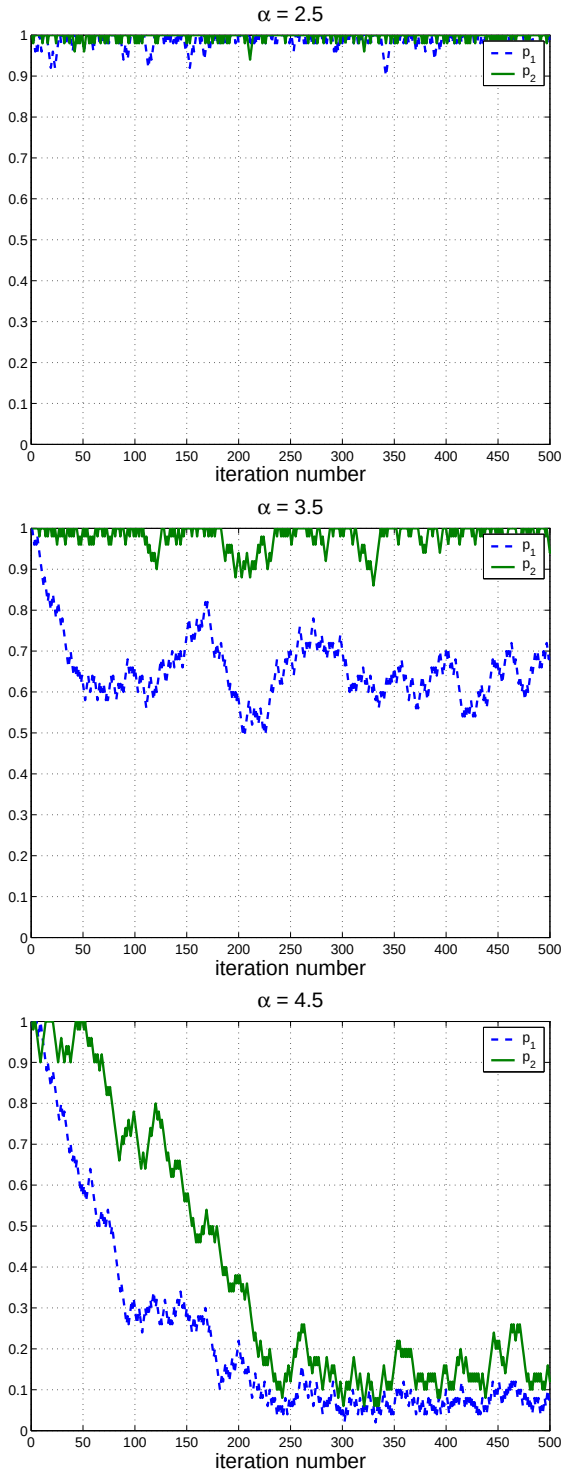

Figure 2.9: Simulations of greedy algorithm under Random Access protocol.

Inputs: $p_1(0), p_2(0), \Delta$

Ouputs: $\mathbf{p}_i = [p_i(1), \ldots, p_i(500)]$, for $i = 1, 2$.

For $t = 1$ to 500

Form estimate $\overline{R}_1(\gamma_1(t-1) + \Delta, \gamma_2(t-1))$

Form estimate $\overline{R}_1(\gamma_1(t-1) - \Delta, \gamma_2(t-1))$

If $\overline{R}_1(\gamma_1(t-1) + \Delta, \gamma_2(t-1)) > \overline{R}_1(\gamma_1(t-1) - \Delta, \gamma_2(t-1))$

$\gamma_1(t) = \min(\gamma_1(t-1) + \Delta, 30\mathsf{dB})$

Else

$\gamma_1(t) = \max(\gamma_1(t-1) - \Delta, -30\mathsf{dB})$

End

Form estimate $\overline{R}_2(\gamma_1(t), \gamma_2(t-1) + \Delta)$

Form estimate $\overline{R}_2(\gamma_1(t), \gamma_2(t-1) - \Delta)$

If $\overline{R}_2(\gamma_1(t), \gamma_2(t-1) + \Delta) > \overline{R}_2(\gamma_1(t), \gamma_2(t-1) - \Delta)$

$\gamma_2(t) = \min(\gamma_2(t-1) + \Delta, 30\mathsf{dB})$

Else

$\gamma_2(t) = \max(\gamma_2(t-1) - \Delta, -30\mathsf{dB})$

End

End

The topology used in the setup is identical to before, the only exception being

that at each iteration of the algorithm, 10 old tx-rx pairs leave each network, and 10 new pairs join in i.i.d. locations drawn uniformly at random. This is to ensure sufficient averaging.

In a similar fashion to before, each network estimates the effect of either increasing or decreasing the silencing threshold and then makes a permanent choice. For the same parameter values, the results of the simulation are displayed in figure 2.10. On the y-axes of these plots we have drawn the fraction of nodes simultaneously scheduled at each iteration, which we denote f_1 and f_2, rather than the silencing thresholds γ_i, in order to draw a simple visual comparison with figure 2.9. For this reason there is more fluctuation in the results, as the fraction of simultaneously scheduled transmissions varies not only due to the up/down movements of the silencing thresholds, but also due to the changing topology.

We conclude from these plots that for small values of α (namely $\alpha = 2.5$) the system converges to a competitive equilibrium, where both networks simultaneously schedule a large fraction of their transmissions, and for large values of α (namely $\alpha = 3.5$ and 4.5) the system converges to a near cooperative equilibrium, where both networks schedule a small fraction of their transmissions.

2.6 Conclusion

This work studied spectrum sharing between wireless devices operating under a random access protocol. The crucial assumption made was that nodes belonging to the same network or coalition cooperate with one another. Competition only exists between nodes belonging to rival networks. It was found that cooperation between devices within each network created the necessary incentive to prevent total anarchy. For pathloss exponents greater than four, we showed that contrary to ones intuition, there can be a natural incentive for devices to cooperate to the extent that each

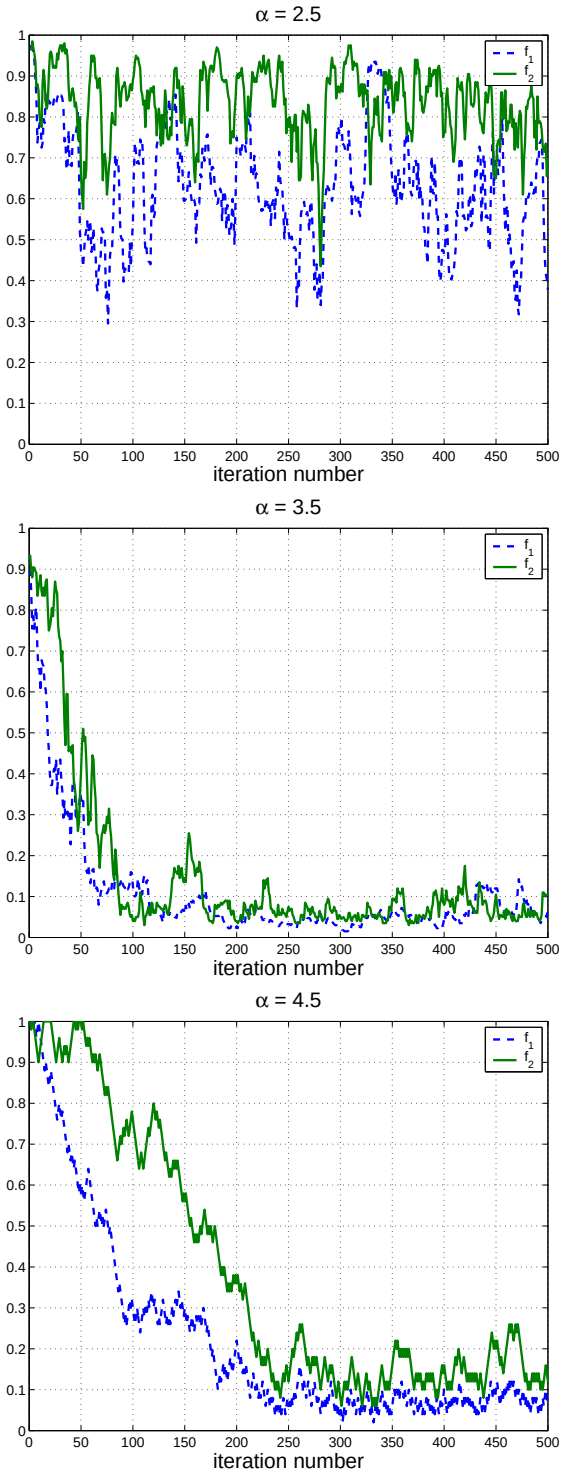

Figure 2.10: Simulations of greedy algorithm under Carrier Sensing Multiple Access protocol

occupies only a fraction of the available bandwidth. Such results are optimistic and encouraging. We demonstrated via simulations that it may be possible to extend them to more complex operating protocols such as those that employ carrier-sensing to determine when the medium is free. More generally one wonders whether a multi-stage game capturing the system dynamics under such a protocol can be formulated, and whether the desirable properties of the single-stage game continue to hold. It would also be worthwhile investigating the incentives wireless links have to form coalitions, as in this work it was in essence assumed that coalitions had been pre-determined.

2.7 Proofs

2.7.1 Theorem 2.3.1

The limiting expression for the average throughput is

$$\mathbb{E}\overline{R}(p_i, \beta_i) \to p_i \log(1+\beta_i) e^{-N_i p_i \beta_i^{2/\alpha}}.$$

Given a β_i there is a single maximum over p_i. By differentiation we have

$$\frac{\partial \mathbb{E}\overline{R}}{\partial p_i} = \left(1 - p_i N_i \beta_i^{2/\alpha}\right) \log(1+\beta_i) e^{-N_i p_i \beta_i^{2/\alpha}},$$

so $p_i^* = \min(1, 1/N_i\beta_i^{2/\alpha})$. Thus

$$\mathbb{E}\overline{R}(p_i^*, \beta_i) = \begin{cases} \log(1+\beta_i)e^{-N_i\beta_i^{2/\alpha}}, & \beta_i \le N_i^{-2/\alpha}, \\ \dfrac{\log(1+\beta_i)e^{-1}}{N_i\beta_i^{2/\alpha}}, & \beta_i > N_i^{-2/\alpha}. \end{cases}$$

Both of these functions have one maximum, but the maximum of the second function is always greater than the maximum of the first as it represents the solution to the

unconstrained problem

$$\max_{p_i>0,\beta_i>0} \mathbb{E}\overline{R}(p_i,\beta_i),$$

whereas the maximum of the first represents the solution to

$$\max_{p_i=1,\beta_i>0} \mathbb{E}\overline{R}(p_i,\beta_i).$$

Thus if the maximum of the second function occurs for $\beta_i > N_i^{-2/\alpha}$, it is the maximum of the entire function, but if it occurs for $\beta_i \leq N^{-2/\alpha}$, the maximum of the entire function is the maximum of the first function over the domain $\beta_i \leq N^{-2/\alpha}$. By differentiation we find the maximum of the second function occurs at the unique solution of

$$\frac{\alpha}{2} = (1+1/\beta_i)\log(1+\beta_i)$$

which is $\beta_i = \Lambda^{*-\alpha/2}$. Thus if $N_i > \Lambda^*$, the solution is $p^* = \Lambda^*/N_i$ and $\beta_i^* = \Lambda^{*-\alpha/2}$. If $N_i \leq \Lambda^*$ the solution is $p^* = 1$ and β_i^* equal to the unique solution of

$$\frac{\alpha}{2N_i\beta_i^{2/\alpha}} = (1+1/\beta_i)\log(1+\beta_i) \tag{2.12}$$

or $N_i^{-2/\alpha}$, whichever is smaller. But as $(1+1/x)\log(1+x)$ is a monotonically increasing function, from the definition of Λ^* we have

$$\frac{\alpha}{2} \leq \left(1+N_i^{\alpha/2}\right)\log\left(1+N_i^{-\alpha/2}\right)$$

whenever $N_i \leq \Lambda^*$. Combining this with equation (2.12) and using the monotonicity of $(1+1/x)\log(1+x)$ we see that the unique solution to equation (2.12) is always smaller than $N_i^{-2/\alpha}$. This establishes the desired result.

2.7.2 Theorem 2.3.4

First we show that any N.E. must lie on the boundary of the strategy space, i.e. $\Lambda_i = 1$ for some i. The utility functions are smooth and continuous. Differentiating U_1 with respect to Λ_1 yields

$$\frac{\partial U_1}{\partial \Lambda_1} = e^{-\Lambda_2/\Lambda_1}\left(\frac{\Lambda_2}{\Lambda_1} - \frac{\alpha}{2\left(1+\Lambda_1^{\alpha/2}\right)\log\left(1+\Lambda_1^{-\alpha/2}\right)} + 1\right)$$

Consider the function $f(x) = (1+x)\log(1+1/x)$. As $f(x)$ is monotonically decreasing for $x \geq 0$ and $\lim_{x\to\infty} f(x) = 1$ we have $f(x) > 1$ for all $x \geq 0$. Thus for $\alpha < 4$, $\partial U_1/\partial \Lambda_1 > 0$ whenever $\Lambda_1 < \Lambda_2$ and similarly $\partial U_2/\partial \Lambda_2 > 0$ whenever $\Lambda_2 < \Lambda_1$. Thus for a N.E. to occur in the interior of the strategy space we must have both $\Lambda_1 > \Lambda_2$ and $\Lambda_2 > \Lambda_1$. As these conditions are mutually exclusive at least one of the constraints of the strategy space must be active at the N.E.. In essence each network is trying to set it's active density higher than the other's. Eventually at least one network maxs out.

First consider the case where the solution to

$$N_1 = x\left(\frac{\alpha}{2\left(1+x^{\alpha/2}\right)\log\left(1+x^{-\alpha/2}\right)} - 1\right). \tag{2.13}$$

occurs for $x < N_2$. Suppose $\Lambda_2^* = N_2$. Then as $N_1 \leq N_2$ we have $\Lambda_1 \leq \Lambda_2^*$, hence $\partial U_1/\partial \Lambda_1 > 0$ for all Λ_1 on the interior and hence $\Lambda_1^* = N_1$. Now the function $U_2(\Lambda_1^*, \Lambda_2)$ has a unique maximum for Λ_2. This maximum satisfies $\partial U_2(\Lambda_1^*, \Lambda_2)\partial \Lambda_2 = 0$, which is equation (2.13) with Λ_2^* substituted for x. But the solution equation (2.13) satisfies $x < N_2$, so $\Lambda_2^* < N_2$, a contradiction. Thus the constraint $\Lambda_2 \leq N_2$ must be inactive. Suppose instead that the constraint $\Lambda_1^* = N_1$ is active. Then by the same arguments the unique Λ_2^* satisfies equation (2.13). This establishes the solution and

it's uniqueness, for the first case.

Second consider the case where the solution to equation (2.13) occurs for $x \geq N_2$. Then it is straightforward to check using similar arguments above, that the unique solution satisfies $(\Lambda_1^*, \Lambda_2^*) = (N_1, N_2)$. This establishes the result.

2.7.3 Theorem 2.3.5

For $\alpha > 2$ the solution to equation (2.8) only goes to infinity for $N_1 \to \infty$. In this limit $(1 + \Lambda_2^{*\alpha/2}) \log(1 + \Lambda_2^{*-\alpha/2}) \to 1$ and

$$\Lambda_2^* \to \frac{2}{\alpha - 2} \Lambda_1^*$$

if $N_1 \leq (\alpha/2 - 1)N_2$. Otherwise, $\Lambda_2^* = N_2$. Computing $p_i^* = \Lambda_i^*/N_i$ produces the stated result.

2.7.4 Theorem 2.3.6

This follows by direct substitution.

2.7.5 Theorem 2.3.7

The proof of this result is more involved than the proof of theorem 2.3. There are three regimes.

First consider the joint spread regime where $N_1 > \sqrt{\Lambda^*(\alpha/2)}$. We show that a N.E. cannot occur on the boundary of the strategy space. Suppose $\Lambda_1^* = N_1$. Then $\Lambda_1^* > \sqrt{\Lambda^*(\alpha/2)}$. As $\sqrt{\Lambda^*(\alpha/2)}$ is the solution to the equation

$$\frac{\alpha}{2\left(1 + \sqrt{\Lambda^*(\alpha/2)}^{\alpha/2}\right) \log\left(1 + \sqrt{\Lambda^*(\alpha/2)}^{-\alpha/2}\right)} - 1 = 1.$$

and $(1+x)\log(1+1/x)$ is a monotonically decreasing function for $x > 0$, we have

$$\frac{\alpha}{2\left(1+\Lambda_1^{*\alpha/2}\right)\log\left(1+\Lambda_1^{*-\alpha/2}\right)} - 1 > 1.$$

If Λ_1^* lies on the boundary of the strategy space then $\partial U_1(\Lambda_1^*, \Lambda_2^*)/\partial\Lambda_1 > 0$ which implies

$$\begin{aligned}\Lambda_2^* &> \Lambda_1^* \left(\frac{\alpha}{2\left(1+\Lambda_1^{*\alpha/2}\right)\log\left(1+\Lambda_1^{*-\alpha/2}\right)} - 1 \right) \\ &> \Lambda_1^* \\ &> \sqrt{\Lambda^*(\alpha/2)}.\end{aligned}$$

This in turn implies

$$\frac{\alpha}{2\left(1+\Lambda_2^{*\alpha/2}\right)\log\left(1+\Lambda_2^{*-\alpha/2}\right)} - 1 > 1.$$

At equilibrium $\partial U_2(\Lambda_1^*, \Lambda_2)/\partial\Lambda_2 \geq 0$ so

$$\begin{aligned}\Lambda_1^* &\geq \Lambda_2^* \left(\frac{\alpha}{2\left(1+\Lambda_2^{*\alpha/2}\right)\log\left(1+\Lambda_2^{*-\alpha/2}\right)} - 1 \right) \\ &> \Lambda_2^*,\end{aligned}$$

a contradiction. Thus $\Lambda_1 < N_1$. Now assume $\Lambda_2 = N_2$. By assumption $N_2 \geq N_1$ so $\Lambda_2^* > \sqrt{\Lambda^*(\alpha/2)}$. By repeating the same arguments we can generate the same style of contradiction and thus $\Lambda_2 < N_2$. This establishes that a N.E. cannot occur on the boundary of the strategy space. In essence each network is trying to undercut the active density of the other. This drags the equilibrium away from the boundary.

Now we establish any N.E. must be symmetric, i.e. $\Lambda_1^* = \Lambda_2^*$. Suppose a N.E. $(\Lambda_1^*, \Lambda_2^*)$ with $\Lambda_1^* \neq \Lambda_2^*$ exists. Then as it must lie on the interior of the strategy space and as the utility functions are symmetric, $(\Lambda_2^*, \Lambda_1^*)$ must also be a N.E.. On the interior of the strategy space the N.E. criterion is $\partial U_1(\Lambda_1^*, \Lambda_2^*)/\partial \Lambda_1 = 0$ and so the function $\Lambda_1^*(\Lambda_2)$ is monotonically increasing in Λ_2. But this implies we cannot have N.E. at both $(\Lambda_1^*, \Lambda_2^*)$ and $(\Lambda_2^*, \Lambda_1^*)$, a contradiction. Thus $\Lambda_1^* = \Lambda_2^*$.

By differentiating the utility functions this implies that at any N.E. Λ_1^* satisfies

$$\frac{\alpha}{2\left(1+\Lambda_1^{*\alpha/2}\right)\log\left(1+\Lambda_1^{*-\alpha/2}\right)} - 1 = 1$$

with $\Lambda_2^* = \Lambda_1^*$. But this is equivalent to $\Lambda_1^* = \sqrt{\Lambda^*(\alpha/2)}$. Thus the N.E. is unique and occurs at $(\Lambda_1^*, \Lambda_2^*) = (\sqrt{\Lambda^*(\alpha/2)}, \sqrt{\Lambda^*(\alpha/2)})$.

Next consider the partial spread and full spread regimes where $N_1 \leq \sqrt{\Lambda^*(\alpha/2)}$. We first show that $\Lambda_1^* = N_1$. Suppose $\Lambda_1^* < N_1$. Then $\Lambda_1^* < \sqrt{\Lambda^*(\alpha/2)}$ which implies

$$\frac{\alpha}{2\left(1+\Lambda_1^{*\alpha/2}\right)\log\left(1+\Lambda_1^{*-\alpha/2}\right)} - 1 < 1.$$

At equilibrium $\partial U_1/\partial \Lambda_1 = 0$ so

$$\begin{aligned}\Lambda_2^* &= \Lambda_1^* \left(\frac{\alpha}{2\left(1+\Lambda_1^{*\alpha/2}\right)\log\left(1+\Lambda_1^{*-\alpha/2}\right)} - 1 \right) \\ &< \Lambda_1^* \\ &< \sqrt{\Lambda^*(\alpha/2)}.\end{aligned}$$

But this in turn implies

$$\frac{\alpha}{2\left(1+\Lambda_2^{*\alpha/2}\right)\log\left(1+\Lambda_2^{*-\alpha/2}\right)}-1<1$$

which in conjunction with the equilibrium condition $\partial U_2/\partial\Lambda_2 = 0$ implies $\Lambda_1^* < \Lambda_2^*$, a contradiction. Thus $\Lambda_1^* = N_1$. Now we can solve for Λ_2^* to conclude that Λ_2^* is the unique solution to equation (2.8) or N_2, whichever is smaller. This concludes the proof.

2.7.6 Theorem 2.3.9

We first tackle the full spread and partial spread regimes. It is shown in lemma 2.8.4 in the appendix that $\Lambda''(\alpha)$ is undefined for $\alpha \leq 4$ and recall $\Lambda''(\alpha)$ is defined to be positive infinity for $\alpha > 4$. Consider the case where $N_1 \leq \Lambda''(\alpha)$. We show that $\Lambda_1^* = N_1$. Suppose the contrary, that $\Lambda_1^* < N_1$. Then $\Lambda_1^* < \Lambda''(\alpha)$. Define the function

$$f(s_1,s_2) \triangleq \frac{\int_0^\infty e^{-(s_1+s_2)x^{2/\alpha}}\dfrac{dx}{1+x}}{s_1\int_0^\infty x^{2/\alpha}e^{-(s_1+s_2)x^{2/\alpha}}\dfrac{dx}{1+x}},$$

for s_1 and s_2 positive. In Lemma 2.8.1 in the appendix it is shown that $f(s,s)$ is a monotonically decreasing function in s. By rearranging equation (2.10) one can check that $f(\Lambda''(\alpha),\Lambda''(\alpha)) = 1$. Thus $f(\Lambda_1^*,\Lambda_1^*) > 1$. For a given Λ_2 it is shown in Lemma 2.8.2 in the appendix that the utility function $U_1(\Lambda_1,\Lambda_2)$ is a smooth continuous function of Λ_1 with a unique maximum (and likewise for U_2 given Λ_1). As $\Lambda_1^* < N_1$ the maximum with respect to Λ_1 occurs at $\partial U_1(\Lambda_1^*,\Lambda_2)/\partial\Lambda_1 = 0$. By rearranging equation (2.11) one can check that this condition is equivalent to $f(\Lambda_1^*,\Lambda_2) = 1$. This means $f(\Lambda_1^*,\Lambda_2^*) < f(\Lambda_1^*,\Lambda_1^*)$. In lemma 2.8.2 we show that $f(s_1,s_2)$ is a monotonically

increasing function in s_2 given s_1. Thus we have $\Lambda_2^* < \Lambda_1^*$ and so also $\Lambda_2^* < \Lambda''(\alpha)$ and $\Lambda_2^* < N_1$. Thus $f(\Lambda_2^*, \Lambda_2^*) > 1$. As by assumption $N_1 \leq N_2$, we have $\Lambda_2^* < N_2$ and so the maximum of U_2 occurs at $\partial U_2(\Lambda_1, \Lambda_2^*)/\partial \Lambda_2 = 0$. This means $f(\Lambda_2^*, \Lambda_1^*) = 1 < f(\Lambda_2^*, \Lambda_2^*)$ which implies $\Lambda_1^* < \Lambda_2^*$. This is a contradiction. Thus we must have $\Lambda_1^* = N_1$ at a N.E.. By maximizing over Λ_2 via differentiation of U_2, we see that Λ_2^* equals the solution of (2.11) or N_2 whichever is smaller. Lemma 2.8.2 establishes the solution of (2.11) always exists and is unique.

Now consider the case where $N_1 > \Lambda''(\alpha)$. We first show that a N.E. cannot occur on the boundary of the strategy space. Suppose $\Lambda_1^* = N_1$. Then $\Lambda_1 > \Lambda''(\alpha)$. This implies $f(\Lambda_1^*, \Lambda_1^*) < 1$. As $\Lambda_1^* = N_1$ the maximum of U_1 occurs at $\partial U_1(\Lambda_1^*, \Lambda_2)/\partial \Lambda_1 \geq 0$ for a given Λ_2. This means $f(\Lambda_1^*, \Lambda_2^*) \geq 1 > f(\Lambda_1^*, \Lambda_1^*)$, thus $\Lambda_2^* > \Lambda_1^*$. We also then have $\Lambda_2^* > \Lambda''(\alpha)$. From the optimality condition for network 2 we then have $\partial U_2(\Lambda_1^*, \Lambda_2)/\partial \Lambda_2 \geq 0$. This means $f(\Lambda_2^*, \Lambda_1^*) \geq 1 > f(\Lambda_2^*, \Lambda_2^*)$ which implies $\Lambda_1^* > \Lambda_2^*$. This is a contradiction. Thus we must have $\Lambda_1^* < N_1$. As $N_2 \geq N_1 > \Lambda''(\alpha)$ we can repeat the argument for Λ_2^* to conclude that we must also have $\Lambda_2^* < N_2$. This proves a N.E. can only occur on the interior of the strategy space.

Now we establish any N.E. must be symmetric, i.e. $\Lambda_1^* = \Lambda_2^*$. Suppose a N.E. $(\Lambda_1^*, \Lambda_2^*)$ with $\Lambda_1^* \neq \Lambda_2^*$ exists. Then as it must lie on the interior of the strategy space and as the utility functions are symmetric, $(\Lambda_2^*, \Lambda_1^*)$ must also be a N.E.. On the interior of the strategy space the N.E. criterion is $\partial U_1(\Lambda_1^*, \Lambda_2^*)/\partial \Lambda_1 = 0$ and so the function $\Lambda_1^*(\Lambda_2)$ is monotonically increasing in Λ_2 by lemma 2.8.3. But this implies we cannot have N.E. at both $(\Lambda_1^*, \Lambda_2^*)$ and $(\Lambda_2^*, \Lambda_1^*)$, a contradiction. Thus $\Lambda_1^* = \Lambda_2^*$.

Finally one can verify that $\Lambda_1^* = \Lambda_2^* = \Lambda''(\alpha)$ is a N.E. by differentiating the utility functions. Thus the unique N.E. is $(\Lambda_1^*, \Lambda_2^*) = (\Lambda''(\alpha), \Lambda''(\alpha))$.

In essence what is going on here is that in the absence of strategy space constraints, when $\Lambda_i < \Lambda''(\alpha)$, network i wants to set $\Lambda_i > \Lambda_j$ and when $\Lambda_i > \Lambda''(\alpha)$ network i wants to set $\Lambda_i < \Lambda_j$. Thus the natural equilibrium is at $(\Lambda_1^*, \Lambda_2^*) = (\Lambda''(\alpha), \Lambda''(\alpha))$.

The problem for $\alpha < 4$ is $\Lambda''(\alpha)$ is infinite and the sparser network winds up maxing out at $\Lambda_1^* = N_1$. When $\alpha > 4$ the function $\Lambda''(\alpha)$ is finite and it is possible to have $N_1 > \Lambda''(\alpha)$, i.e. both networks have a sufficiently high density of nodes so as not to be constrained by the strategy space. In this case they get to set their access probabilities so as to achieve the natural equilibrium.

2.8 Appendix

Lemma 2.8.1. *The function $f(s, s)$ is monotonically decreasing in s.*

Proof. By changing variables we can rewrite $f(s, s)$ as

$$f(s,s) \triangleq \frac{\int_0^\infty g_s(x)dx}{\int_0^\infty x g_s(x)dx}$$

where

$$g_s(x) = \frac{x^{\alpha/2-1}e^{-2x}}{s^{\alpha/2} + x^{\alpha/2}}.$$

Choose a pair of values for s_1 and s_2 satisfying $0 \leq s_1 \leq s_2$ and then observe that for any $x_1 \leq x_2$ the following inequality holds

$$\frac{g_{s_2}(x_2)}{g_{s_1}(x_2)} \geq \frac{g_{s_2}(x_1)}{g_{s_1}(x_1)}.$$

Thus

$$\begin{aligned}
\int_0^\infty \int_0^{x_2} (x_2 - x_1) g_{s_1}(x_1) g_{s_2}(x_2) dx_1 dx_2 &= \int_0^\infty \int_{x_1}^\infty (x_2 - x_1) g_{s_1}(x_1) g_{s_2}(x_2) dx_2 dx_1 \\
&= \int_0^\infty \int_{x_2}^\infty (x_1 - x_2) g_{s_1}(x_2) g_{s_2}(x_1) dx_1 dx_2 \\
&\geq \int_0^\infty \int_{x_2}^\infty (x_1 - x_2) g_{s_1}(x_1) g_{s_2}(x_2) dx_1 dx_2.
\end{aligned}$$

Then

$$\int_0^\infty \int_0^\infty (x_2 - x_1) g_{s_1}(x_1) g_{s_2}(x_2) dx_1 dx_2 \geq 0$$

and so

$$\int_0^\infty \int_0^\infty x_2 g_{s_1}(x_1) g_{s_2}(x_2) dx_1 dx_2 \geq \int_0^\infty \int_0^\infty x_1 g_{s_1}(x_1) g_{s_2}(x_2) dx_1 dx_2$$

which implies

$$\int_0^\infty g_{s_1}(x) dx \int_0^\infty x g_{s_2}(x) dx \geq \int_0^\infty x g_{s_1}(x) dx \int_0^\infty g_{s_2}(x) dx$$

and thus $f(s_1, s_1) \geq f(s_2, s_2)$. □

Lemma 2.8.2. *The function*

$$U_i(\Lambda_1, \Lambda_2) = \Lambda_i \int_0^\infty e^{-(\Lambda_1 + \Lambda_2)x^{2/\alpha}} \frac{dx}{1+x}$$

is smooth and continuous in Λ_i with a unique maximum Λ_i^*.

Proof. As the integral is well-defined for all positive Λ_1 and Λ_2, the function is smooth and continuous by inspection. To see that a unique maximum exists set the derivative to zero to obtain $f(\Lambda_i, \Lambda_j) = 1$. For fixed Λ_j it is straightforward to show $f(\Lambda_i, \Lambda_j)$ is monotonically decreasing in Λ_i using arguments similar to those in lemma 2.8.1. For $\Lambda_i \to 0$ we find $f(\Lambda_i, \Lambda_j) \to \infty$ and for $\Lambda_i \to \infty$ we find $f(\Lambda_i, \Lambda_j) \to 2/\alpha$ which is always less than 1 for $\alpha > 2$. Thus there always exists a single Λ_i^* satisfying $f(\Lambda_i^*, \Lambda_j) = 1$ and hence a unique maximum always exists. □

Lemma 2.8.3. *The function $f(s_1, s_2)$ is monotonically increasing in s_2 given s_1.*

Proof. The proof mirrors that of lemma 2.8.1, the only difference being that now

$$\frac{g_{s_2}(x_2)}{g_{s_1}(x_2)} \leq \frac{g_{s_2}(x_1)}{g_{s_1}(x_1)},$$

i.e. the inequality goes the other way. We omit the details for brevity. □

Lemma 2.8.4. *The function $\Lambda''(\alpha)$ is undefined for $\alpha \leq 4$ and uniquely defined for $\alpha > 4$.*

Proof. $\Lambda''(\alpha)$ is the solution to $f(\Lambda''(\alpha), \Lambda''(\alpha)) = 1$. The function $f(s, s)$ is a monotonically decreasing in s by lemma 2.8.1. By taking $s \to 0$ we find $f(s, s) \to \infty$ and by taking $s \to \infty$ we find $f(s, s) \to 4/\alpha$. Thus when $\alpha \leq 4$ there is no s for which $f(s, s) = 1$ and hence $\Lambda''(\alpha)$ is undefined. When $\alpha > 4$ there is a single s at which $f(s, s)$ crosses the value 1 and hence $\Lambda''(\alpha)$ is uniquely defined. □

Chapter 3

Fundamental Constraints on Multicast Capacity Regions

3.1 Introduction

The broadcast channel has predominantly been studied in the context of unicast messaging, where the transmitter wishes to send one private message to each of the L receivers (see [7] for example). We refer to this as unicasting. The transmitter may however wish to send different messages to different subsets of receivers. We refer to this as multicasting. The most general multicast structure comprises of $2^L - 1$ messages (the powerset). For $L = 2$ there are three messages, one required only by the first receiver, one required only by the second receiver, and one required by both receivers.

The multicast capacity region for a broadcast channel is the set of 2^L-1-dimensional rate vectors that are achievable. For $L = 2$ this is the set of achievable rate vectors (R_1, R_2, R_{12}), where R_{12} denotes the rate of the common message. One question of interest is, can the multicast capacity region be inferred from the unicast capacity

region? That is, can we always compute the multicast capacity region from the unicast capacity region, i.e. without knowing the structure of the channel? For certain broadcast channels this is true, although it is not true in general. Thus the multicast capacity region provides additional information about the communication limits of the channel beyond that of the unicast capacity region.

Multicasting has received significant attention in the network-coding literature. In [1] and [18] the maximum rate at which a common message can be sent from a source node through a network of directed noiseless links to a collection of sink nodes, is shown to equal the minimum-cut of the associated graph. In [8] and [23] the multicast capacity region for one-source-two-sink networks is fully characterized.[1] It is again given by the minimum-cuts of the associated graph. For three or more sinks this is not the case and the problem is open. In this exposition we shed light on it by characterizing some of the structure for three-sink networks.

There is an oddity to multicasting. Suppose we have a two-user broadcast channel that can support a rate vector $(1, 1, 1)$. That is the transmitter can simultaneously deliver one bit of private information to the first receiver, one bit of private information to the second receiver, and one bit of common information to both receivers. An important point to clarify is that there is *no secrecy requirement* –"private" information sent to the first receiver may or may not be decodable by the second receiver and vice versa. Then the channel can also support a rate vector $(2, 1, 0)$. The transmitter merely uses the common bit to send private information to the first receiver. Ofcourse the second receiver is capable of decoding this bit too, but the information is of no interest to it. By symmetry the achievability of rate vector $(1, 1, 1)$ also implies the achievability of rate vector $(1, 2, 0)$. There is one more implication in this vein: the achievability of $(1, 1, 1)$ implies the achievability of $(0, 0, 2)$. The reasoning is similar.

[1] To be more precise, we define the multicast capacity region of a network as the convex-hull of the union of all multicast capacity regions of broadcast channels that arise from specifying the encoding and decoding operations at intermediate nodes in the network.

The transmitter sends the same information on the two private bits. In this way the first user receives the same private bit as the second user, in addition to the same common bit. Thus two common bits have been sent. These three manipulations are summarized in figure 3.1 as *extremal rays* stemming from $(1, 1, 1)$ and represent three distinct encoding/decoding operations that can always be performed, regardless of the structure of the broadcast channel. In this sense they are universal. By time-sharing one can achieve any point in the polytope indicated in figure 3.1. To summarize: if a rate-vector $(1, 1, 1)$ is achievable, so must be the region illustrated, regardless of the channel. Is this set of operations complete? Put in reverse, are there any rate vectors outside the polytope in figure 3.1 that are achievable on for all broadcast channels for which $(1, 1, 1)$ is achievable? The answer is that there are not –there exists a broadcast channel where the rate vector $(1, 1, 1)$ is achievable, but no rate vector outside the polytope in figure 3.1 is. Thus for the two-user broadcast channels the three operations discussed form a complete set -they are the only *distinct universal encoding/decoding operations*.

It is straightforward to generalize these operations to broadcast channels with an arbitrary number of users. Consider for example the three user broadcast channel. There are seven messages. Suppose a rate vector $(R_1, R_2, R_3, R_{12}, R_{13}, R_{23}, R_{123}) = (1, 1, 1, 1, 1, 1, 1)$ is achievable (for example, R_{13} represents the rate of the message intended for receivers 1 and 3). Then for any two subsets of receivers $\mathcal{I} \subset \mathcal{J}$ we can perform the operation $R_{\mathcal{I}} \to R_{\mathcal{I}}+1, R_{\mathcal{J}} \to R_{\mathcal{J}}-1$, and for any two subsets of receivers $\mathcal{I} \neq \mathcal{J}$ we can perform the operation $R_{\mathcal{I}} \to R_{\mathcal{I}} - 1, R_{\mathcal{J}} \to R_{\mathcal{J}} - 1, R_{\mathcal{I}\cup\mathcal{J}} \to R_{\mathcal{I}\cup\mathcal{J}} + 1$. For instance we may swap the first and second receivers' private bits for a common bit that is sent to the pair, so that the rate vector $(0, 0, 1, 2, 1, 1, 1)$ is achieved. Similarly the rate vector $(0, 1, 1, 1, 1, 0, 2)$ can be achieved by using the first receivers private bit and the bit common to the second and third receivers, to send information common to all three receivers. It can be shown that the number of distinct operations of this

form is 15. That is, if the rate vector $(1, 1, 1, 1, 1, 1)$ is achievable, so is the set of points contained within a 15-edged polytope, which is the generalization to $L = 3$ of the polytope in figure 3.1.

Again we ask the question, is this set of operations complete? Are there any points outside this 15-edged polytope that are universally achievable on any three-user broadcast channel? The answer, perhaps surprisingly, is yes. There exists a sixteenth distinct universal encoding/decoding operation. It does not involve a mere relabeling of common and private bits. It enables the rate vector $(1, 1, 1, 0, 0, 0, 3)$ to be achieved. This new operation together with the fifteen trivial ones forms the complete set of distinct universal encoding/decoding operations for $L = 3$. That is, all other rate vectors universally achievable from $(1, 1, 1, 1, 1, 1, 1)$ can be achieved by time sharing between these 16 distinct universal encoding/decoding operations.

Now we turn to the multiple access channel (MAC) with L users. The MAC has also typically been studied in the context of unicast messaging where it's capacity region has in many cases been completely characterized. For multicasting the capacity of the discrete memoryless MAC is computed in [26] and a conjecture regarding the generalization of this result to an arbitrary number of users is given.

Let us apply the reasoning we applied above for the broadcast channel, to the MAC. Consider a two user MAC. Each transmitter wishes to send a private message of rate R_i to the receiver for $i \in \{1, 2\}$. In addition there is a common message of rate R_{12} that both transmitters share, and desire to be sent to the receiver. Suppose for a given MAC a rate vector $(R_1, R_2, R_{12}) = (1, 1, 1)$ is achievable. Then the first transmitter could just label its rate-one bit stream as common information and send it to the transmitter. Thus the rate vector $(0, 1, 2)$ is also achievable. By symmetry the second transmitter could do the same so $(1, 0, 2)$ is achievable too. Are there any other operations that tradeoff between elements of the rate vector?[2] The answer

[2]We could combine these two arguments to conclude $(0, 0, 3)$ is achievable but we will not be

is no. For the broadcast channel we could swap common information for private, but not so for the MAC. More specifically we cannot relabel common information as private, as a common bitstream may require both transmitters have access to it in order for it to be passed to the receiver. A private bitstream assumes only a single transmitter has access to it. The $(1, 1, 1)$-multicast region for the two-user MAC is plotted in figure 3.2. There are three extremal rays and correspondingly three distinct universal/encoding decoding operations. The first two are stated above and the third consists of merely lowering the common rate so as to arrive at the point $(1, 1, 0)$.

Unlike the broadcast channel, this structure directly generalizes to L users. For three users there are ten universal encoding/decoding operations. Six result from relabeling private information as pairwise. Three result from relabeling pairwise as common and the last results from lowering the common rate. Thus the multicast capacity region of the multiple access channel has a less intricate structure than that of the broadcast.

In this paper we characterize the complete set of distinct universal encoding/decoding operations and the associated region of achievable rate vectors, for both the broadcast channel and the MAC channel, for $L = 3$. In essence this is a characterization of the universal constraints on the multicast capacity region of these channels.

Section II describes the notation we use. In section III we describe the problem in detail. Section IV presents the results and section V and VI the proofs.

3.2 Preliminary Notation

We briefly describe some of the notation that will be used. Typically $\mathcal{I}$ and $\mathcal{J}$ will be used to denote subsets of $\{1, 2, 3\}$. For example we may have $\mathcal{I} = \{2, 3\}$, which would imply $R_{\mathcal{I}} \equiv R_{\{2,3\}} \equiv R_{23}$. Rates in bold font represent tuples, for example

interested in this operation as it can be expressed as a linear combination of others.

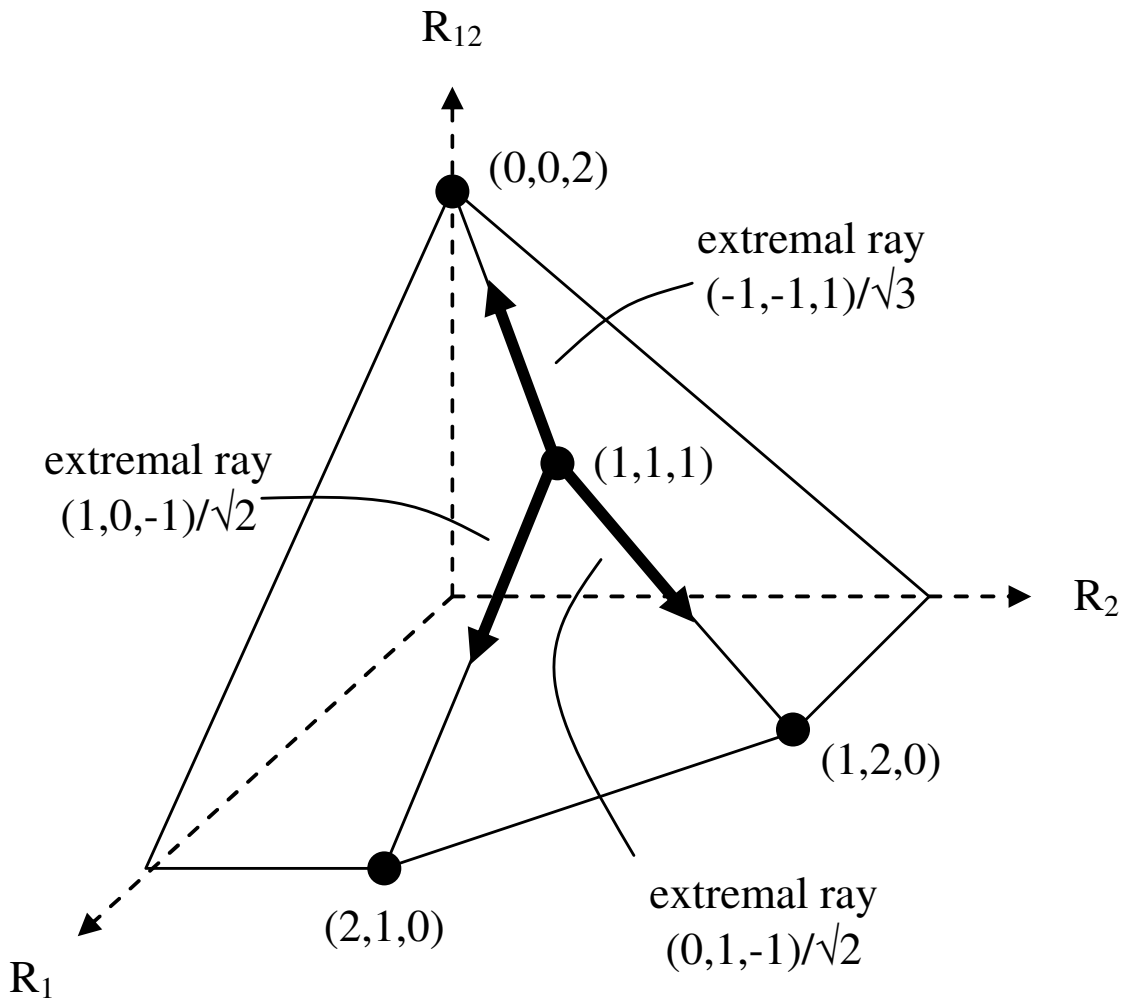

Figure 3.1: The $(1, 1, 1)$-multicast region for the broadcast channel, $L = 2$.

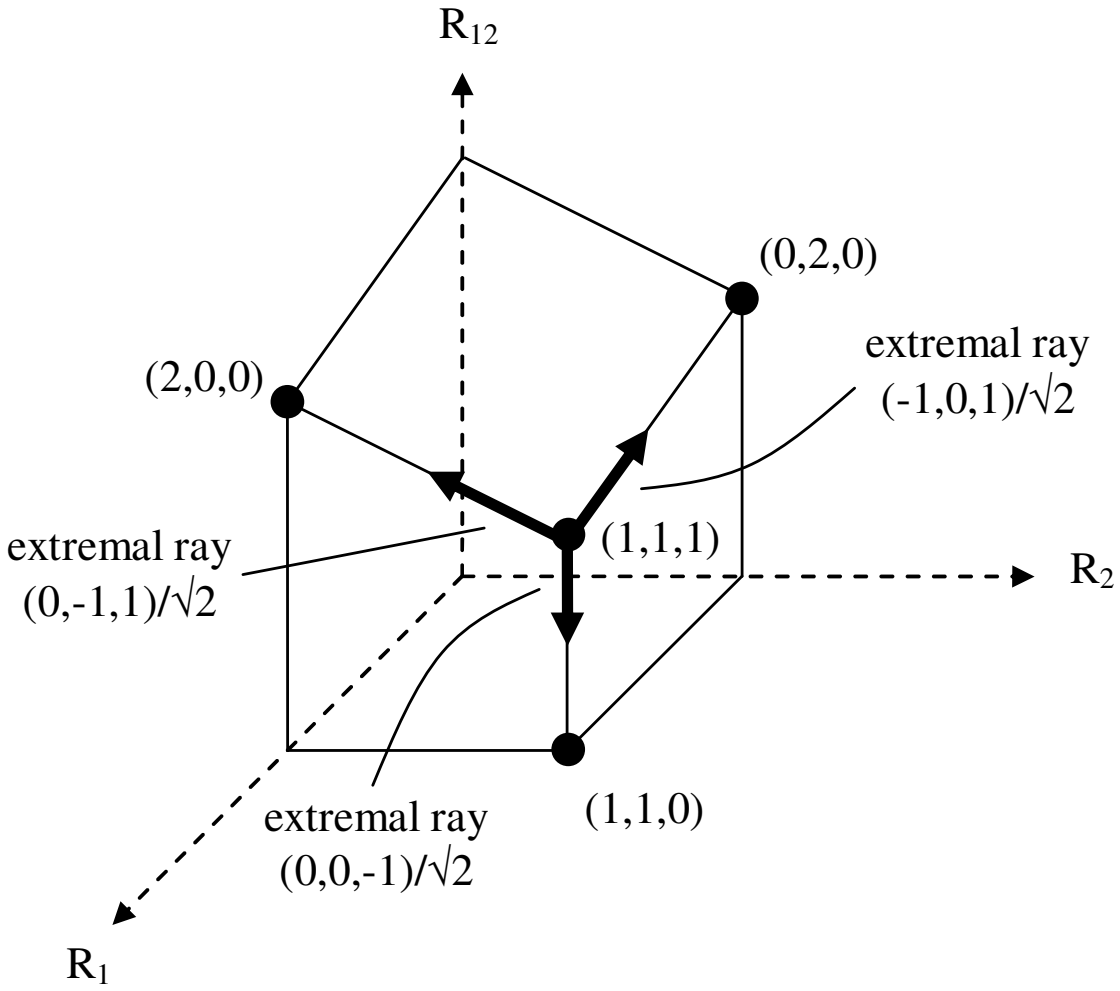

Figure 3.2: The $(1,1,1)$-multicast region for the multiple access channel, $L = 2$.

we may have $\mathbf{R} = (R_1, R_2, R_{12})$. Elements of time series are indicated by a index in parentheses following the variable, for example $Y(i)$. An entire time series is represented by bold font, for example $\mathbf{W}_1 = [W_1(1), \ldots, W_1(n)]$ If $\mathcal{S}$ is a set then 2^S denotes the powerset (the set of all subsets of S) excluding the nullset, e.g. if $S = \{1, 2\}$ then $2^S \equiv \{\{1\}, \{2\}, \{1, 2\}\}$. We denote the nullset by ϕ. The symbol $\preceq$ denotes element-wise inequality.

3.3 Problem Setup

Consider a broadcast channel with three receivers. The input alphabet is denoted $\mathcal{X}$ and the output alphabets $\mathcal{Y}_1, \mathcal{Y}_2, \mathcal{Y}_3$. The probability transition function is $p(y_1, y_2, y_3|x)$. The message vector is

$$(W_1, W_2, W_3, W_{12}, W_{13}, W_{23}, W_{123}).$$

The subscript denotes the subset of receivers for which the message in intended, for example message W_{23} is intended for receivers 2 and 3. Denote the rate vector $\mathbf{R} = (R_1, R_2, R_3, R_{12}, R_{13}, R_{23}, R_{123})$. A $(2^{n\mathbf{R}}, n)$ code consists of an encoder

$$x^n : \prod_{\mathcal{I} \subseteq \{1,2,3\}} \{1, \ldots, 2^{nR_{\mathcal{I}}}\} \to \mathcal{X}^n$$

and twelve decoders

$$\hat{W}_{i,\mathcal{I}} : \mathcal{Y}_i^n \to 2^{nR_{\mathcal{I}}}$$

where $i \in \{1, 2, 3\}$ denotes the receiver and $\mathcal{I} \subseteq \{1, 2, 3\}$ with $i \in \mathcal{I}$ denotes the message index. Thus each receiver decodes four messages (the first receiver decodes $W_1, W_{12}, W_{13}, W_{123}$, etc...). The probability of error $P_e^{(n)}$ is defined to be the probabil-

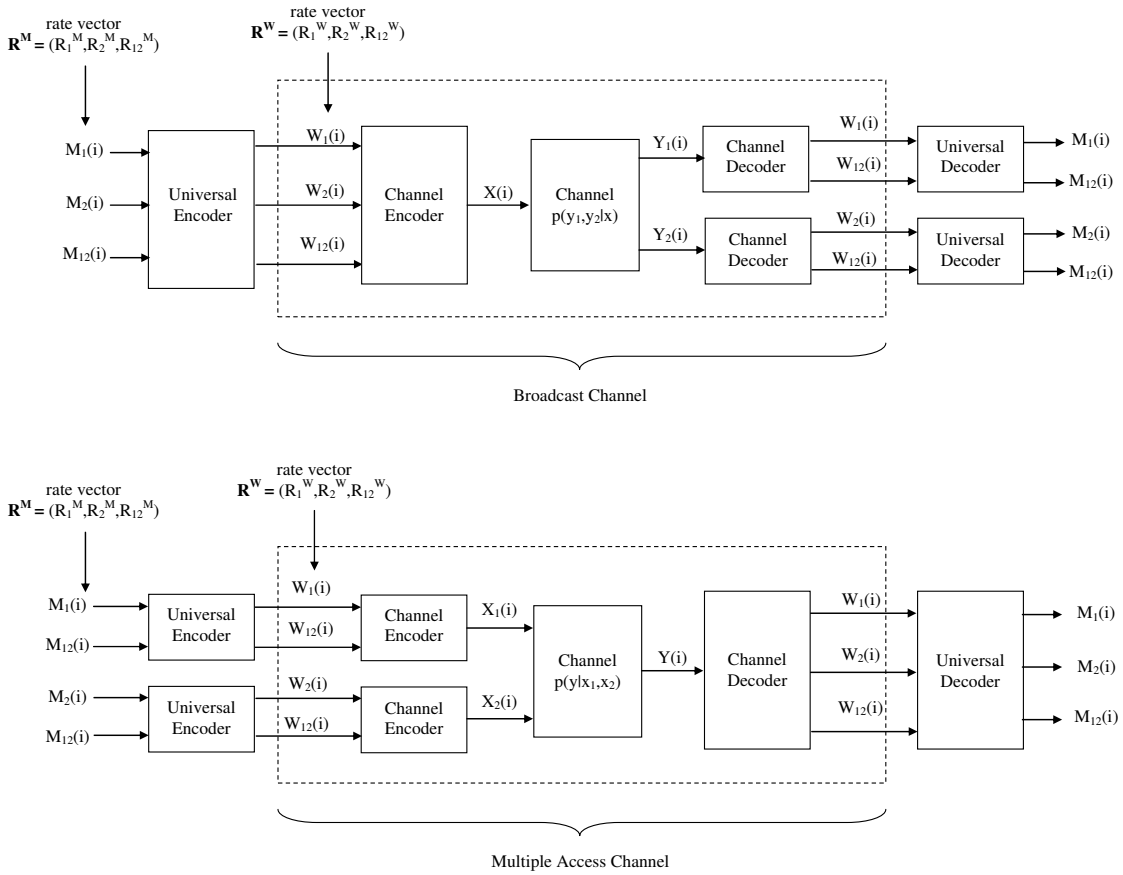

Figure 3.3: System diagrams for $L = 2$.

ity that at least one of the decoded messages is not equal to the transmitted message, i.e.

$$P_e^{(n)} = P\left(\bigcup_{\substack{\mathcal{I} \subseteq \{1,2,3\} \\ \text{s.t. } i \in \mathcal{I}}} \left\{\hat{W}_{i,\mathcal{I}}(Y_i^n) \neq W_{i,\mathcal{I}}\right\}\right).$$

where the seven messages are assumed to be mutually independent and uniformly distributed over $\prod_{\mathcal{I}\in\{1,2,3\}}\{1,\ldots,2^{nR_{\mathcal{I}}}\}$.

Definition 3.3.1. *A multicast rate vector* $\mathbf{R}$ *is said to be achievable for the broadcast channel if there exists a sequence of* $(2^{n\mathbf{R}}, n)$ *codes with* $P_e^{(n)} \to 0$.

Definition 3.3.2. *The multicast capacity region of the broadcast channel is the closure of the set of achievable multicast rate vectors. It is denoted* $\mathcal{C}_{p(y_1,y_2,y_3|x)}$ *or* $\mathcal{C}$ *for short.*

Often we will omit the adjective 'multicast'.

We now give a defintion that makes precise the operation of swapping common and private messages, and quantifies the change in the rate vector. Let $\mathbf{R}^W$ and $\mathbf{R}^M$ be two rate vectors.

Definition 3.3.3. *A* $(d\mathbf{R}, n)$*-universal encoding/decoding operation is a pair of mappings*

$$W_{\mathcal{J}} : \prod_{\mathcal{I}\subseteq\{1,2,3\}} \{1,\ldots,2^{nR_{\mathcal{I}}^M}\} \to \{1,\ldots,2^{nR_{\mathcal{J}}^W}\}, \text{ and}$$

$$\hat{M}_{i,\mathcal{I}} : \prod_{\substack{\mathcal{J}\subseteq\{1,2,3\} \\ s.t.\ i\in\mathcal{J}}} \{1,\ldots,2^{nR_{\mathcal{J}}^W}\} \to \{1,\ldots,2^{nR_{\mathcal{I}}^M}\}$$

for all $\mathcal{J} \subseteq \{1,2,3\}$ *and all* $i \in \{1,2,3\}$ *for all* $\mathcal{I} \subseteq \{1,2,3\}$ *such that* $i \in \mathcal{I}$*, with the properties* $\hat{M}_{i,\mathcal{I}} = \hat{M}_{j,\mathcal{I}}$ *for all* $i,j \in \{1,2,3\}$*,* $\mathbf{R}^M \neq \mathbf{R}^W$ *and*

$$\frac{\mathbf{R}^M - \mathbf{R}^W}{\|\mathbf{R}^M - \mathbf{R}^W\|} = d\mathbf{R},$$

$W(M)$ *being the universal encoder output and* $\hat{M}(\hat{W})$ *being the universal decoder output. The vector* $d\mathbf{R}$ *is referred to as the 'normalized difference vector'.*

The property $\hat{M}_{i,\mathcal{I}} = \hat{M}_{j,\mathcal{I}}$ for all $i,j \in \{1,2,3\}$ ensures that all users agree on the common messages they decode. See figure 3.3 for a system diagram that illustrates the relationship between $M, W, \hat{M}$ and $\hat{W}$.

Example 3.3.4. *Suppose* $\mathbf{R}^W = (1,0,0,1,0,0,0)$ *and* $\mathbf{R}^M = (2,0,0,0,0,0,0)$. *Let* $n = 1$. *Then the mapping* $W_1(\mathbf{M}) = M_1(1)$, $W_{12}(\mathbf{M}) = M_1(2)$ *is a universal encoding operation with* $d\mathbf{R} = (1,0,0,-1,0,0,0)/\sqrt{2}$. *The universal decoding operation is the inverse mapping given by* $\hat{M}_1(\hat{\mathbf{W}}) = [\hat{W}_1, \hat{W}_{12}]$.

Definition 3.3.5. *A* $d\mathbf{R}$*-universal encoding/decoding operation is called 'distinct' if the vector* $d\mathbf{R}$ *cannot be expressed as positive linear combination of vectors* $\{d\mathbf{R}_i\} \neq d\mathbf{R}$ *for which there exist* $d\mathbf{R}_i$*-universal encoding/decoding operations for* $i = 1, 2, \ldots$. *The (rays associated with the) normalized difference vectors corresponding to distinct* $d\mathbf{R}$*-universal encoding/decoding operations are called 'extremal rays'.*

By positive linear combination we mean a weighted linear sum with non-negative coefficients.

Example 3.3.6. *It will be evident later that the universal encoding/decoding operation given in example 3.3.4 is distinct and thus* $(1,0,0,-1,0,0,0)/\sqrt{2}$ *is an extremal ray. By symmetry* $(0,1,0,-1,0,0,0)/\sqrt{2}$ *is also an extremal ray. Note distinctness does not imply uniqueness –the universal encoding/decoding operation that moves from rate vector* $\mathbf{R}^W = (1,0,0,1,0,0,0)$ *to rate vector* $\mathbf{R}^M = (1.5,0,0,0.5,0,0,0)$ *is also classified as distinct, but it has the same normalized difference vector. An example of a universal encoding/decoding operation that is not distinct is one that moves from rate vector* $\mathbf{R}^W = (1,0,0,1,0,0,0)$ *to rate vector* $\mathbf{R}^M = (1.5,0.5,0,0,0,0,0)$. *Denote the corresponding normalized difference vector is* $d\mathbf{R}_A \triangleq (0.5,0.5,0,-1,0,0,0)/\sqrt{1.5}$. *The universal encoding/decoding operations that achieve this shift correspond to time-sharing between two operations, one with normalized difference vector*

$$d\mathbf{R}_B \triangleq \frac{1}{\sqrt{2}}(1,0,0,-1,0,0,0),$$

the other with normalized difference vector

$$d\mathbf{R}_C \triangleq \frac{1}{\sqrt{2}}(0,1,0,-1,0,0,0).$$

Indeed we have

$$d\mathbf{R}_A = \frac{1}{\sqrt{3}}d\mathbf{R}_B + \frac{1}{\sqrt{3}}d\mathbf{R}_C.$$

We now give a formal definition of the region alluded to in figure 3.1. Let

$$\mathbf{R}^* = (R_1^*, R_2^*, R_3^*, R_{12}^*, R_{13}^*, R_{23}^*, R_{123}^*)$$

be a parameter.

Definition 3.3.7. *The '$\mathbf{R}^*$-multicast region' is the intersection of the capacity regions of all broadcast channels for which the rate vector $\mathbf{R}^*$ is achievable, i.e.*

$$\bigcap_{p(y_1,y_2,y_3|x):\mathbf{R}^*\in\mathcal{C}_{p(y_1,y_2,y_3|x)}} \mathcal{C}_{p(y_1,y_2,y_3|x)}$$

See figures 3.1 for examples of this region.

As the problem setup for the multiple access channel is entirely analogous to the aforementioned setup for the broadcast channel, we do not explicitly describe it. An example of the $\mathbf{R}^*$-multicast region is given in figure 3.2

The aim of this paper is to characterize the $\mathbf{R}^*$-multicast cones for both the broadcast and multiple access channels.

$$\mathbf{G}_{BC,2} = \begin{bmatrix} 1 & 0 & 1 \\ 0 & 1 & 1 \\ 1 & 1 & 1 \end{bmatrix} \qquad \mathbf{H}_{BC,2} = \begin{bmatrix} 1 & 0 & -1 \\ 0 & 1 & -1 \\ -1 & -1 & 1 \end{bmatrix}$$

$$\mathbf{G}_{MAC,2} = \begin{bmatrix} 1 & 0 & 1 \\ 0 & 1 & 1 \\ 1 & 1 & 1 \end{bmatrix} \qquad \mathbf{H}_{MAC,2} = \begin{bmatrix} 1 & 0 & -1 \\ 0 & 1 & -1 \\ -1 & -1 & 1 \end{bmatrix}$$

Figure 3.4: Results for $L = 2$.

$$\mathbf{G}_{BC,3} = \begin{bmatrix} 1 & 0 & 0 & 1 & 1 & 0 & 1 & 1 & 1 & 1 & 1 & 2 & 2 & 1 & 2 \\ 0 & 1 & 0 & 1 & 0 & 1 & 1 & 1 & 1 & 1 & 1 & 2 & 1 & 2 & 2 \\ 0 & 0 & 1 & 0 & 1 & 1 & 1 & 1 & 1 & 1 & 1 & 1 & 2 & 2 & 2 \\ 1 & 1 & 0 & 1 & 1 & 1 & 1 & 2 & 1 & 1 & 2 & 2 & 2 & 2 & 2 \\ 1 & 0 & 1 & 1 & 1 & 1 & 1 & 1 & 2 & 1 & 2 & 2 & 2 & 2 & 2 \\ 0 & 1 & 1 & 1 & 1 & 1 & 1 & 1 & 1 & 2 & 2 & 2 & 2 & 2 & 2 \\ 1 & 1 & 1 & 1 & 1 & 1 & 1 & 2 & 2 & 2 & 2 & 3 & 3 & 3 & 3 \end{bmatrix}$$

$$\mathbf{H}_{BC,3} = \begin{bmatrix} -1 & -1 & 0 & 1 & 0 & 0 & 1 & 0 & 0 & -1 & 0 & 0 & 0 & 0 & 0 & 0 \\ -1 & 0 & -1 & 0 & 1 & 0 & 0 & -1 & 0 & 0 & 1 & 0 & 0 & 0 & 0 & 0 \\ 0 & -1 & -1 & 0 & 0 & -1 & 0 & 0 & 1 & 0 & 0 & 1 & 0 & 0 & 0 & 0 \\ 1 & 0 & 0 & -1 & -1 & -1 & 0 & 0 & 0 & 0 & 0 & 0 & 1 & 0 & 0 & -1 \\ 0 & 1 & 0 & 0 & 0 & 0 & -1 & -1 & -1 & 0 & 0 & 0 & 0 & 1 & 0 & -1 \\ 0 & 0 & 1 & 0 & 0 & 0 & 0 & 0 & 0 & -1 & -1 & -1 & 0 & 0 & 1 & -1 \\ 0 & 0 & 0 & 0 & 0 & 1 & 0 & 1 & 0 & 1 & 0 & 0 & -1 & -1 & -1 & 2 \end{bmatrix}$$

$$\mathbf{G}_{MAC,3} = \begin{bmatrix} 1 & 0 & 0 & 1 & 1 & 0 & 1 & 1 & 1 & 1 & 1 \\ 0 & 1 & 0 & 1 & 0 & 1 & 1 & 1 & 1 & 1 & 1 \\ 0 & 0 & 1 & 0 & 1 & 1 & 1 & 1 & 1 & 1 & 1 \\ 0 & 0 & 0 & 1 & 0 & 0 & 0 & 1 & 1 & 1 & 1 \\ 0 & 0 & 0 & 0 & 1 & 0 & 1 & 0 & 1 & 1 & 1 \\ 0 & 0 & 0 & 0 & 0 & 1 & 1 & 1 & 0 & 1 & 1 \\ 0 & 0 & 0 & 0 & 0 & 0 & 0 & 0 & 0 & 0 & 1 \end{bmatrix}$$

$$\mathbf{H}_{MAC,3} = \begin{bmatrix} 1 & 1 & 0 & 0 & 0 & 0 & 0 & 0 & 0 & 0 \\ 0 & 0 & 1 & 1 & 0 & 0 & 0 & 0 & 0 & 0 \\ 0 & 0 & 0 & 0 & 1 & 1 & 0 & 0 & 0 & 0 \\ -1 & 0 & -1 & 0 & 0 & 0 & 1 & 0 & 0 & 0 \\ 0 & -1 & 0 & 0 & -1 & 0 & 0 & 1 & 0 & 0 \\ 0 & 0 & 0 & -1 & 0 & -1 & 0 & 0 & 1 & 0 \\ 0 & 0 & 0 & 0 & 0 & 0 & -1 & -1 & -1 & 1 \end{bmatrix}$$

Figure 3.5: Results for $L = 3$.

3.4 Results

Theorem 3.4.1. *For $L = 3$ the $\mathbf{R}^*$-multicast region of the broadcast channel is the set of all $\mathbf{R} \in \mathbb{R}_+^7$ satisfying*

$$\mathbf{G}_{BC,3}^T (\mathbf{R} - \mathbf{R}^*) \preceq 0 \tag{3.1}$$

where $\mathbf{G}_{BC,3}$ is given in figure 3.4. This region is a polytope, characterized by the cone $\{\mathbf{R} \in \mathbb{R}^7 : \mathbf{G}_{BC,3}^T \mathbf{R} \preceq 0\}$. We refer to this cone as the $L = 3$ 'multicast cone'. The sixteen extremal rays of this cone are given by the columns of the matrix $\mathbf{H}_{BC,3}$ in figure 3.4. Thus there are 16 distinct universal encoding/decoding operations for $L = 3$.

The $(1, 1, 1)$-multicast region for the broadcast channel for $L = 2$ is illustrated in figure 3.1. For $L = 2$ there are 3 distinct universal encoding/decoding operations. The $\mathbf{G}_{BC,2}$ and $\mathbf{H}_{BC,2}$ matrices are given in the above figure.
The columns of $\mathbf{G}_{BC,2}$ are the normal vectors to the three hyperplanes bounding the region. The columns of $\mathbf{H}_{BC,2}$ are the three extremal rays (see figure 3.1).

Theorem 3.4.2. *For $L = 3$ the $\mathbf{R}^*$-multicast region of the multiple access channel is the set of all $\mathbf{R} \in \mathbb{R}_+^7$ satisfying*

$$\mathbf{G}_{MAC,3}^T (\mathbf{R} - \mathbf{R}^*) \preceq 0 \tag{3.2}$$

where $\mathbf{G}_{MAC,3}$ is given in figure 3.4. This region is also a polytope characterized by the cone $\{\mathbf{R} \in \mathbb{R}^7 : \mathbf{G}_{MAC,3}^T \mathbf{R} \preceq 0\}$. The 10 extremal rays of this cone are given by the columns of the matrix $\mathbf{H}_{MAC,3}$ in figure 3.4. Thus there are 10 distinct universal encoding/decoding operations for $L = 3$.

The $(1, 1, 1)$-multicast region for the MAC for $L = 2$ is illustrated in figure

3.2. There are 3 distinct universal encoding/decoding operations. The $\mathbf{G}_{MAC,2}$ and $\mathbf{H}_{MAC,2}$ matrices are given in figure **??**.

An alternative interpretation of theorem 3.4.1 is the following (the same interpretation applies for 3.4.2). For notational simplicity we denote the capacity region of an arbitrary broadcast channel by $\mathcal{C}$. Let

$$\mathbf{R}^*(\alpha) = \arg\max_{R\in\mathcal{C}} \alpha^T\mathbf{R}$$

$\mathbf{R}^*(\alpha)$ is the rate vector lying on the boundary of the capacity region in the direction of α. Let

$$\mathcal{C}^*(\alpha) = \left\{\mathbf{R}\in\mathbb{R}_+^7 \,\middle|\, \alpha^T\mathbf{R} \le \alpha^T\mathbf{R}^*(\alpha)\right\}.$$

$\mathcal{C}^*(\alpha)$ is the halfspace of all rate vectors lying underneath the hyperplane $\alpha^T\mathbf{R} = \alpha^T\mathbf{R}^*(\alpha)$. The region $\mathcal{C}$ is convex and thus we can characterize it by its support function $\mathcal{C}^*(\alpha)$, i.e.

$$\mathcal{C} = \bigcap_{\alpha\in\mathbb{R}_+^7} \mathcal{C}(\alpha).$$

However this is not the minimal dual representation of $\mathcal{C}$. Let

$$\mathcal{H}_3^* \triangleq \left\{\alpha\in\mathbb{R}_+^7 \,\middle|\, \alpha^T\mathbf{H}_{BC,3} \preceq 0\right\}$$

Corollary 3.4.3. *The multicast capacity region of an any broadcast channel with three receivers can be expressed as*

$$\mathcal{C} = \bigcap_{\alpha\in\mathcal{H}} \mathcal{C}(\alpha).$$

if and only if

$$\mathcal{H} \supseteq \mathcal{H}_3^*.$$

This says the following: when computing the multicast capacity region of a broadcast channel by maximizing the weighted sum-rate, the smallest set that one need vary the weighting coefficients α over is $\mathcal{H}_3^*$. Put another way, the normal vector α to any point on the boundary of the multicast capacity region is always contained in the set $\mathcal{H}_3^*$. See figure 3.6.

3.5 Proof of Theorem 3.4.1

The direct part of the proof consists of showing that for any broadcast channel, if a rate vector $\mathbf{R}^*$ is achievable then all rate vectors in the region given by equation (1) are achievable. This establishes that the $\mathbf{R}^*$-multicast region is 'at least as large' as the region given by equation (1). The converse part of the proof consists of illustrating, for each $\mathbf{R}^* \in \mathbb{R}_+^7$, a broadcast channel for which no rate vector outside the region given by equation (1) is achievable. This establishes that the $\mathbf{R}^*$-multicast region is 'at least as small' as the region given by equation (1). We start with the direct part. For notational simplicity we drop the broadcast channel (BC) subscript.

3.5.1 Direct Part

Suppose that $\mathbf{R}^*$ is achievable for a particular broadcast channel. We show that any rate-vector $\mathbf{R} \in \mathbb{R}_+^7$ satisfying

$$\mathbf{R} \preceq \mathbf{R}^* + \mathbf{H}_{BC,3}\Delta \tag{3.3}$$

for $\Delta \in \mathbb{R}_+^{16}$ is also achievable. We then show that this region is precisely the one given in equation (1). Let Δ_i denote the ith element of Δ and $\mathbf{H}_{BC,3}(i)$ denote the ith column of $\mathbf{H}_{BC,3}$. To show that any rate-vector satisfying equation (2) is achievable,

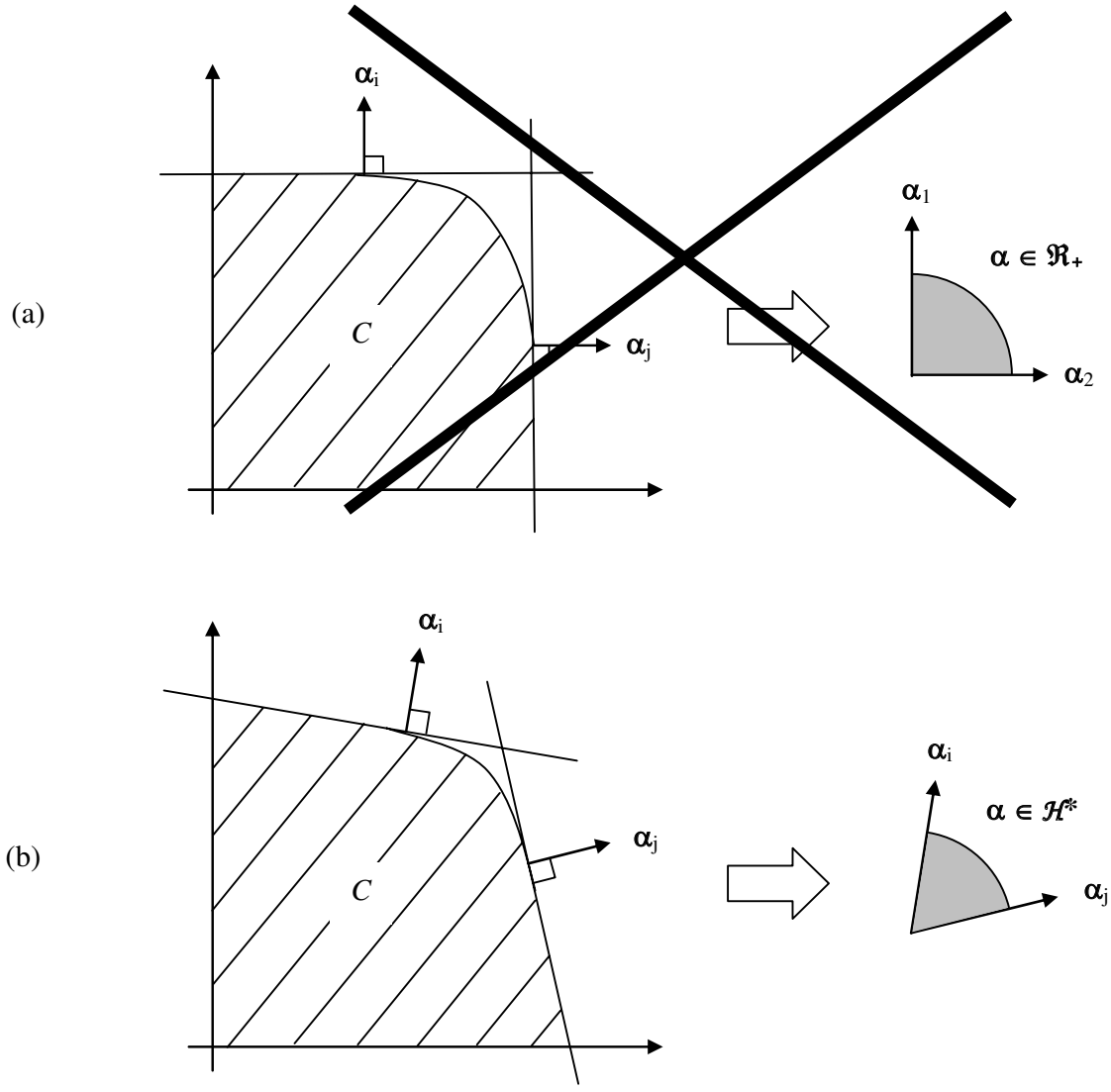

Figure 3.6: The normal vector α of the broadcast channel capacity region satisfies $\alpha^T \in \mathcal{H}^*$. (a) A capacity region that cannot occur. (b) A capacity region that can occur.

we show that each of the 16 rate-vectors given by

$$\mathbf{R}^{(i)} = \mathbf{R}^* + \mathbf{H}_{BC,3}(i)\Delta_i^*, \qquad i = 1, \ldots, 16 \tag{3.4}$$

are achievable where

$$\Delta_i^* = \max_{\mathbf{H}_{BC,3}(i)\Delta_i \preceq \mathbf{R}^*} \Delta$$

By time sharing between these vectors the entire boundary region $\{\mathbf{R}^* - \mathbf{H}_{BC,3}\Delta | \Delta \in \mathbb{R}_+^{16}\}$ is achieved and hence any point within it (i.e. satisfying equation (2)) can also be achieved.

Let $\mathbf{M}, \hat{\mathbf{M}}$ correspond to the binary message vector and estimate of the message vector, respectively, that the transmitter wishes to send at rate vector $\mathbf{R}^{(i)}$. We illustrate the achievability of equation (3) for $i = 3$.

To universally encode for $i = 3$, assume without loss of generality that $R_1^* \leq R_2^*$. In what follows we ignore rounding effects as it will be clear that in the limit $n \to \infty$ they are negligible. Set

$$\begin{aligned} W_1^n &= [M_{12}(1), \ldots, M_{12}(nR_1^*)] \\ W_2^n &= [M_{12}(1), \ldots, M_{12}(nR_1^*), M_2(1), \ldots, M_2(nR_2^* - nR_1^*)] \\ W_{12}^n &= [M_{12}(nR_1^* + 1), \ldots, M_{12}(nR_1^* + nR_{12}^*)] \end{aligned}$$

In words, the information common to receivers 1 and 2 is split into two parts. The first part is replicated and sent separately down both receiver 1 and receiver 2's private channels. The second part is sent down the channel common to both receivers. As receiver 2's private channel can accommodate a higher bit-rate than receiver 1's, there is some bandwidth left over. This is allocated to sending some of receiver 2's private information.

For all other subsets $\mathcal{I}$ of $\{1, 2, 3\}$ set $W_{\mathcal{I}}^n = M_{\mathcal{I}}^n$ and $\hat{M}_{\mathcal{I}}^n = \hat{W}_{\mathcal{I}}^n$. Universal

decoding is straightforward. The first receiver sets

$$\begin{aligned}\hat{M}^n_{1,12} &= [\hat{W}^n_1, \hat{W}^n_{12}] \\ \hat{M}^n_{1,13} &= \hat{W}^n_{13} \\ \hat{M}^n_{1,123} &= \hat{W}^n_{123}\end{aligned}$$

and in this way successfully recovers its message, as the achievability of $\mathbf{R}^*$ implies that $\mathbf{W}$ was decoded correctly. The second receiver sets

$$\begin{aligned}\hat{M}^n_{2,2} &= [\hat{W}_2(nR^*_1 + 1), \ldots, \hat{W}_2(nR^*_2)] \\ \hat{M}^n_{2,12} &= [\hat{W}_2(1), \ldots, \hat{W}_2(nR^*_1), \hat{W}^n_{12}] \\ \hat{M}^n_{2,23} &= \hat{W}^n_{23} \\ \hat{M}^n_{2,123} &= \hat{W}^n_{123}\end{aligned}$$

and is similarly successful in decoding. The third receivers sets $\hat{M}^n_{\mathcal{I}} = \hat{W}^n_{\mathcal{I}}$ for all of its messages. Then we have achieved a rate vector of

$$\begin{aligned}\mathbf{R}^{(3)} &= \mathbf{R}^* + \begin{bmatrix} -1 \\ -1 \\ 0 \\ 1 \\ 0 \\ 0 \\ 0 \end{bmatrix} R^*_1 \\ &= \mathbf{R}^* + \mathbf{H}_{BC,3}(3)\Delta_3.\end{aligned}$$

with $\Delta_3 = R^*_1$. The universal encoding and decoding procedures for all other $i \in$

$\{1, \ldots, 15\}$ are similar and follow from the structure of the columns of the matrix $\mathbf{H}_{BC,3}$.

Universal encoding and decoding for $i = 16$ is different. Assume without loss of generality that $R^*_{12} \leq R^*_{13} \leq R^*_{23}$. To encode, set $W^n_i = M^n_i$ for $i = 1, 2, 3$ and

$$\begin{aligned}
W^n_{12} &= [M_{123}(1), \ldots, M_{123}(nR^*_{12})] \\
W^n_{13} &= [M_{123}(nR^*_{12}+1), \ldots, M_{123}(2nR^*_{12}), M_{13}(1), M_{13}(nR_{13} - nR_{12})] \\
W^n_{23} &= [M_{123}(1) \oplus M_{123}(nR^*_{12}+1), \ldots, M_{123}(nR^*_{12}) \oplus M_{123}(2nR^*_{12}), \\
&\qquad M_{23}(1), \ldots, M_{23}(nR_{23} - nR_{12})] \\
W^n_{123} &= [M^n_{123}(2nR^*_{12}), \ldots, M^n_{123}(2nR^*_{12} + nR^*_{123})]
\end{aligned}$$

In words, the information common to all receivers is split into three streams. The first and second are sent at rate R^*_{12} using the three pairwise links. The third stream is sent at rate R^*_{123} across the link common to all receivers.

The first receiver decodes by setting $\hat{M}^n_{1,1} = \hat{W}^n_1$ and

$$\begin{aligned}
M^n_{13} &= [W_{13}(nR^*_{12}+1), \ldots, W_{13}(nR^*_{13})] \\
M^n_{123} &= [W^n_{12}, W^n_{13}, W^n_{123}].
\end{aligned}$$

The second receiver decodes by setting $\hat{M}^n_{1,2} = \hat{W}^n_2$ and

$$\begin{aligned}
M^n_{23} &= [W_{23}(nR^*_{12}+1), \ldots, W_{23}(nR^*_{23})] \\
M^n_{123} &= [W^n_{12}, W^n_{12} \oplus W^n_{23}, W^n_{123}].
\end{aligned}$$

The third receiver decodes by setting $\hat{M}^n_{1,3} = \hat{W}^n_3$ and

$$\begin{aligned} M^n_{13} &= [W_{13}(nR^*_{12}+1), \ldots, W_{13}(nR^*_{13})] \\ M^n_{23} &= [W_{23}(nR^*_{12}+1), \ldots, W_{23}(nR^*_{23})] \\ M^n_{123} &= [W^n_{13}, W^n_{13} \oplus W^n_{23}, W^n_{123}]. \end{aligned}$$

Then we have achieved a rate vector of

$$\begin{aligned} \mathbf{R}^{(3)} &= \mathbf{R}^* + \begin{bmatrix} 0 \\ 0 \\ 0 \\ -1 \\ -1 \\ -1 \\ 2 \end{bmatrix} R^*_{12} \\ &= \mathbf{R}^* + \mathbf{H}_{BC,3}(16)\Delta_{16}. \end{aligned}$$

with $\Delta_{16} = R^*_{12}$. Thus the 16 rate vectors satisfying equation (3) are achievable and by time sharing between them, all rate vectors in the region given by equation (2) are achievable.

It remains to show that this region is equivalent to the one in equation (1), i.e. that for any $\mathbf{R}^* \in \mathbb{R}^7_+$

$$\left\{ \mathbf{R} \in \mathbb{R}^7_+ \middle| \, \mathbf{G}^T_{BC,3}\mathbf{R} \preceq \mathbf{G}^T_{BC,3}\mathbf{R} \right\} \equiv \left\{ \mathbf{R} \in \mathbb{R}^7_+ \middle| \, \mathbf{R} \preceq \mathbf{R}^* + \mathbf{H}_{BC,3}\Delta, \forall \Delta \in \mathbb{R}^{16}_+ \right\}.$$

On the left is the characterization of the polytope in terms of the hyperplanes bounding it. On the right is the dual characterization in terms of the edges of the polytope

(1-dimensional facets). This equivalence can be demonstrated using computer software such as *polymake*.

3.5.2 Converse Part

To establish the converse we now present, for each $\mathbf{R}^*$, a particular (deterministic) broadcast channel and show its capacity region is equal to (1). Let the input alphabet $\mathcal{X} = \prod_{\mathcal{I}\subseteq\{1,2,3\}}\{0,\ldots,2^{nR^*_{\mathcal{I}}}-1\}$ with the ith channel input

$$X(i) = [X_1(i), X_2(i), X_3(i), X_{12}(i), X_{13}(i), X_{23}(i), X_{123}(i)]$$

so that each $X_{\mathcal{I}} \in \{0,\ldots,2^{nR^*_{\mathcal{I}}}-1\}$, and let $\mathcal{Y}_i \in \prod_{\mathcal{I}\subseteq\{1,2,3\},i\in I}\{0,\ldots,2^{nR^*_{\mathcal{I}}}-1\}$ for $i = 1,2,3$ with

$$\begin{aligned} Y_1(i) &= [X_1(i), X_{12}(i), X_{13}(i), X_{123}(i)] \\ Y_2(i) &= [X_2(i), X_{12}(i), X_{23}(i), X_{123}(i)] \\ Y_3(i) &= [X_3(i), X_{13}(i), X_{23}(i), X_{123}(i)]. \end{aligned}$$

See figure 3.7 for an illustration of the channel. Suppose the channel is used n times. The messages to be transmitted are $W_{\mathcal{I}} \sim U(\{1,\ldots,2^{nR_{\mathcal{I}}}\})$ and mutually independent. Denote the length-n vector of channel inputs by $\mathbf{X}$ and the length-n vectors of channel outputs by $\mathbf{Y}_1, \mathbf{Y}_2$ and $\mathbf{Y}_3$. Let $\mathbf{G}_{BC,3}(i)$ denote the ith column of $\mathbf{G}_{BC,3}$. We wish to show

$$\mathbf{G}_{BC,3}(i)^T\mathbf{R} \leq \mathbf{G}_{BC,3}(i)^T\mathbf{R}^* \tag{3.5}$$

for $i = 1,\ldots,15$. Before this we introduce some notation. Suppose $\mathcal{A}$ is a collection of subsets of $\{1,2,3\}$, for example $\mathcal{A} = \{1,2,12,13,123\}$. The collection $\mathcal{A}$ should

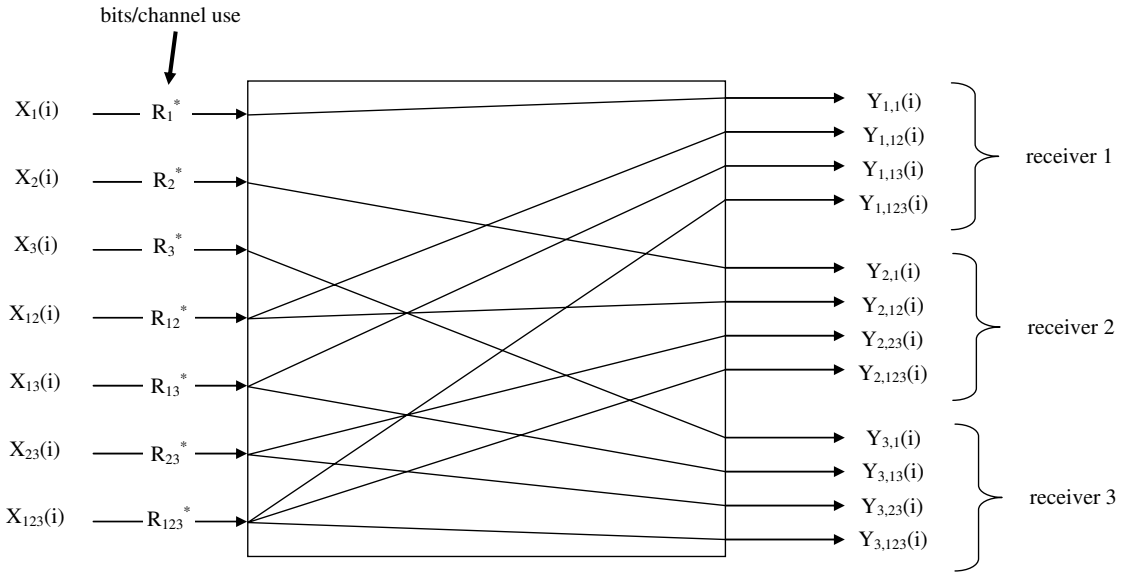

Figure 3.7: Illustration of the deterministic broadcast channel used in converse.

be thought as the indices of a subset of the seven channel links (see figure 3.7), for example $\mathcal{A} = \{1, 123\}$ corresponds to two links, the private one from X_1 to $Y_{1,1}$ and the common one from X_{123} to $Y_{1,123}, Y_{2,123}, Y_{3,123}$. By $\lfloor \mathcal{A} \rfloor$ we denote the indices of the messages intended for those receivers cut by $\mathcal{A}$. For example if $\mathcal{A} = \{1, 2, 12, 13, 123\}$ then all links to the first receiver are cut, but not all links to the second or the third. As the first receiver is sent the messages W_1, W_{12}, W_{13} and W_{123}, we have $\lfloor \mathcal{A} \rfloor = \{1, 12, 13, 123\}$. As another example let $\mathcal{A} = \{2, 3, 12, 13, 23, 123\}$. Then all links to both the second and third receivers are cut and $\lfloor \mathcal{A} \rfloor = \{2, 3, 12, 13, 23, 123\} = \mathcal{A}$. As a final example if $\mathcal{A} = \{1, 12, 23, 123\}$ no receivers are completely cut, and thus $\lfloor A \rfloor = \phi$.

Lemma 3.5.1. *Let $\mathcal{A}_1, \mathcal{A}_2$ and $\mathcal{A}_3$ be three collections of subsets of $\{1, 2, 3\}$ such that*

either $\mathcal{A}_1 \subseteq \mathcal{A}_2 \cup \mathcal{A}_3$, $\mathcal{A}_2 \subseteq \mathcal{A}_1 \cup \mathcal{A}_3$ *or* $\mathcal{A}_3 \subseteq \mathcal{A}_1 \cup \mathcal{A}_2$. *Then*

$$\sum_{\mathcal{I} \in \lfloor \mathcal{A}_1 \cup \mathcal{A}_2 \cup \mathcal{A}_3 \rfloor} R_{\mathcal{I}} + \sum_{\substack{\mathcal{I} \in \lfloor \mathcal{A}_1 \cup \mathcal{A}_2 \rfloor \cap \\ \lfloor \mathcal{A}_1 \cup \mathcal{A}_3 \rfloor \cap \lfloor \mathcal{A}_2 \cup \mathcal{A}_3 \rfloor}} R_{\mathcal{I}} + \sum_{\substack{\mathcal{I} \in \lfloor \mathcal{A}_1 \rfloor \cap \\ \lfloor \mathcal{A}_2 \rfloor \cap \lfloor \mathcal{A}_3 \rfloor}} R_{\mathcal{I}} \leq \sum_{\mathcal{I} \in \mathcal{A}_1} R^*_{\mathcal{I}} + \sum_{\mathcal{I} \in \mathcal{A}_2} R^*_{\mathcal{I}} + \sum_{\mathcal{I} \in \mathcal{A}_3} R^*_{\mathcal{I}}$$

This lemma is a generalization of the cutset bounds to multiple subsets of cuts. Indeed if we set $\mathcal{A}_2 = \phi$ and $\mathcal{A}_3 = \phi$ we are left with

$$\sum_{\mathcal{I} \in \lfloor \mathcal{A}_1 \rfloor} R_{\mathcal{I}} \leq \sum_{\mathcal{I} \in \mathcal{A}_1} R^*_{\mathcal{I}}$$

which are precisely the cutset bounds.

Proof.

$$\begin{aligned}
& n \left(\sum_{\mathcal{I} \in \mathcal{A}_1} R^*_{\mathcal{I}} + \sum_{\mathcal{I} \in \mathcal{A}_2} R^*_{\mathcal{I}} + \sum_{\mathcal{I} \in \mathcal{A}_3} R^*_{\mathcal{I}} \right) \\
& \quad \geq \sum_{\mathcal{I} \in \mathcal{A}_1} H(\mathbf{X}_{\mathcal{I}}) + \sum_{\mathcal{I} \in \mathcal{A}_2} H(\mathbf{X}_{\mathcal{I}}) + \sum_{\mathcal{I} \in \mathcal{A}_3} H(\mathbf{X}_{\mathcal{I}}) \\
& \quad \geq H\left(\cup_{\mathcal{I} \in \mathcal{A}_1} \mathbf{X}_{\mathcal{I}}\right) + H\left(\cup_{\mathcal{I} \in \mathcal{A}_2} \mathbf{X}_{\mathcal{I}}\right) + H\left(\cup_{\mathcal{I} \in \mathcal{A}_3} \mathbf{X}_{\mathcal{I}}\right) \\
& \quad = H\left(\cup_{\mathcal{I} \in \mathcal{A}_1 \cup \mathcal{A}_2 \cup \mathcal{A}_3} \mathbf{X}_{\mathcal{I}}\right) + I\left(\cup_{\mathcal{I} \in \mathcal{A}_1 \cup \mathcal{A}_2} \mathbf{X}_{\mathcal{I}}; \cup_{\mathcal{I} \in \mathcal{A}_1 \cup \mathcal{A}_3} \mathbf{X}_{\mathcal{I}}; \cup_{\mathcal{I} \in \mathcal{A}_2 \in \mathcal{A}_3} \mathbf{X}_{\mathcal{I}}\right) \\
& \qquad + I\left(\cup_{\mathcal{I} \in \mathcal{A}_1} \mathbf{X}_{\mathcal{I}}; \cup_{\mathcal{I} \in \mathcal{A}_2} \mathbf{X}_{\mathcal{I}}; \cup_{\mathcal{I} \in \mathcal{A}_3} \mathbf{X}_{\mathcal{I}}\right) \\
& \quad \geq H\left(\cup_{\mathcal{I} \in \lfloor \mathcal{A}_1 \cup \mathcal{A}_2 \cup \mathcal{A}_3 \rfloor} \mathbf{W}_{\mathcal{I}}\right) + H\left(\cup_{\mathcal{I} \in \lfloor \mathcal{A}_1 \cup \mathcal{A}_2 \rfloor \cap \lfloor \mathcal{A}_1 \cup \mathcal{A}_3 \rfloor \cap \lfloor \mathcal{A}_2 \cup \mathcal{A}_3 \rfloor} \mathbf{W}_{\mathcal{I}}\right) \\
& \qquad + H\left(\cup_{\mathcal{I} \in \lfloor \mathcal{A}_1 \rfloor \cap \lfloor \mathcal{A}_2 \rfloor \cap \lfloor \mathcal{A}_3 \rfloor} \mathbf{W}_{\mathcal{I}}\right) + \epsilon_n \\
& \quad = n \left(\sum_{\mathcal{I} \in \lfloor \mathcal{A}_1 \cup \mathcal{A}_2 \cup \mathcal{A}_3 \rfloor} R_{\mathcal{I}} + \sum_{\mathcal{I} \in \lfloor \mathcal{A}_1 \cup \mathcal{A}_2 \rfloor \cap \lfloor \mathcal{A}_1 \cup \mathcal{A}_3 \rfloor \cap \lfloor \mathcal{A}_2 \cup \mathcal{A}_3 \rfloor} R_{\mathcal{I}} + \sum_{\mathcal{I} \in \lfloor \mathcal{A}_1 \rfloor \cap \lfloor \mathcal{A}_2 \rfloor \cap \lfloor \mathcal{A}_3 \rfloor} R_{\mathcal{I}} \right)
\end{aligned}$$

where the third step follows from lemma 3.7.2 in the appendix and the fourth from the requirement $P_e^{(n)} \to 0$ (Fano's inequality) and lemma 3.7.1 in the appendix. □

Applying lemma 5.1 to the sets of indices in table 1 establishes equation (3.1) for columns $i = 1, 2, 3, 4, 5, 6, 7, 8, 9, 10, 12, 13, 14, 15$ of $\mathbf{G}_{BC,3}$. Unfortunately for column $i = 11$ the condition that either $\mathcal{A}_1 \subseteq \mathcal{A}_2 \cup \mathcal{A}_3$, $\mathcal{A}_2 \subseteq \mathcal{A}_1 \cup \mathcal{A}_3$ or $\mathcal{A}_3 \subseteq \mathcal{A}_1 \cup \mathcal{A}_2$ must hold, is violated. Consequently the 11th converse bound is established in a different fashion.

Let $\mathcal{A}_1, \mathcal{A}_2, \mathcal{A}_3$ be defined by the 11th row of table 1. Then

$$
\begin{aligned}
& n\left(\sum_{\mathcal{I}\in\mathcal{A}_1} R^*_{\mathcal{I}} + \sum_{\mathcal{I}\in\mathcal{A}_2} R^*_{\mathcal{I}} + \sum_{\mathcal{I}\in\mathcal{A}_3} R^*_{\mathcal{I}}\right) \\
& \geq \sum_{\mathcal{I}\in\mathcal{A}_1} H(\mathbf{X}_{\mathcal{I}}) + \sum_{\mathcal{I}\in\mathcal{A}_2} H(\mathbf{X}_{\mathcal{I}}) + \sum_{\mathcal{I}\in\mathcal{A}_3} H(\mathbf{X}_{\mathcal{I}}) \\
& \geq H\left(\cup_{\mathcal{I}\in\mathcal{A}_1}\mathbf{X}_{\mathcal{I}}\right) + H\left(\cup_{\mathcal{I}\in\mathcal{A}_2}\mathbf{X}_{\mathcal{I}}\right) + H\left(\cup_{\mathcal{I}\in\mathcal{A}_3}\mathbf{X}_{\mathcal{I}}\right) \\
& \geq H\left(\cup_{\mathcal{I}\in\mathcal{A}_1}\mathbf{X}_{\mathcal{I}}\right) + H\left(\cup_{\mathcal{I}\in\mathcal{A}_2}\mathbf{X}_{\mathcal{I}}\right) + H\left(\cup_{\mathcal{I}\in\mathcal{A}_3\cup\{123\}}\mathbf{X}_{\mathcal{I}}\right) - H\left(\mathbf{X}_{123}\right) \\
& \geq H(\cup_{\mathcal{I}\in\mathcal{A}_1}\mathbf{X}_{\mathcal{I}}|\mathbf{W}_1, \mathbf{W}_{12}, \mathbf{W}_{13}, \mathbf{W}_{123}) + H(\mathbf{W}_1, \mathbf{W}_{12}, \mathbf{W}_{13}, \mathbf{W}_{123}) \\
& \quad + H(\cup_{\mathcal{I}\in\mathcal{A}_2}\mathbf{X}_{\mathcal{I}}|\mathbf{W}_2, \mathbf{W}_{12}, \mathbf{W}_{23}, \mathbf{W}_{123}) + H(\mathbf{W}_2, \mathbf{W}_{12}, \mathbf{W}_{23}, \mathbf{W}_{123}) \\
& \quad + H(\cup_{\mathcal{I}\in\mathcal{A}_3\cup\{123\}}\mathbf{X}_{\mathcal{I}}|\mathbf{W}_3, \mathbf{W}_{13}, \mathbf{W}_{23}) + H(\mathbf{W}_3, \mathbf{W}_{13}, \mathbf{W}_{23}) - H(\mathbf{X}_{123}) \\
& \geq H(\mathbf{X}_{123}|\mathbf{W}_1, \mathbf{W}_{12}, \mathbf{W}_{13}, \mathbf{W}_{123}) + H(\mathbf{W}_1, \mathbf{W}_{12}, \mathbf{W}_{13}, \mathbf{W}_{123}) \\
& \quad + H(\mathbf{X}_{123}|\mathbf{W}_2, \mathbf{W}_{12}, \mathbf{W}_{23}, \mathbf{W}_{123}) + H(\mathbf{W}_2, \mathbf{W}_{12}, \mathbf{W}_{23}, \mathbf{W}_{123}) \\
& \quad + H(\mathbf{X}_{123}|\mathbf{W}_3, \mathbf{W}_{13}, \mathbf{W}_{23}) + H(\mathbf{W}_3, \mathbf{W}_{13}, \mathbf{W}_{23}) - H(\mathbf{X}_{123}) \\
& \geq H(\mathbf{W}_1, \mathbf{W}_{12}, \mathbf{W}_{13}, \mathbf{W}_{123}) + H(\mathbf{W}_2, \mathbf{W}_{12}, \mathbf{W}_{23}, \mathbf{W}_{123}) + H(\mathbf{W}_3, \mathbf{W}_{13}, \mathbf{W}_{23}) \\
& = H(\mathbf{W}_1) + H(\mathbf{W}_2) + H(\mathbf{W}_3) + 2H(\mathbf{W}_{12}) + 2H(\mathbf{W}_{13}) + 2H(\mathbf{W}_{23}) + 2H(\mathbf{W}_{123}) \\
& = n(R_1 + R_2 + R_3 + 2R_{12} + 2R_{13} + 2R_{23} + 2R_{123})
\end{aligned}
$$

where the fourth step follows from the requirement $P_e^{(}n) \to 0$ (Fano's inequality), the sixth from lemma 3.7.3 and the seventh from the independence of the messages.

i	$\mathcal{A}_1$	$\mathcal{A}_2$	$\mathcal{A}_3$
1	$\{1\},\{12\},\{13\},\{123\}$	ϕ	ϕ
2	$\{2\},\{12\},\{23\},\{123\}$	ϕ	ϕ
3	$\{3\},\{13\},\{23\},\{123\}$	ϕ	ϕ
4	$\{1\},\{2\},\{12\},\{13\},\{23\},\{123\}$	ϕ	ϕ
5	$\{1\},\{3\},\{12\},\{13\},\{23\},\{123\}$	ϕ	ϕ
6	$\{2\},\{3\},\{12\},\{13\},\{23\},\{123\}$	ϕ	ϕ
7	$\{1\},\{2\},\{3\},\{12\},\{13\},\{23\},\{123\}$	ϕ	ϕ
8	$\{1\},\{3\},\{12\},\{13\},\{123\}$	$\{2\},\{12\},\{23\},\{123\}$	ϕ
9	$\{1\},\{2\},\{12\},\{13\},\{123\}$	$\{3\},\{13\},\{23\},\{123\}$	ϕ
10	$\{1\},\{2\},\{12\},\{23\},\{123\}$	$\{3\},\{13\},\{23\},\{123\}$	ϕ
11	$\{1\},\{12\},\{13\},\{123\}$	$\{2\},\{12\},\{23\},\{123\}$	$\{3\},\{13\},\{23\}$
12	$\{1\},\{2\},\{12\},\{13\},\{123\}$	$\{2\},\{3\},\{12\},\{23\},\{123\}$	$\{3\},\{13\},\{23\},\{123\}$
13	$\{1\},\{3\},\{13\},\{23\},\{123\}$	$\{1\},\{2\},\{12\},\{23\},\{123\}$	$\{1\},\{12\},\{13\},\{123\}$
14	$\{1\},\{2\},\{12\},\{13\},\{123\}$	$\{2\},\{12\},\{23\},\{123\}$	$\{1\},\{3\},\{13\},\{23\},\{123\}$
15	$\{1\},\{2\},\{12\},\{13\},\{123\}$	$\{2\},\{3\},\{12\},\{23\},\{123\}$	$\{1\},\{3\},\{13\},\{23\},\{123\}$

Figure 3.8: The $(1,1,1)$-multicast region for the broadcast channel, $L=2$.

3.6 Proof of Theorem 4.2

The direct part of this proof is entirely analogous to the direct part for the broadcast channel. This establishes the universal achievability of the $\mathbf{R}^*$-multicast region. The converse part is different. For each $\mathbf{R}^*$ we present a sequence of channels. The limiting intersection of the capacity regions of these channels is the region in equation (3.2). The capacity regions of these channels are not precisely computed, but only outer bounded in a manner sufficient to establish their limiting intersection.

3.6.1 Direct part

As this part of the proof is trivial and entirely analogous section 5.1 we only provide a sketch. In essence we need to establish that each of the columns of $\mathbf{H}_{MAC,3}$ are achievable in the sense of section 5.1. The first column is achieved by transmitting additional M_{12} bits on the W_1 channel, the second column is achieved by transmitting additional M_{13} bits on the W_1 channel, the third column is achieved by transmitting

additional M_{12} bits on the W_2 channel, and so on. The last column is achieved by lowering the rate of the M_{123} message.

3.6.2 Converse part

For each $\mathbf{R}^*$ we present a sequence of deterministic channels with capacity region tending to the region in equation (3.2). The capacity regions of these channels are not explicitly computed, only outer bounded, but we show the limiting outer bound is tight. The sequence is parameterized by the integer k.

Let $\mathbf{R}^*$ be given and assume its elements are rational. Denote their numerators and denominators by $N_{\mathcal{I}}$ and $D_{\mathcal{I}}$, for $\mathcal{I} \subseteq \{1,2,3\}$ so that $\mathbf{R}^* = (N_1/D_1, \ldots, N_{123}/D_{123})$. Let $l = LCM(D_1, \ldots, D_{123})$. The kth channel is defined as follows. See figure 3.10 for a pictorial representation. Every $k \times l$ time steps the channel takes in a triple of inputs and outputs one symbol. The input alphabet is $\mathcal{X} = \mathcal{X}_1 \times \mathcal{X}_2 \times \mathcal{X}_3$ where

$$\begin{aligned}
\mathcal{X}_1 &= \{0,1\}^{kN_1} \times \{0,1\}^{kN_{12}} \times \{0,1\}^{kN_{13}} \times \{0,1\}^{kN_{123}} \\
\mathcal{X}_2 &= \{0,1\}^{kN_2} \times \{0,1\}^{kN_{12}} \times \{0,1\}^{kN_{13}} \times \{0,1\}^{kN_{123}} \\
\mathcal{X}_3 &= \{0,1\}^{kN_3} \times \{0,1\}^{kN_{13}} \times \{0,1\}^{kN_{23}} \times \{0,1\}^{kN_{123}}
\end{aligned}$$

The output alphabet is

$$\begin{aligned}
&\mathcal{Y} = \{0,1\}^{kN_1} \times \{0,1\}^{kN_2} \times \{0,1\}^{kN_3} \\
&\times \left(\{0,1\}^{kN_{12}} \cup \{e\}\right) \times \left(\{0,1\}^{kN_{13}} \cup \{e\}\right) \times \left(\{0,1\}^{kN_{23}} \cup \{e\}\right) \times \left(\{0,1\}^{kN_{123}} \cup \{e\}\right)
\end{aligned}$$

where e is an output symbol that can be thought of as an erasure. The channel thus decomposes into one with $4 \times 3 = 12$ inputs and 7 outputs. The outputs at time i

are related deterministically to the inputs at time i via

$$Y_1(i) = X_{1,1}(i)$$
$$Y_2(i) = X_{2,1}(i)$$
$$Y_3(i) = X_{3,1}(i)$$

$$Y_{12}(i) = \begin{cases} X_{1,12}(i) & \text{if } X_{1,12}(i) = X_{2,12}(i) \\ e & \text{otherwise} \end{cases}$$
$$Y_{13}(i) = \begin{cases} X_{1,13}(i) & \text{if } X_{1,13}(i) = X_{3,13}(i) \\ e & \text{otherwise} \end{cases}$$
$$Y_{23}(i) = \begin{cases} X_{2,23}(i) & \text{if } X_{2,23}(i) = X_{3,23}(i) \\ e & \text{otherwise} \end{cases}$$

$$Y_{123}(i) = \begin{cases} X_{1,123}(i) & \text{if } X_{1,123}(i) = X_{2,123}(i) = X_{3,123} \\ e & \text{otherwise} \end{cases}$$

The input streams thus consist of blocks of kN_i bits. The output streams $Y_1(i), Y_2(i), Y_3(i)$ match their associated input streams. The output stream $Y_{12}(i)$ matches its associated input streams if and only if the input streams match at each bit, otherwise the erasure symbol is outputted. Likewise for the other output streams. For this reason the boxes inside the channel in figure 3.9 are labeled 'coordination channel'. See figure 3.10 for a pictorial example of one such coordination channel. The idea of the coordination channels is that in the limit of large k, they only let common information through. This should be intuitive from their definition and from the figure.

We now bound the capacity region of this channel. It is clear that we can fur-

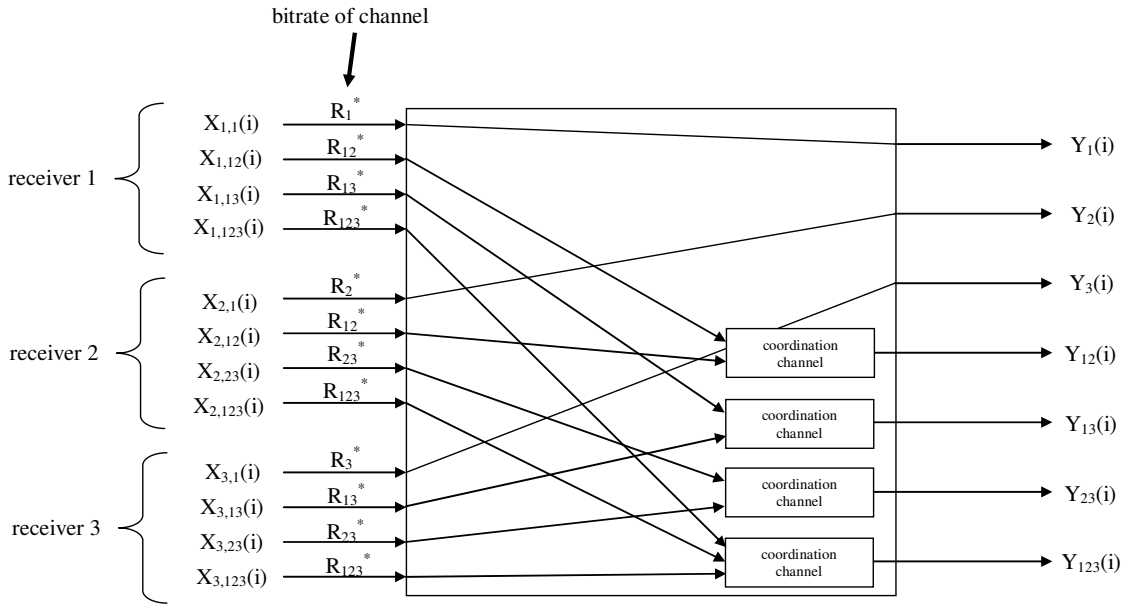

Figure 3.9: Illustration of the deterministic multiple access channel used in converse.

ther decompose the channel into seven parallel channels, one linking $X_{1,1}$ and Y_1, one linking $X_{2,1}$ and Y_2, one linking $X_{3,1}$ and Y_3, one linking $(X_{1,12}, X_{2,12})$ and Y_{12}, one linking $(X_{1,13}, X_{3,13})$ and Y_{13}, one linking $(X_{2,23}, X_{3,23})$ and Y_{23}, and one linking $(X_{1,123}, X_{2,123}, X_{3,123})$ and Y_{123}. The capacity region of the channel in question is thus the Minkowski sum of the capacity regions of these seven channels. Denote these seven capacity regions by $\mathcal{C}_{\mathcal{I}}^k$ for $\mathcal{I} \subseteq \{1,2,3\}$. Then the capacity region of our channel is given by

$$\mathcal{C}^k = \sum_{\mathcal{I} \subseteq \{1,2,3\}} \mathcal{C}_{\mathcal{I}}^k.$$

where sigma denotes the Minkowski sum. In particular we wish to compute the

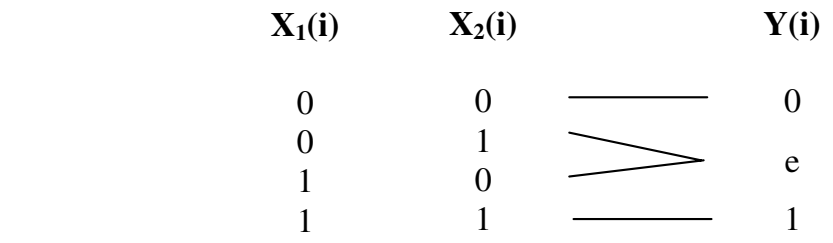

(a)

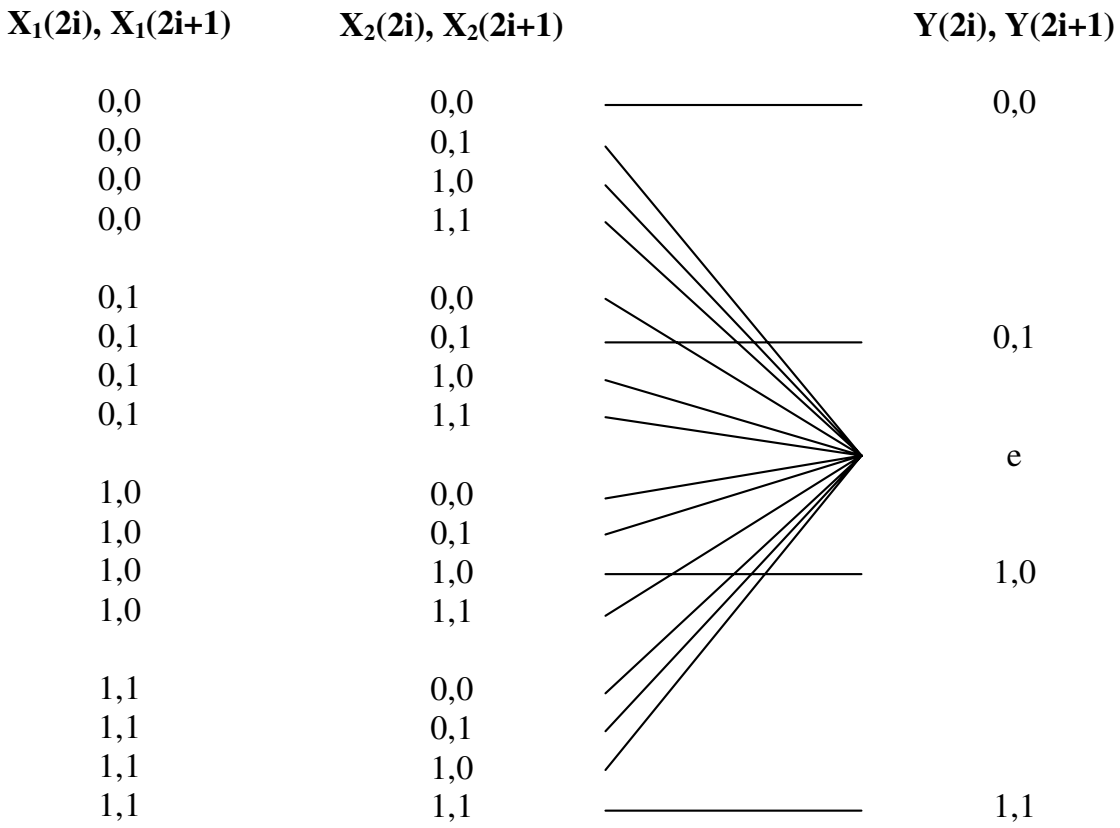

(b)

Figure 3.10: (a) a coordination channel for $k = 1$. (b) a coordination channel for $k = 2$.

limiting intersection of these regions

$$\begin{aligned}\mathcal{C} &= \lim_{K\to\infty} \bigcap_{k=1}^{K} \mathcal{C}^k \\ &= \sum_{\mathcal{I}\subseteq\{1,2,3\}} \lim_{K\to\infty} \bigcap_{k=1}^{K} \mathcal{C}_{\mathcal{I}}^k \\ &= \sum_{\mathcal{I}\subseteq\{1,2,3\}} \mathcal{C}_{\mathcal{I}}.\end{aligned}$$

Lemma 3.6.1.

1. *The region* $\mathcal{C}_1$ *is the set of all* $\mathbf{R} \in \mathbb{R}_+^7$ *satisfying* $R_1 + R_{12} + R_{13} + R_{123} \leq R_1^*$ *and* $R_{\mathcal{I}} = 0$ *for* $\mathcal{I} \in \{2, 3, 23\}$,

2. *The region* $\mathcal{C}_2$ *is the set of all* $\mathbf{R} \in \mathbb{R}_+^7$ *satisfying* $R_2 + R_{12} + R_{23} + R_{123} \leq R_2^*$ *and* $R_{\mathcal{I}} = 0$ *for* $\mathcal{I} \in \{1, 3, 13\}$,

3. *The region* $\mathcal{C}_3$ *is the set of all* $\mathbf{R} \in \mathbb{R}_+^7$ *satisfying* $R_3 + R_{13} + R_{23} + R_{123} \leq R_3^*$ *and* $R_{\mathcal{I}} = 0$ *for* $\mathcal{I} \in \{1, 2, 12\}$,

4. *The region* $\mathcal{C}_{12}$ *is the set of all* $\mathbf{R} \in \mathbb{R}_+^7$ *satisfying* $R_{12} + R_{123} \leq R_{12}^*$ *and* $R_{\mathcal{I}} = 0$ *for* $\mathcal{I} \in \{1, 2, 3, 13, 23\}$,

5. *The region* $\mathcal{C}_{13}$ *is the set of all* $\mathbf{R} \in \mathbb{R}_+^7$ *satisfying* $R_{13} + R_{123} \leq R_{13}^*$ *and* $R_{\mathcal{I}} = 0$ *for* $\mathcal{I} \in \{1, 2, 3, 12, 23\}$,

6. *The region* $\mathcal{C}_{23}$ *is the set of all* $\mathbf{R} \in \mathbb{R}_+^7$ *satisfying* $R_{23} + R_{123} \leq R_{23}^*$ *and* $R_{\mathcal{I}} = 0$ *for* $\mathcal{I} \in \{1, 2, 3, 12, 13\}$,

7. *The region* $\mathcal{C}_{123}$ *is the set of all* $\mathbf{R} \in \mathbb{R}_+^7$ *satisfying* $R_{123} \leq R_{123}^*$ *and* $R_{\mathcal{I}} = 0$ *for* $\mathcal{I} \in \{1, 2, 3, 12, 13, 23\}$.

Proof. The first three regions are trivial. We establish the fourth. The messages $\mathbf{W}_{\mathcal{I}}$ are uniformly distributed on $\{1, \ldots, 2^{nR_{\mathcal{I}}}\}$ and mutually independent for fixed n. Denote the n-length output sequence by $\mathbf{Y}_{12}$. By Fano's inequality we must have $H(\cup_{\mathcal{I}\subseteq\{1,2,3\}}\mathbf{W}_{\mathcal{I}}|\mathbf{Y}_{12}) \leq \epsilon_n$ with $\epsilon_n \to 0$ as $n \to \infty$ in order for the error probability to be made arbitrarily small. Thus by the mutual independence of the messages we have

$$\begin{aligned} n(R_1 + R_2 + R_3 + R_{13} + R_{23}) &= H(\mathbf{W}_1) + H(\mathbf{W}_2) + H(\mathbf{W}_{13}) + H(\mathbf{W}_{23}) \\ &\leq H(\cup_{\mathcal{I}\subseteq\{1,2,3\}}\mathbf{W}_{\mathcal{I}}, \mathbf{Y}_{12}) - H(\mathbf{W}_{12}, \mathbf{W}_{123}) \\ &\leq H(\mathbf{Y}_{12}) - H(\mathbf{W}_{12}, \mathbf{W}_{123}) + \epsilon_n \\ &= H(\mathbf{Y}_{12}|\mathbf{W}_{12}, \mathbf{W}_{123}) + \epsilon_n \end{aligned}$$

Assume for simplicity that $n = mk$ where m is an integer. We write $\mathbf{Y}_{12} = [\mathbf{Y}_{12}^1, \ldots, \mathbf{Y}_{12}^m]$ where $\mathbf{Y}_{12}^i$ represents the ith block of k symbols in $\mathbf{Y}$. Similarly $\mathbf{X}^i$ represents the ith block of k symbols in $\mathbf{X}$. We also use the shorthand $\mathbf{W} \equiv \{\mathbf{W}_{12}, \mathbf{W}_{123}\}$. We proceed to show that $H(\mathbf{Y}_{12}|\mathbf{W})$ is sufficiently small.

$$\begin{aligned} H(\mathbf{Y}_{12}|\mathbf{W}) &\leq \sum_{i=1}^{m} H(\mathbf{Y}_{12}^i|\mathbf{W}) \\ &= -\sum_{i=1}^{m}\sum_{\mathbf{w}} P(\mathbf{W} = \mathbf{w}) \sum_{x} P(\mathbf{Y}_{12}^i = x|\mathbf{W} = \mathbf{w}) \log P(\mathbf{Y}_{12}^i = x|\mathbf{W} = \mathbf{w}) \end{aligned}$$

From the channel definition we have

$$P(\mathbf{Y}_{12}^i = x|\mathbf{W} = \mathbf{w}) = \begin{cases} P(\mathbf{X}_{1,12}^i = x, \mathbf{X}_{2,12}^i = x|\mathbf{W} = \mathbf{w}) & x \neq e; \\ P(\mathbf{X}_{1,12}^i \neq \mathbf{X}_{2,12}^i|\mathbf{W} = \mathbf{w}) & x = e. \end{cases}$$

Using this expression and the conditional independence of $\mathbf{X}_{1,12}^i$ and $\mathbf{X}_{2,12}^i$ given $\mathbf{W}$ we have

$$
\begin{aligned}
&-\sum_x P(\mathbf{Y}_{12}^i = x|\mathbf{W}=\mathbf{w}) \log P(\mathbf{Y}_{12}^i = x|\mathbf{W}=\mathbf{w}) \\
&\quad = -P(\mathbf{X}_{1,12}^i \neq \mathbf{X}_{2,12}^i|\mathbf{W}=\mathbf{w}) \log P(\mathbf{X}_{1,12}^i \neq \mathbf{X}_{2,12}^i|\mathbf{W}=\mathbf{w}) \\
&\qquad - \sum_x P(\mathbf{X}_{1,12}^i = x|\mathbf{W}=\mathbf{w}) P(\mathbf{X}_{2,12}^i = x|\mathbf{W}=\mathbf{w}) \log P(\mathbf{X}_{1,12}^i = x|\mathbf{W}=\mathbf{w}) \\
&\qquad - \sum_x P(\mathbf{X}_{1,12}^i = x|\mathbf{W}=\mathbf{w}) P(\mathbf{X}_{2,12}^i = x|\mathbf{W}=\mathbf{w}) \log P(\mathbf{X}_{2,12}^i = x|\mathbf{W}=\mathbf{w}).
\end{aligned}
$$

The first term can be upper bounded by 1 (as $-x \log_2 x < 1$ for all $x \in \mathbb{R}$). The second term can also be upper bounded by 1. To see this, maximize first over the distribution $P(\mathbf{X}_{2,12}^i|\mathbf{W}=\mathbf{w})$ and then over the distribution $P(\mathbf{X}_{1,12}^i|\mathbf{W}=\mathbf{w})$,

$$
\begin{aligned}
&\max_{\substack{P(\mathbf{X}_{1,12}^i|\mathbf{W}=\mathbf{w}) \\ P(\mathbf{X}_{2,12}^i|\mathbf{W}=\mathbf{w})}} \sum_x P(\mathbf{X}_{1,12}^i = x|\mathbf{W}=\mathbf{w}) P(\mathbf{X}_{2,12}^i = x|\mathbf{W}=\mathbf{w}) \log P(\mathbf{X}_{1,12}^i = x|\mathbf{W}=\mathbf{w}) \\
&\quad = \max_{P(\mathbf{X}_{1,12}^i|\mathbf{W}=\mathbf{w})} \left[\max_x P(\mathbf{X}_{1,12}^i = x|\mathbf{W}=\mathbf{w})\right] \log \left[\max_x P(\mathbf{X}_{1,12}^i = x|\mathbf{W}=\mathbf{w})\right] \\
&\quad \leq 1
\end{aligned}
$$

Likewise the third term can be upper bounded by 1. Thus putting this all together we have

$$
\begin{aligned}
H(\mathbf{Y}_{12}|\mathbf{W}) &< 3 \sum_{i=1}^{m} \sum_{\mathbf{w}} P(\mathbf{W}=\mathbf{w}) \\
&= 3m
\end{aligned}
$$

and so

$$\begin{aligned} R_1 + R_2 + R_3 + R_{13} + R_{23} &< 3m/n \\ &= 3/k \end{aligned}$$

Then by letting $k \to \infty$ we have $R_{\mathcal{I}} = 0$ for $\mathcal{I} \in \{1, 2, 3, 13, 23\}$. From the structure of the coordination channel it is clear that we can achieve points $(R_{12}, R_{123}) = (R_{12}^*, 0)$ and $(R_{12}, R_{123}) = (0, R_{12}^*)$. By time-sharing we can achieve all points in the region $R_{12} + R_{123} \leq R_{12}^*$. Conversely from Fano's inequality we have

$$\begin{aligned} n(R_{12} + R_{123}) &= H(\mathbf{W}_{12}) + H(\mathbf{W}_{123}) \\ &\leq H(\mathbf{Y}) \\ &\leq \log(2^{kR_{12}^*} + 1)^m \\ &= n(R_{12}^* + \delta_k) \end{aligned}$$

where $\delta_k \to 0$ as $k \to \infty$. This establishes the fourth component of the lemma. The remaining components are established in the same manner. We omit the details. □

It remains to show that the region $\sum_{\mathcal{I} \subseteq \{1,2,3\}} \mathcal{C}_{\mathcal{I}}$, corresponds to the region in equation (3.2).

3.7 Appendix

Lemma 3.7.1. *Let $\mathcal{X}_1, \mathcal{X}_2$ and $\mathcal{X}_3$ be three sets of random variables satisfying at least one of the properties $\mathcal{X}_1 \subseteq \mathcal{X}_2 \cup \mathcal{X}_3$, $\mathcal{X}_2 \subseteq \mathcal{X}_1 \cup \mathcal{X}_3$ or $\mathcal{X}_3 \subseteq \mathcal{X}_1 \cup \mathcal{X}_2$. Let W be a random variable that satisfies $H(W|\mathcal{X}_i) = 0$ for $i = 1, 2, 3$. Then*

$$I(\mathcal{X}_1; \mathcal{X}_2; \mathcal{X}_3) \geq H(W)$$

Proof.

$$\begin{aligned}
I(\mathcal{X}_1;\mathcal{X}_2;\mathcal{X}_3) &= I(W,\mathcal{X}_1;W,\mathcal{X}_2;W,\mathcal{X}_3)\\
&= H(W,\mathcal{X}_1)+H(W,\mathcal{X}_2)+H(W,\mathcal{X}_3)\\
&\quad - H(W,\mathcal{X}_1,\mathcal{X}_2)-H(W,\mathcal{X}_1,\mathcal{X}_3)-H(W,\mathcal{X}_2,\mathcal{X}_3)+H(W,\mathcal{X}_1,\mathcal{X}_2,\mathcal{X}_3)\\
&= H(W)+H(\mathcal{X}_1|W)+H(\mathcal{X}_2|W)+H(\mathcal{X}_3|W)\\
&\quad - H(\mathcal{X}_1,\mathcal{X}_2|W)-H(\mathcal{X}_1,\mathcal{X}_3|W)-H(\mathcal{X}_2,\mathcal{X}_3|W)+H(\mathcal{X}_1,\mathcal{X}_2,\mathcal{X}_3|W)\\
&= H(W)+I(\mathcal{X}_1;\mathcal{X}_2;\mathcal{X}_3|W)\\
&\geq H(W)
\end{aligned}$$

where the last step follows from lemma 3.7.4. □

Lemma 3.7.2.

$$H(A)+H(B)+H(C)=H(A,B,C)+I(A,B;A,C;B,C)+I(A;B;C)$$

Proof. ITIP □

Lemma 3.7.3. *Let $X_1,\ldots,X_n$ be a set of mutually independent r.v's. Let $\mathcal{X}_1,\mathcal{X}_2$ and $\mathcal{X}_3$ be three subsets of these r.v.'s with the property $\mathcal{X}_1\cap\mathcal{X}_2\cap\mathcal{X}_3=\phi$. Then for any r.v. Y*

$$H(Y|\mathcal{X}_1)+H(Y|\mathcal{X}_2)+H(Y|\mathcal{X}_3)\geq H(Y).$$

Proof.

$$
\begin{aligned}
&H(Y|\mathcal{X}_1) + H(Y|\mathcal{X}_2) + H(Y|\mathcal{X}_3) \\
&\quad \geq H(Y|\mathcal{X}_1, \mathcal{X}_2^c) + H(Y|\mathcal{X}_2, \mathcal{X}_3^c) + H(Y|\mathcal{X}_3, \mathcal{X}_1^c) \\
&\quad = H(Y, \mathcal{X}_1, \mathcal{X}_2^c) + H(Y, \mathcal{X}_2, \mathcal{X}_3^c) + H(Y, \mathcal{X}_3, \mathcal{X}_1^c) - H(\mathcal{X}_1, \mathcal{X}_2^c) - H(\mathcal{X}_2, \mathcal{X}_3^c) - H(\mathcal{X}_3, \mathcal{X}_1^c) \\
&\quad = H(Y, \mathcal{X}_1, \mathcal{X}_2, \mathcal{X}_3) + I(Y, \mathcal{X}_1, \mathcal{X}_2^c; Y, \mathcal{X}_2, \mathcal{X}_3^c; Y, \mathcal{X}_3, \mathcal{X}_1^c) \\
&\qquad + I(Y, \mathcal{X}_1, \mathcal{X}_2, \mathcal{X}_3; Y, \mathcal{X}_1, \mathcal{X}_2, \mathcal{X}_3; Y, \mathcal{X}_1, \mathcal{X}_2, \mathcal{X}_3) \\
&\qquad - H(\mathcal{X}_1, \mathcal{X}_2^c) - H(\mathcal{X}_2, \mathcal{X}_3^c) - H(\mathcal{X}_3, \mathcal{X}_1^c) \\
&\quad = 2H(Y, \mathcal{X}_1, \mathcal{X}_2, \mathcal{X}_3) + I(Y, \mathcal{X}_1, \mathcal{X}_2^c; Y, \mathcal{X}_2, \mathcal{X}_3^c; Y, \mathcal{X}_3, \mathcal{X}_1^c) \\
&\qquad - 2H(\mathcal{X}_1 \backslash \mathcal{X}_2 \cup \mathcal{X}_3) - 2H(\mathcal{X}_2 \backslash \mathcal{X}_1 \cup \mathcal{X}_3) - 2H(\mathcal{X}_3 \backslash \mathcal{X}_1 \cup \mathcal{X}_2) \\
&\qquad - 2H(\mathcal{X}_1 \cap \mathcal{X}_2 \backslash \mathcal{X}_3) - 2H(\mathcal{X}_1 \cap \mathcal{X}_3 \backslash \mathcal{X}_2) - 2H(\mathcal{X}_2 \cap \mathcal{X}_3 \backslash \mathcal{X}_1) - 3H(\mathcal{X}_1 \cap \mathcal{X}_2 \cap \mathcal{X}_3) \\
&\quad = 2H(Y, \mathcal{X}_1, \mathcal{X}_2, \mathcal{X}_3) + I(Y, \mathcal{X}_1, \mathcal{X}_2^c; Y, \mathcal{X}_2, \mathcal{X}_3^c; Y, \mathcal{X}_3, \mathcal{X}_1^c) \\
&\qquad - 2H(\mathcal{X}_1 \backslash \mathcal{X}_2 \cup \mathcal{X}_3) - 2H(\mathcal{X}_2 \backslash \mathcal{X}_1 \cup \mathcal{X}_3) - 2H(\mathcal{X}_3 \backslash \mathcal{X}_1 \cup \mathcal{X}_2) \\
&\qquad - 2H(\mathcal{X}_1 \cap \mathcal{X}_2 \backslash \mathcal{X}_3) - 2H(\mathcal{X}_1 \cap \mathcal{X}_3 \backslash \mathcal{X}_2) - 2H(\mathcal{X}_2 \cap \mathcal{X}_3 \backslash \mathcal{X}_1) - 2H(\mathcal{X}_1 \cap \mathcal{X}_2 \cap \mathcal{X}_3) \\
&\quad = 2H(Y, \mathcal{X}_1, \mathcal{X}_2, \mathcal{X}_3) + I(Y, \mathcal{X}_1, \mathcal{X}_2^c; Y, \mathcal{X}_2, \mathcal{X}_3^c; Y, \mathcal{X}_3, \mathcal{X}_1^c) - 2H(\mathcal{X}_1, \mathcal{X}_2, \mathcal{X}_3) \\
&\quad \geq I(Y, \mathcal{X}_1, \mathcal{X}_2^c; Y, \mathcal{X}_2, \mathcal{X}_3^c; Y, \mathcal{X}_3, \mathcal{X}_1^c) \\
&\quad \geq H(Y)
\end{aligned}
$$

where the third step follows from lemma 3.7.2, the fourth from a set expansion made possible by the mutual independence of the underlying r.v.'s $X_1, \ldots, X_n$, the fifth from the property $\mathcal{X}_1 \cap \mathcal{X}_2 \cap \mathcal{X}_3 = \phi$, the sixth by a set relationship, and the eighth by lemma 3.7.1. □

Lemma 3.7.4. *Let $\mathcal{X}_1, \mathcal{X}_2$ and $\mathcal{X}_3$ be sets of random variables. If either $\mathcal{X}_1 \subseteq \mathcal{X}_2 \cup \mathcal{X}_3$,*

$\mathcal{X}_2 \subseteq \mathcal{X}_1 \cup \mathcal{X}_3$ *or* $\mathcal{X}_3 \subseteq \mathcal{X}_1 \cup \mathcal{X}_2$ *then for any r.v.* W*,*

$$I(\mathcal{X}_1; \mathcal{X}_2; \mathcal{X}_3|W) \geq 0.$$

Proof. Assume without loss of generality that the first *containment* property $\mathcal{X}_3 \subseteq \mathcal{X}_1 \cup \mathcal{X}_2$ holds. Then

$$\begin{aligned}
&I(\mathcal{X}_1, \mathcal{X}_2, \mathcal{X}_3|W) \\
&\quad = H(\mathcal{X}_1|W) + H(\mathcal{X}_2|W) + H(\mathcal{X}_3|W) \\
&\qquad - H(\mathcal{X}_1, \mathcal{X}_2|W) - H(\mathcal{X}_1, \mathcal{X}_3|W) - H(\mathcal{X}_2, \mathcal{X}_3|W) + H(\mathcal{X}_1, \mathcal{X}_2, \mathcal{X}_3|W) \\
&\quad = H(\mathcal{X}_1|W) + H(\mathcal{X}_2|W) + H(\mathcal{X}_3|W) - H(\mathcal{X}_1, \mathcal{X}_2|W) - H(\mathcal{X}_1, \mathcal{X}_3|W) \\
&\quad = I(\mathcal{X}_1; \mathcal{X}_3|W) + I(\mathcal{X}_2; \mathcal{X}_3|W) - H(\mathcal{X}_3|W) \\
&\quad \geq H(\mathcal{X}_1 \cap \mathcal{X}_3|W) + H(\mathcal{X}_2 \cap \mathcal{X}_3|W) - H(\mathcal{X}_1 \cap \mathcal{X}_3, \mathcal{X}_2 \cap \mathcal{X}_3|W) \\
&\quad = I(\mathcal{X}_1 \cap \mathcal{X}_3; \mathcal{X}_2 \cap \mathcal{X}_3|W) \\
&\quad \geq 0.
\end{aligned}$$

The second step follows from the containment property $\mathcal{X}_1 \subseteq \mathcal{X}_2 \cup \mathcal{X}_3$. The first term in the fourth step follows by applying lemma 3.7.6 with $W = W$, $X = \mathcal{X}_1$, $Y = \mathcal{X}_3$ and $Z = \mathcal{X}_1 \cap \mathcal{X}_3$, the second term by applying the same lemma with $W = W$, $X = \mathcal{X}_2$, $Y = \mathcal{X}_3$ and $Z = \mathcal{X}_2 \cap \mathcal{X}_3$. The third term in the third and fourth steps are equal by the containment property. □

Lemma 3.7.5. *If* $H(Z|X) = 0$ *and* $H(Z|Y) = 0$ *then* $I(X; Y|W) \geq H(Z|W)$*.*

Proof.

$$\begin{aligned} I(X;Y|W) &= I(X,Z;Y,Z|W) \\ &= H(X,Z|W) + H(Y,Z|W) - H(X,Y,Z|W) \\ &= H(Z|W) + H(X|W,Z) + H(Z|W) + H(Y|W,Z) - H(Z|W) - H(X,Y|W,Z) \\ &= H(Z|W) + I(X;Y|W,Z) \\ &\geq H(Z|W). \end{aligned}$$

□

Lemma 3.7.6. *If* $H(Z|X) = 0$ *and* $H(Z|Y) = 0$ *then* $I(X;Y|W) \geq H(Z|W)$.

Bibliography

[1] R. Ahlswede, N. Cai, S. -Y. R. Li, R. W. Yeung, "Network information flow," *IEEE Trans. on Inform. Theory,* vol. 46, pp 1204-1216, July 2000.

[2] F. Baccelli, B. Blaszczyszyn, P. Mühlethaler, "An Aloha Protocol for Multihop Mobile Wireless Networks," *IEEE Trans. Info. Theory*, vol. 52, pp. 421-436, Feb. 2006.

[3] L. Berlemann, G. R. Hiertz, B. H. Walke, S. Mangold, "Radio resource sharing games: enabling QoS support in unlicensed bands," *IEEE Network*, vol. 19, iss. 4, pp. 59-65, July-Aug. 2005.

[4] B. Bollobas, *Random Graphs*, Cambridge University Press, 2001.

[5] V. Cadambe, S. Jafar, "Interference Alignment and Degrees of Freedom for the K user Interference Channel," in *IEEE Trans. Info. Theory*, Vol. 54, Iss. 8, pp. 3425-3441, Aug. 2008.

[6] S. T. Chung, S. Kim, J. Lee, J. M. Cioffi, "A game-theoretic approach to power allocation in frequency-selective Gaussian interference channels," *Proc. of IEEE International Symposium on Information Theory*, pp. 316-316, July 2003.

[7] T. M. Cover, "Comments on Broadcast Channels," *IEEE Trans. Inform. Theory*, Vol. 44, No. 6, Oct. 1998, pp. 2524-2530.

[8] E. Erez, M. Feder, "Capacity Region and network codes for two receivers multicast with private and common data," *Proc. Workshop on Coding, Cryptography and Combinatorics*, China, 2003

[9] R. Etkin, A. Parekh, D. Tse, "Spectrum sharing for unlicensed bands," *IEEE J. Sel. Areas Comm.*, vol. 25, is. 3, pp. 517-528, Apr. 2007.

[10] M. Félegyházi, M. Cagalj, S. S. Bidokhti, J. -P. Hubaux, "Non-cooperative multi-radio channel allocation in wireless networks," *Proc. INFOCOM*, pp. 1442-1450, May 2007.

[11] M. Franceschetti, M. D. Migliore, P. Minero, "The Capacity of Wireless Networks: Information-theoretic and Physical Limits," submitted to *IEEE Trans. Info. Theory*.

[12] P. Gupta, P. R. Kumar, "The Capacity of Wireless Networks," in *IEEE Trans. Info. Theory*, Vol. 46, Iss. 2., pp. 388-404, Mar. 2000.

[13] M. M. Halldórsson, J. Y. Halpern, Li (Erran) Li, Vahab S. Mirrokni, "On spectrum sharing games," *Proc. of Annual ACM Symposium on Principles of Distributed Computing*, pp. 107-114, 2004.

[14] S. A. Jafar, S. Shamai, "Degrees of Freedom Region for the MIMO X Channel," in *IEEE Trans. Info. Theory*, Vol. 54, No. 1, pp. 151-170, Jan. 2008.

[15] N. Jindal, J. G. Andrews, S. Weber, "Optimizing the SIR operating point of Spatial Networks," *Workshop on Information Theory and its Applications, U.C. San Diego*, available at arXiv:cd.IT/0702030v1, Feb 2007.

[16] N. Jindal, J. G. Andrews, S. Weber, "Bandwidth partitioning in Decentralized Wireless Networks," submitted to *IEEE Trans. Wireless Comm.*, Nov. 2007.

[17] N. Jindal, S. Weber, J. G. Andrews, "Fractional Power Control for Decentralized Wireless Networks," submitted to *IEEE Trans. Wireless Comm.*, Dec. 2007.

[18] R. Koetter, M. Medard, "An Algebraic Approach to Network Coding," *IEEE/ACM Trans. on Networking,* vol. 11, no. 5, Oct. 2003.

[19] A. B. MacKenzie, S. B. Wicker, "Selfish users in Aloha: a game-theoretic approach," *Proc. of IEEE Vehicular Technology Conference*, vol. 3, pp. 1354-1357, Oct. 2001.

[20] M. Maddah-Ali, A. Motahari, and A. Khandani, "Signaling over MIMO multi-base systems - combination of multi-access and broadcast schemes," in *Proc. of ISIT*, pp. 21042108, July 2006.

[21] M. H. Manshaei, M. Félegyházi, J. Freudiger, J. -P. Hubaux, P. Marbach, "Spectrum Sharing Games of Network Operators and Cognitive Radios," *Cognitive Wireless Networks: Concepts, Methodologies and Visions*, Springer, 2007.

[22] S. Mathur, L. Sankaranarayanan, N. B. Mandayam, "Coalitional games in receiver cooperation for spectrum sharing," *Proc. of IEEE Inform. Sci. and Systems*, pp. 949-954, March 2006.

[23] C. K. Ngai, R. W. Yeung, "Multisource Network Coding with Two Sinks," *Proc. Internation Conference on Communications, Circuits and Systems*, vol. 1, pp. 34-37, June 2004.

[24] A. Özgür, O. Lévêque and D. N. C. Tse, "Hierarchical Cooperation Achieves Optimal Capacity Scaling in Ad Hoc Networks," in *IEEE Trans. Info. Theory*, Vol. 53, No. 10, Oct. 2007.

[25] O. Simeone, Y. Bar-Ness, "A game-theoretic view on the interference channel with random access," *Proc. of IEEE New Frontiers in Dynamic Spectrum Access Networks*, pp. 13-21, April 2007.

[26] D. Slepian, J. K. Wolf, "A Coding Theorem for Multiple Access Channels With Correlated Sources," *Bell Sys. Tech. Journal,* vol. 52, pp. 1037-1076, Sep. 1973.

[27] T. Tao and V. H. Vu, *Additive Combinatorics*, Cambridge University Press, 2006.

[28] D. N. C. Tse, P. Viswanath, *Fundamentals of Wireless Communication*, Cambridge Univeristy Press, 2005.

[29] S. Weber, J. G. Andrews, "The Effect of Fading, Channel Inversion, and Threshold Scheduling on *Ad Hoc* Networks," *IEEE Trans Info. Theory*, vol. 53, no. 11, Nov. 2007.

[30] W. Yu, G. Ginis, J. M. Cioffi, "Distributed multiuser power control for digital subscriber lines," *IEEE J. Sel. Areas Comm.* vol. 20, no. 5, June 2002.

[31] F. Zuyuan, B. Bensaou,"Fair bandwidth sharing algorithms based on game theory frameworks for wireless ad-hoc networks," *Proc. 23rd Annual Joint Conference of the IEEE Computer and Communications Societies (INFOCOM)*, vol. 2, pp. 1284-1295, Mar. 2004.